UNESCO-IHE
Institute for Water Education

Universidad del Valle

PERFORMANCE OF A FIXED BED REACTOR FOR MERCURY REMOVAL BY BIOSORPTION USING AGRICULTURAL RESIDUE

Carlos Miguel Torrado Cuellar

San Juan production unit, Suarez, Cauca

PERFORMANCE OF A FIXED BED REACTOR FOR MERCURY REMOVAL BY BIOSORPTION USING AGRICULTURAL RESIDUE

Master of Science Thesis
by
Carlos Miguel Torrado Cuellar

Mentors
Carlos Arturo Madera, Ph.D

Examination Committee
Eldon R. Rene, Ph.D
Alberto Albis Arrieta Ph.D

This research is done for the partial fulfilment of requirements for the Master of Science degree at the UNESCO-IHE Institute for Water Education, Delft, the Netherlands
Delft
January 2018

Although the author and UNESCO-IHE Institute for Water Education have made every effort to ensure that the information in this thesis was correct at press time, the author and UNESCO-IHE do not assume and hereby disclaim any liability to any party for any loss, damage, or disruption caused by errors or omissions, whether such errors or omissions result from negligence, accident, or any other cause.

© By Carlos Miguel Torrado Cuellar, 2018.
This work is licensed under a Creative Commons Attribution-NonCommercial 4.0 International License. 

Abstract

This research was aimed to evaluate the performance of a technology for mercury removal. This study was performed in a mining area located in Cauca, Colombia. The purpose of this project was to asses a low cost alternative for removal of mercury in the wastewater of a mining production unit (MPU) which produces gold. Activated carbons generated with coconut shell and coffee husk were evaluated as a treatment alternative for the removal of mercury released to the water after the amalgamation process.

Thus, an evaluation of the MPU in terms of the wastewater characterization and the performance and conditions of the main processes used for gold production was carried out. Mercury losses were estimated throughout the units prior to the discharge point as an important factor contributing to the contamination pathways in the MPU. Coconut shell and coffee husk were ground and activated with a physical mechanism using a muffle furnace, nitrogen gas as the reducing atmosphere and steam as the activating agent. The activated biosorbents were characterized and compared based on their surface area, mesopore and micropore distribution, density and adsorption capacity by performing batch tests. Desorption test was applied for the biosorbent that showed the highest performance in the adsorption batch tests. A laboratory scale fixed bed reactor was evaluated for 10 days, in a semi continuous regimen, with the same conditions as that of the real MPU.

Mercury, suspended solids and COD concentrations were found to exceed the Colombian national permissible limits of wastewater discharge with a maximum mercury, suspended solids and COD concentrations of 7.71, 18496, and 303 mg l^{-1} O_2, respectively. A primary sedimentation tank was designed as a starting point of the treatment train. The sedimentation process was used to remove the majority of solids before the use of the biosorbents for the mercury removal. Coconut shell and coffee husk were activated with maximum yields of 30.0 % and 23.7 %, respectively, obtained from the amount of precursor material introduced to the muffle furnace and the amount of activated carbon generated. Coconut shell activated at a carbonization temperature of 300 °C and an activation temperature of 600 °C showed the highest adsorption capacity and surface area with results of 0.0036 mg g^{-1} and 539.59 m^2 g^{-1}, respectively.

The fixed bed reactor did not achieve its breakthrough point or capacity after 10 days of operation and showed good mercury removal. The effluent quality complies with the national permissible limit of 0.002 mg l^{-1} of mercury. Coconut shell activated carbon proved to offer a better alternative for the removal of mercury in effluents from the gold mining industry.

Keywords: Gold mining, amalgamation, mercury, biosorption, wastewater

Acknowledgment

Firstly, I would like to express my deepest gratitude to Cecilia Cuellar; every step, every dream and every one of my successes will always be achieved because of her and for her. Thank you Mom for always believing in me. I hope I have made you proud from where you are now. Secondly I want to thank to the rest of my family as well for always believing in me, to my father, sisters, nieces and nephews for being the reason I want to be better a human every day. I want to thank those ones, who are friends but feel like sisters to myself, thank you Liby and Doly for always having my back and remind me what I am made of.

I sincerely want to thank Universidad del Valle and UNESCO-IHE for the incredible opportunity of completing this Master, thanks for every lesson inside and outside the classroom. I want to thank to professors Luis Fernando Marmolejo and Juan Pablo Silva for helping me during important moments of this process. Thanks to Leonie Zweekhorst and Yvette van Dongen for being my adoptive family in the Netherlands. Thanks to Bill & Melinda Gates foundation for giving me the opportunity to become a better engineer and person, I will always be grateful. Thanks to 2016 - 2017 sanitary engineering class for all your support, love and company, may life bring us together again. Last but not least thanks to professor Eldon R. Rene and Carlos Arturo Madera for helping me as mentors in this last stage, I will always remember all of your lessons.

Table of Contents

List of Tables

List of Figures

CHAPTER 1

Introduction

The mining industry in Colombia is a growing activity where gold is one of the principal interests of several Colombian and foreign companies. Different gold mining districts in Colombia have been characterized by exploitation, processing and marketing of precious metals with no prevision (Gaviria and Meza, 2006). Mercury contamination in the surrounding environment of the mining production units (MPU) is a major concern in Colombia. This phenomenon is produced by the amalgamation process carried out for the benefit of recovering gold.

It is necessary that the impacts produced by the mining industry on the environment get drastically reduced during extractive operation and more importantly during the production and extraction/recovery of gold through amalgamation (Oyarzun et al., 2011). The municipality of Suárez, located in Cauca department, Colombia, has one of the highest numbers of mining development in the whole department and shows the greatest potential resources in the area where various sub-surface minerals like gold, coal, sand and clay are extracted. Waste resulting from the benefit plants or MPU sometimes is directed to the storage sites that contain significant amounts of free gold and mercury, which is unable to be captured during the washing and amalgamation process. According to the Unidad de planeación minero energética (UPME, Unidad de planeación minero energética), for each pound of gold produced per month, 1.75 pounds of mercury is used without recovery in the department of Cauca, Colombia (UPME, 2007).

Innovative processes for treating industrial wastewater containing heavy metals often involve technologies for the reduction of toxicity in order to meet technology-based treatment standards. A particular attention is given to innovative physico-chemical removal processes such as, adsorption, membrane filtration, electrodialysis and photocatalysis (Barakat, 2011). Natural and plant materials, industrial and agricultural wastes are receiving attention as low cost sorption materials (Acheampong et al., 2010). Coconut shell and coffee husk are agricultural wastes produced near the municipality of Suárez, their capacity to become precursor materials of activated carbon for the removal of heavy metals has been studied previously. However, it is important to assess the use of this waste for the removal of mercury under the prevailing conditions existing in the mining industry.

Low cost alternatives and the improvement of the wastewater treatment train of San Juan MPU may be achieved by characterizing the nature of the sorbent materials, evaluating their efficiency and establishing the performance of adsorption models that describes the mechanism of adsorption at the laboratory scale. This research intended to assess the mercury removal

efficiency of coconut shell and coffee husk activated carbon in batch and fixed bed reactors. These biosorbents were found to have a significant affinity with mercury and a good mercury removal from the wastewater was obtained. This provides valuable information for stablishing a low cost alternative for this kind of industry.

CHAPTER 2

Problem statement

2.1 Background

Colombia is a rich country in resources such as gold, a mineral whose exploitation is largely carried out on a small-scale using traditional/artisanal methods. During the benefit of metal, many UPM use mercury, cyanide and other high toxicity substances that cause serious damage to health and the environment when handled improperly (UPME, 2007). Whether legal or illegal gold mining in Colombia has been an important activity. According to the Ministerio de minas y energía et al. (2014), it was estimated in 2013 that 66 ton of gold were produced, and its value was > 6% of the official goal and at least 17,000 people worked in an artisanal way, while other 51,000 people worked without having a legal license.

Gold mining in Colombia has severe impacts in the water bodies, as it requires up to 1,060 liters of water for the extraction of 1 g of gold. In 2012, it was estimated that 179 municipalities located in 15 departments discharged a load of 205 ton of mercury to the ground and water bodies. It is noteworthy to mention that ~72.5% of this load was produced by the gold processing industry (IDEAM, 2015). This load is released because of the amalgamation process, which produces residual mercury into wastewater in the gold benefit process. Mercury exists in three oxidation states (Hg(II), Hg(I) and Hg^0) and may form different compounds such as mercuric chloride ($HgCl_2$), methyl mercuric chloride (CH_3HgCl), dimethyl mercury (CH_3HgCH_3) and diethyl mercury ($CH_2H_5HgC_2H_5$) (Khunphonoi et al., 2015), these species and some other may be present in the wastewater of the mining industry.

Mining in some municipalities of Cauca department is an important factor for their economic dynamics. It requires special attention because of the way in which it is practiced. While most of the mining industries are at the small scale, most of the people have appropriated this activity as their own with no real technical knowledge or skills on the use and management of toxic substances that are harmful to the environment and human health. The residual water that contains these toxic compounds needs to be treated in order to avoid significant negative impacts on the environment and human health.

2.2 Justification

Mercury is one of the toxic chemicals that is used commonly for the benefit of gold. It is found naturally, but in recent decades it has increased its concentration in the atmosphere due to human factors caused by industrial and mining activities, accumulation in the air, soil and water (Jaramillo et al., 2015). Mercury can cause brain damage, heart, and lung diseases in human beings (Mishra & Upadhyay, 2008). Therefore, its removal in industrial effluents is essential before disposal into the aquatic environment (Rai & Tripathi, 2009).

Most of the gold MPU in Suárez have no appropriate technologies for gold processing and wastewater treatment. After amalgamation, the water with residual gold and mercury is flushed to the tailing dams where the settled sludge should be recovered. However, these dams are often under-designed, poorly managed, and they lead to severe infiltrating into the ground or is operated incorrectly. Just a few MPU in Suárez use chemical conditioning to remove mercury, while the rest have no treatment before it is being discharged to the river. According to the Colombian regulations for gold mining and precious metals, a maximum limit of 0.002 mg l^{-1} of Hg has been recommended (MADS, 2015). On the other hand, an average of 4 ounces is added per every 40 kg of mineral, this amount may vary depending on the amount of gold present in the mineral.

San Juan production unit is located 50 m upstream from the local community of Suárez municipality. It has no treatment of the produced wastewater and the dams do not provide proper conditions for the sludge removal. It is therefore necessary to establish a low cost technology that meets the legal requirements for discharge of wastewater that can be implemented in the gold processing plants in the municipality of Suárez. Biosorption is a low-cost green technology for water pollution decontamination. According to Anastopoulos & Kyzas (2015), new adsorbent materials (raw or modified) have been synthesized and tested for a wide variety of pollutants. Therefore, it is important to evaluate this technology with low cost materials provided by the nearby agricultural industries.

It is also important to evaluate a low cost alternative for the small scale MPUs that is able to recover mercury instead of only confining or retaining it. Adsorption with agricultural by-products is a promising solution for this resource recovery. In this manner, the efficiency of adsorption can be evaluated at the laboratory scale according to the conditions present locally. This will be an innovative solution for all the mining factories in the area. The major reason for this is the fact that, most of the industries are just beginning to comply with regulations in the mining and environmental sector.

2.3 Research question

What is the adsorption capacity of coconut (*Cocos nucifera*) shell and coffee (*Coffea sp.*) husk for the removal of mercury?

2.4 Hypothesis

Coconut (*Cocos nucifera*) shell and coffee (*Coffea sp.*) husk activated carbon may offer high mercury removal efficiency for biosorption in a fixed bed column reactor.

CHAPTER 3

Research objectives

3.1 Main objective

To evaluate the performance of a fixed bed biosorption column for mercury removal from the effluent of San Juan gold processing plant in Suárez, Cauca, Colombia.

3.2 Specific objectives

i. To compare the mercury adsorption capacity of coconut (*Cocos nucifera*) shell and coffee (*Coffea sp.*) husk in batch tests.
ii. To determine the adsorption mechanism, adsorption kinetics and parameters for various adsorption models.
iii. To assess the performance of a fixed bed column for mercury removal using the most suitable adsorbent.

CHAPTER 4

Fundamental concepts

4.1 Introduction to fundamental concepts

This chapter starts by showing an overview of the environmental conditions of the municipality of Suárez, in the department of Cauca. Like many of the municipalities in Colombia, Suárez is a territory, where a poor and undeveloped economy stands in conflict with the natural resources. It is an area rich in minerals and with a great potential; therefore, it is necessary to recognize the environmental and social dynamics in order to design an accessible and replicable technology. Information provided herein, presents the geographical location, the biotic and physical aspects in order to build the scenario where small scale gold mining develops. Also, a list of the environmental impacts caused by the mining industry to this area is mentioned.

Since there are different types of mining in terms of the extraction mode and the gold recovery technologies, a conceptual framework on gold mining in Suárez is provided. Mining terminology may vary from one country to the other, so it is important to establish a common language regarding the scale of mining and extraction mode used. A short definition of the mineral composition found in the area and the stages of gold mining process under these conditions are also provided.

The amalgamation process is defined as the main mechanism used for gold recovery in the area. Hence, it is very important for this chapter to explain the properties, species and toxicology of mercury. Tailing dams play an important role in the mining production units of Suárez. Therefore, a definition of the sedimentation mechanism and the solids retention units implemented in the area is also offered. After presenting the global context of the industry where the fixed bed reactor is evaluated, it is important to give a clear definition of the process carried out, specifically in San Juan MPU, in order to consider the number of units involved in the amalgamation step and the units used for sludge retention.

At last, this chapter intends to present the evolution of adsorption technology as a useful alternative for the removal of heavy metals by explaining the advantages of using activated carbon from low cost adsorption materials over the traditionally prepared activated carbon. The characterization parameters of low cost sorbent materials showing different activation conditions, sources, pore sizes and metal uptake are also presented. Physical and chemical adsorption has been presented as the key mechanisms of the sorption process, while their main challenges and limitations were also reviewed in this chapter.

4.2 Suárez municipality - geographical framework

4.2.1 Geographical location of the Municipality of Suárez

The gold mining district of Suárez, is located on the eastern edge of the western mountain range and geographically corresponds to a strip parallel to the Cauca River and involves a big area of the Salvajina dam. The most representative areas of exploitation of underground gold are: La Toma, El Carmen, El Peñón, Gelima, la Montaña, el Desquite, Maravelez, Guayabillas, Tamboral, El Calvario, El Danubio, La Carolina and La Turbina. The extension of the mining region was initially estimated to be less than 120 km^2 (Alcaldía municipal Suárez, 2017). Figure 1 shows the location of the municipality of Suárez in the department of Cauca.

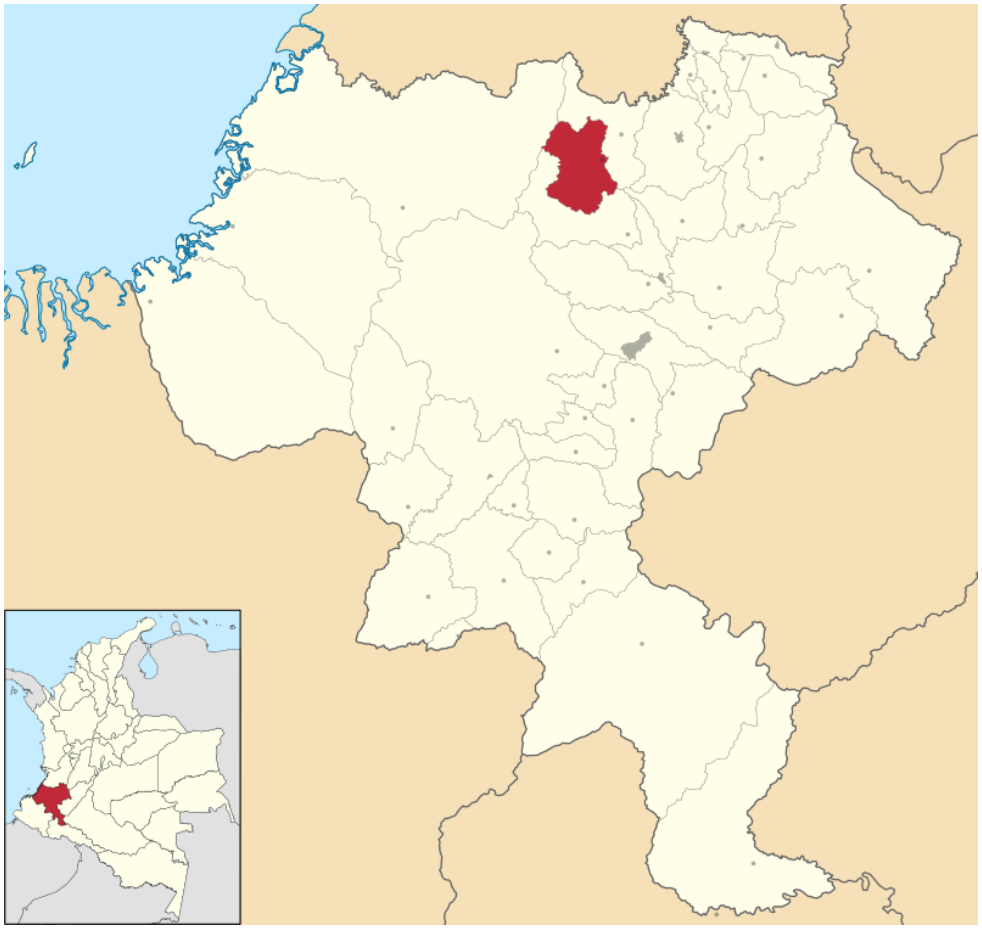

Figure 1. Location of the municipality of Suárez in the department of Cauca. Mapa de Colombia, departamento del Cauca
Source: Alcaldía municipal Suárez (2017)

It limits to the north and east with the municipality of Buenos Aires, to the South with the Municipality of Morales and to the West with Lopez de Micay. It has an extension of 389.87 km^2, of which 3.57 km^2 corresponds to the urban area (Alcaldía municipal Suárez, 2017). Figure 2 shows the districts and villages that are located in the Municipality of Suárez and the Salvajina dam location.

Figure 2. Politic map of the municipality of Suárez, Cauca - districts and villages
Source: Alcaldía municipal de Suárez (2017)

4.2.2 Physical and biotic aspects

4.2.2.1 Climate

Because of its geographical location, the area has a humid, tropical - temperate climate, with well-defined summer and winter seasons. The altitudinal gradient is marked approximately between 1,100 and 2,050 meters, with an average temperature of 19º C and an average annual rainfall of 2,600 mm.

4.2.2.2 Hydrography

The mining district of Suárez is surrounded from south to north by the Cauca River, in whose basin the Salvajina dam is located. The River Ovejas is located in the northwestern sector and

flows into the Cauca River. The basin of this river is very important for its reception of wastewater and mining waste. To the west, the drainage flows to the River Inguito, which finally drains to the Cauca River.

4.2.2.3 Vegetation cover

The vast majority of the area is covered by natural pastures and to a lesser extent by stubble, forest and permanent crops.

4.2.2.4 Soils

According to the topographic conditions and the base material, soils of different characteristics are present. Most of them are relatively poor in nutrients and of little thickness, with serious restrictions of their use.

4.2.3 Socioeconomic aspects

4.2.3.1 Population

The municipality of Suárez has a total of 23,668 inhabitants, of whom 8,296 are settled in the urban area and 15,932 in the rural area. In the mining districts, there are around 5,500 people.

4.2.3.2 Economic activities

It emphasizes agricultural activities, business trade and gold mining; considering the latter a generator of economic resources that allows about 45% of employment in the mining region. The generation of electric energy is an economic activity of greater scale; however, this production has very little economic redistribution and employment in the region.

4.2.3.3 Mining organization

The Suárez Miners´ Cooperative (in Spanish Cooperativa de mineros de Suárez) groups most of the miners, MPU in the region and performs the intermediation of mining inputs (explosives). After proper discussion with relevant parties, these groups have managed to legalize mining activities in different areas of the region. However, despite the efforts, so far there has been very little formal titles of mining establishments or industries, which leads to the existence of informal (illegal) mining in the area. The possible granting of titles to multinational companies in ancestral mining areas is an aggravating factor for regional stability, so that the base organizations in conjunction/cooperation with the municipal administration should lead the process of legalization.

4.2.4 Environmental impacts of gold mining industry in Suárez

Mining, as a generator of employment and regional economy, has caused serious damage to the environmental balance due to the high load of solids dumped to the rivers Ovejas, Cauca and

Inguito and the La Salvajina dam. Visual aesthetic pollution caused by improperly located waste streams and a new threat from the inadequate use of mercury and cyanide adds to the persisting environmental problems. The environmental impacts generated from the gold mining activity in the mining district of Suárez are serious and cumulative and many of them are permanent. The main causes can be summarized as follows:

- Deforestation processes
- Erosion processes
- Processes of deterioration of soil, water sources and basins
- Instability processes (sinking, sliding, mass removal)
- Discharge of toxic substances

The main impacts arising from the mining of precious metals in the gold region of Suárez are:

- Contribution of sediments
- Introduction of heavy metals, especially mercury, into the natural system

This leads to:

- Contamination of marshes and wetlands
- Accumulation of mercury in fish and hydro-biological resources
- Accumulation of mercury in settled communities (Lopez, 2006)

4.3 Conceptual framework on gold mining

4.3.1 Mining

Mining is a different economic activity than the others. The term “mining production” is often used inappropriately. In this case, it is an activity where the resources extracted are non-renewable resources, whose extraction is carried out by progressive levels. As the resource runs out, the work progresses, increasing both the economic and environmental costs, since the material is increasingly present in less accessible places. Places where the removal of materials is necessary, the implementation of large machinery generates greater removal, the production of large quantities of waste (sterile) and socio-environmental effects (Díaz & Pilar, 2011).

In its early stages of development, mining was a purely extractive activity, but with the industrial revolution, it was transformed into a vertically integrated industrial activity. Presently, it is known as the mining-metallurgical industry, because in order to be used, mineral resources need an industrial transformation. In addition, mining makes intensive, but temporary use of space, whose repercussions extend over the long term (Saavedra & Sanchez, 2011).

4.3.1.1 Small-scale mining

In terms of small-scale mining or small-scale mining, the first thing to be said is that the mining legislation in force in Colombia does not discriminate or stratify any of the different mining

exploitation scales, so the same requirements must be met for large mining establishments and the small miner.

In Colombia, the only reference that is made in this respect is the one of the Mining Technical Glossary, which states that small mining exploitations are considered “with simple tools and implements for manual use, powered by human force, and whose quantity is not in any case exceeds two hundred and fifty (250) tons per year of material”. However, this definition has no legal implications.

According to this, small mining includes the realization of the activity in a rudimentary way which means that it is a type of artisanal mining which has been defined as the set of mining activities that develop in a rudimentary, anti-technical and instinctive, i.e. without the use of conventional techniques of geological exploration, drilling, proven reserves, or engineering studies. However, it should be clarified that artisanal mining can also be carried out at the medium and large scale (Guiza, 2013).

4.3.1.2 Underground mining

Underground mines are those that are accessed through galleries or tunnels, or vertical wells. Underground mining can be sub-divided into soft rock mining and hard rock mining. It is called “soft rock” when it does not require the use of explosives in the extraction process. Hard rock mining uses explosives as a method of extraction. Most of hard rock mines extraction is done by drilling and blasting.

First, holes are drilled with compressed air or hydraulic drills. Thereafter, drill holes are inserted into the holes and exploded, causing the rock to fracture and be extracted. Then, special loading machines, often with diesel engines and tires, are used to load the exploded rock, to carry it and later to be transported to the processing plant. In order to access the ore deposit, a network of access galleries, which is usually spread over the waste rock surrounding the deposit, is to be excavated (Salvarore & La Barbera, 2005).

4.3.2 Mineralization

Suárez gold deposits offer ore composed mainly of chalcopyrite, pyrite sphalerite, galena, pyrrhotite, hematite and ilmenite, due to the large amount of sulphides within the rock crack. It could first be classified as a post-orogenic deposit of high sulphuration. In between the gangue, the quartz is the main mineral (Lopez, 2006).

4.3.3 Stages and gold mining activities

4.3.3.1 Prospecting and exploration

Exploration activities allow the proper planning of exploitation in order to obtain greater productive efficiency and avoid the high waste of the mineral. This is primarily due to lack of knowledge of the characteristics of the deposit. Geological prospecting aims to locate anomalies due to mineral deposits.

4.3.3.2 Exploitation

As far as the exploitation is concerned, the diversity of the geological environments where the country's gold reserves are found, generate different ore exploitation systems and the types of mining vary according to several factors. These include the following: depth, shape and inclination of the deposits, the distribution of mineral laws, the geo-mechanical characteristics of the rocks and the mineral itself, the physical and cultural conditions of the area, the magnitude of the operation, and the machinery used. In the case of gold mining, the exploitation systems used are underground and open pit.

The exploitation stage includes planning and assembly, development, benefit and transformation and closure.

- Planning and assembly: It comprises the set of activities that go from the organization, design, establishment of infrastructure and equipment to advance the exploitation of the mineral. In the case of small and medium Colombian mining for the alluvial and underground system this stage is not fulfilled in the vast majority of the gold regions. The starting methods/tools used for this type of mining are usually hand made. The drilling is done manually with smaller tools (pick, shovels, holes) or mechanized using mechanical or pneumatic drills, hydraulic excavator, as is the case in the departments of Antioquia, Tolima and Santander.

- Mineral benefit and transformation: In the case of metallic minerals, the objective of this stage is to eliminate gangue material, to increase the tenor or metallic content in the form of concentrates of more easy handling and greater added value. In Colombia, the benefit of the mineral is carried out in the immediate areas to the exploitation or in the municipal head towns and consists of the following unit operations:

    - Size classification: The separation of rock into fractions by size is done visually and manually by the small mining using sieves, meshes or angeos, hydroclassifier or cyclones in the medium mining.
    - Crushing: In this operation, the size of the material is reduced to suit grinding. Jaw and jaw crushers are used or manually with a baton or saddle.
    - Grinding: It intends to reduce the ore to reach a degree of release to be recovered gravimetrically or by amalgamation. The process is carried out in Californian, pistons, balls or bars mills.
    - Concentration: It can be carried out gravimetrically (table, pestle, gutter, dense media) by physical and chemical methods (flotation, agglomeration, flocculation), or by magnetic and electrostatic methods. The alluvial exploitation of small mining is carried out using rafts, elevators, monitors, gutter, and concentration table. Medium-sized enterprises use a hydraulic trap or centrifugal concentrator of the Knelson type (Ministerio del Medio Ambiente, 2002).
    - Amalgamation: It is a process of concentration based on the preferential adherence of gold by mercury, in the presence of water and air. If the amalgamation process is applied to the whole ore, mercury losses are generated in the tailings (70%), with a gold recovery of 50%. Amalgamation tailings, with a content close to 70%

of gold of the ore, are stored in the plant where it is recovered to around 90% of the residual gold from the tailings (Valderrama et al., 2012).

- Closure: Once the productive stage or the exhaustion of the mine's reserves is finished, it comes to a closure. It includes the dismantling and removal of facilities, machinery and equipment. The various activities of recovery and morphological rehabilitation of the areas are applied, according to the mining-environmental plan and the intended use post mining, all with the respective control and supervision. The stage of closure, in Colombia, for small and medium mining is rarely performed (Ministerio del Medio Ambiente, 2002).

According to the above, the processes that comprise the activities of benefit of gold, demand high consumption of energy, water, toxic substances like mercury. Besides, it also affects the health of the workers (Caicedo, 2014).

4.3.4 Hazardous materials in gold mining

In all the mining operations, heavy metals are used as inputs that cause serious environmental damages and human health without proper management. Among these the most important are cyanide and mercury. The environmental management plans should also include measures to prevent severe impacts of cyanide and mercury spills on the environment.

4.3.4.1 Cyanide

Cyanide is acutely toxic to humans. Toxicological studies have indicated that short-term exposure to high levels of cyanide causes rapid breathing, tremors and other neurological effects; while long-term exposure causes weight loss, thyroid effects, nerve damage and death (Dash et al., 2008). Skin contact with liquids containing cyanide may produce irritation and sores. Clearly, heavy metal and cyanide pollution of the environment is of great concern due to their health risk to humans and threats to the ecosystem (Acheampong et al., 2010).

4.3.4.2 Mercury

Mercury is a metal that exists naturally in the environment and has several chemical forms (Table 1). The metallic mercury is a liquid, odorless, bright white-silver color. When heated, it becomes an odorless and colorless gas. Mercury is combined with other elements, for example chlorine, sulfur or oxygen to form inorganic mercury compounds or "salts," which are generally white powders or crystals. Mercury also combines with carbon to form organic mercury compounds.

The most common, methylmercury, is produced mainly by the microscopic organisms in soil and water. The greater the amount of mercury in the environment, the greater the amount of methylmercury these microorganisms produce. Metallic mercury is used in the production of chlorine gas and caustic soda and is also used in thermometers, dental fillers and batteries. Mercury salts are used in creams to lighten the skin and in antiseptic creams and ointments.

Table 1. Mercury species in the environment

Name	Chemical formula
Metal mercury	
Mercury	Hg
Mercury amalgams with gold, silver, copper and zinc	Au - Hg, Ag - Hg, Cu - Hg, Zn - Hg
Inorganic mercury	
Mercury chloride	Cl_2Hg_2
Mercuric chloride	Cl_2Hg
Mercuric sulphide (cinnabar)	SHg
Mercuric nitrate	$Hg(NO_3)_2$
Mercuric oxide	HgO
Mercuric Bromide	$HgBr_2$
Organic mercury	
Ethyl mercury	C_2H_5Hg
Methyl mercury	CH_3Hg
Dimethyl mercury	$(CH_3)_2Hg$
Methyl mercury chloride	CH_3HgCl
Methyl mercury	C_5H_5Hg

Source: Adapted from Lopez (2006)

4.3.5 Physical properties of mercury

Mercury is a bright silver metal, which at room temperature is in a liquid state: its melting temperature is -38.9 °C and its boiling point is 357.3 °C. Its specific weight is 13.6 g/cm^3 (0 °C). Metallic mercury, due to its high vapor pressure 163×10^{-3} Pa, evaporates easily at ambient temperature: at 20 °C, its concentration in the air can reach up to 0.014 g/m^3, at 100 °C up to 2.4 g/m^3.

Mercury vapor is generally referred to when elemental mercury is present in the atmosphere or of metallic mercury when in its liquid form. A large number of metals, and mostly gold and silver, form alloys with metallic mercury, which are called amalgams. This property makes it attractive for gold recovery in small gold mining. The solubility of mercury in water depends strongly on the temperature (Montenegro & Arturo, 2002).

4.3.6 Mercury toxicology

Mercury is a heavy metal and its presence in the human body is toxic from certain critical levels that depend fundamentally on a knowledge of dose-effect and dose-response relationships. It also depends on the knowledge of variations in exposure, absorption, metabolism and excretion in any given situation. Therefore, whenever there is talk of mercury in relation to Public Health (general population) and Occupational Health (workers with exposure to mercury), it is necessary to take into account the following aspects:

- Underground level of the particular area under study. For example, the most important mercury deposits are located almost exclusively in the Mediterranean, Himalayan and

the Pacific belt. Besides, the geographic, demographic, geological, climatic and socioeconomic characteristics should also be considered.

- Mercury possesses a great variety of physical and chemical states (elemental/inorganic/organic), with toxic properties intrinsic to each of them. Toxicologically speaking, organic mercury and primarily methylmercury have a much higher toxicity than elemental mercury and inorganic compounds.

- Consider a number of factors that have a decisive influence on the toxicity of mercury, for example, its physicochemical status, pathways of penetration into the body, individual metabolism, excretion rates and synergistic and/or antagonistic effects of other agents (Español, 2001).

4.3.7 Routes of entry and effects in the organism

4.3.7.1 Inhalation

It is the main route of entry to the body for elemental mercury. This occurs because it is easily vaporized at room temperature and is absorbed by the lungs and then distributed through the blood. Approximately 1% of the absorbed metal is stored in the mammalian brain, where it can remain for a long time, while the remaining mercury is distributed in the liver and kidney where it is secreted through bile and urine.

Inhalation of mercury vapors is associated with systematic toxicity in humans and animals. Because of its high diffusibility and liposolubility, which facilitates its distribution and movement through the body, about 80% of the mercury vapor is absorbed by the lungs and rapidly reaches the bloodstream.

4.3.7.2 Ingestion

The danger of mercury intake to the body is usually in the form of methyl mercury through foods that contains it. Methyl mercury is one of the most dangerous metals for health. Various incidents of human exposure to methyl mercury have shown to cause neurotoxic effects. The effects of methyl mercury vary, as discussed above, depending on dose, response, and associated symptoms.

The groups most vulnerable to exposure to methyl mercury are children, the fetus and the mother. Methyl mercury passes through the blood, brain barrier and reaches the central nervous system. Clinical symptoms of methyl mercury poisoning in children and adults include: paraesthesia (limbs and sleeping surroundings), ataxia (difficulty walking), dysarthria (difficulty in speaking), visual field impairment, deafness, tremors, intellectual impairment, and in some cases, motor paralysis (Comisión nacional del medio ambiente, 2008).

4.3.8 Sludge retention in mining production units

4.3.8.1 Sedimentation

Sedimentation is the gravitational removal of the suspended particles present in the water. These particles must have a specific gravity greater than the fluid. Removal of suspended particles in water can be achieved by sedimentation or filtration. Hence, both processes are considered complementary. Sedimentation removes denser particles while filtration removes particles which have a density very close to the density of water or have been re-suspended and therefore could not be removed in the previous process.

Sedimentation is, in essence, a purely physical phenomenon and constitutes one of the processes used in the treatment of water to achieve clarification. It is exclusively related to the dropping/settling properties of the particles present in water. When sedimentation occurs from a suspension of particles, the final result will always be a clarified fluid and a more concentrated suspension (Centro panamericano de ingeniería sanitaria y ciencias del ambiente, 2004).

4.3.8.2 Tailing dams management

The residual discharge of the mining MPU in Suárez usually flow through a series of "tanks" or sedimentation dams where the sands are deposited such as the one shown in Figure 3. After these dams, sludge and wastewater is taken to a final sedimentation lagoon (Figure 4), where the water is discharged without any treatment to the receiving body.

Figure 3. Tailing dams in San Juan mining production unit.

Figure 4. Sedimentation pond of San Juan mining production unit.

As the sludge from the dams and the ponds accumulate to a maximum level, they are emptied manually. This material, often called tailings, is stacked near the mills. It remains exposed to the environment for a long time as shown in Figure 5, and it is subsequently processed again in the mills in order to recover pieces of gold. Other MPU have facilities for a cyanidation process to recover the gold.

Figure 5. Sludge storage area from a mining production unit in Buenos Aires, Cauca

4.3.8.3 Location and description of San Juan mining production unit

San Juan MPU has an area of approximately 64 m^2, and the activities take places at the back of a carwash service. It is located in the urban area of the Municipality of Suárez, at a distance of approximately 60 m, from the main park on the road to the south. The area of influence presents a slightly undulating topography with free flood zones and favorable drainage of the rainwater. Residential, commercial and recreational areas are located around 60 m from the MPU, and the soil type is mainly clay. The Cauca river is located around 100 m distance from San Juan (Figure 6).

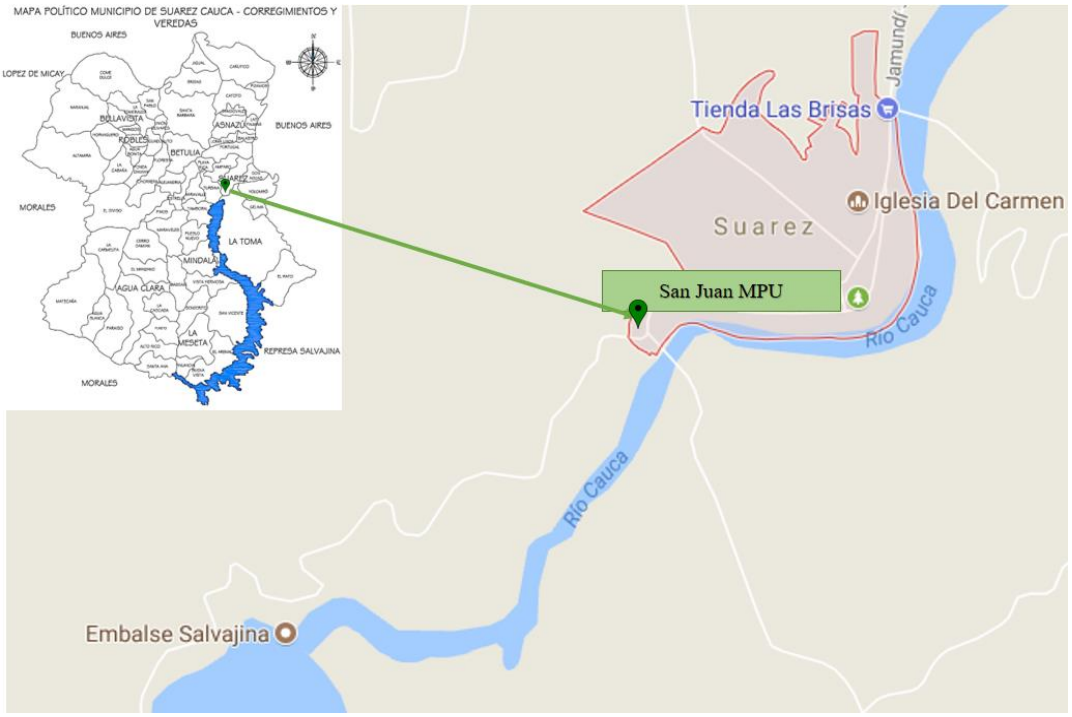

Figure 6. Cauca River and San Juan mining production unit location. Suarez political map.
Source: Adapted from Alcaldia Municipal de Suarez (2017); Google (2017)

The previous figure shows the receiving water body of Zanjón Grande stream where the wastewater from San Juan MPU is being discharged. The production unit has three tailing dams in series and a sedimentation pond where the sludge is retained inefficiently according to the high solids concentrations in the wastewater discharge at plain sight. All these characteristics make it a plant that offers great advantages for the miner in the acquisition of mining supplies, easy access for the discharge and loading of ores from the different mines in the region. The law 1658, June 2013 (Colombia) prohibits new plants for the benefit of precious metals and this law controls the existing minerals that is made. The location of new gold beneficiation plants that use and burn amalgam of mercury in residential, commercial, institutional or recreational areas is prohibited. Figure 7 shows San Juan MPU.

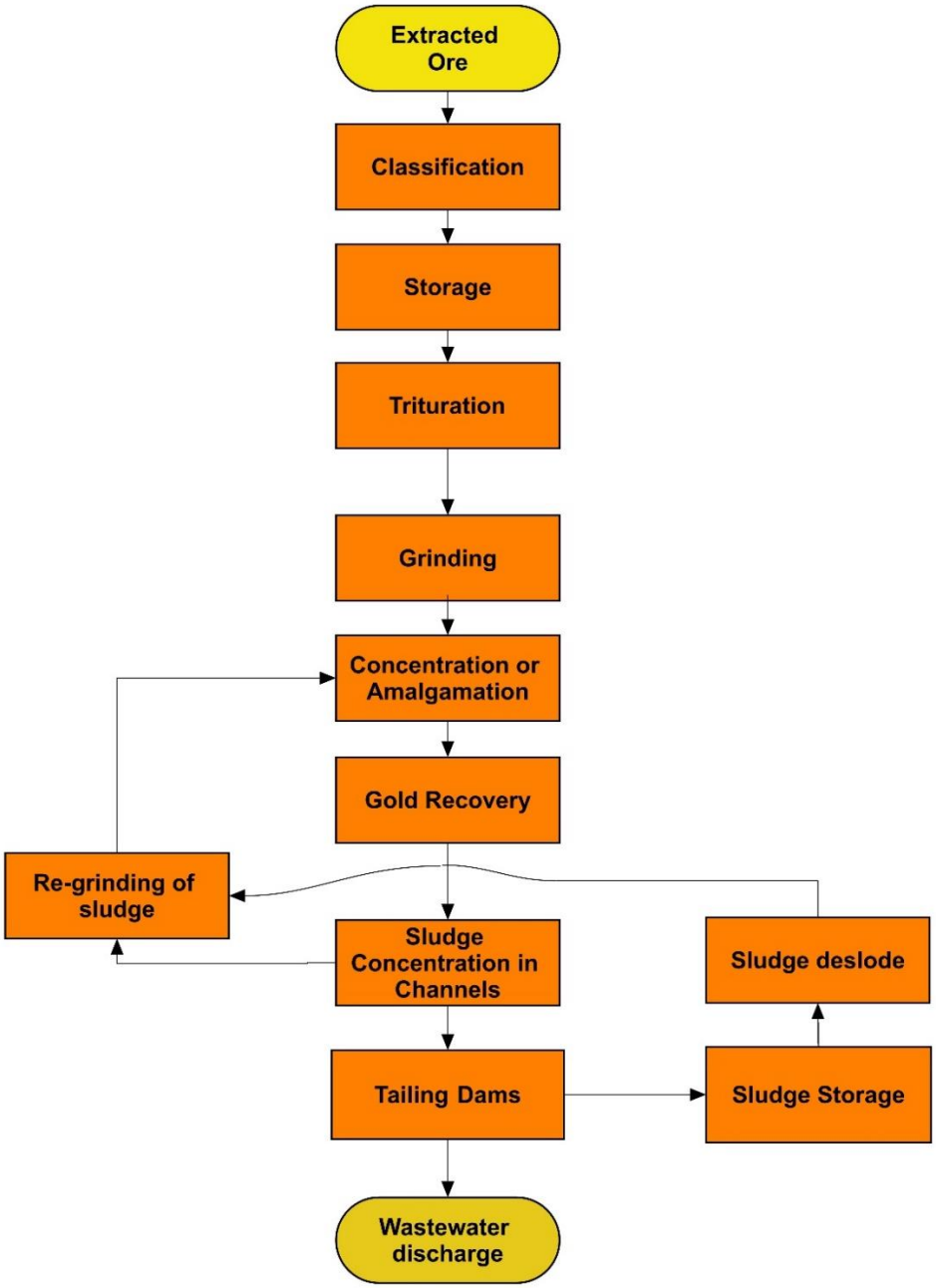

Figure 7. General process flow diagram in San Juan mining production unit

Currently, the plant has 22 barrels or amalgamator drums. It is also in under expansion plans in order to meet the high demand of ore which is extracted from the different mines in the region. The extraction of materials is done by pneumatic hammers of 90 lb that are driven by an air compressor, allowing the miner to have a greater yield and larger amounts of material. Subsequently, this material is directed towards the crushing plants for the benefit of gold by the processes illustrated in Figure 7.

Usually, deposits of gold with very small particles need mercury for a good recovery of the same, in the open circuits. The amalgamation process is done in barrels or drums as shown in Figure 8, as grinding of the rocky mineral, the mineral along with the water plus mercury and other products. Other substances, such as lemon, in a state of decomposition and detergents serve as degreasers, so fine gold does not get washed away by the water streams.

Cane molasses is commonly used as a cleaner and reducer of mercury losses during grinding. In a span of 1 to 3 h, the barrels are opened to perform the washing step, where water plus mineral ground with mercury is poured into a conditioning tank, and gold is trapped by the mercury in an aqueous pulp to form a highly viscous substance and bright white color, called the amalgam. In order to recover the gold trapped in the amalgam of mercury, a fine cloth is used, which is strongly squeezed for the purpose of separating gold from mercury.

Figure 8. Configuration of drums in San Juan mining production unit

In addition, several re-grinding steps (×4) are repeated with the resulting sludge. This step varies according to the quantities of gold obtained in the first washing of the ground mineral. The sands or sludge with very fine fractions of mercury pass through a gutter that goes directly to the tailing dams. Some of these fractions are recovered in the tailing dams and others are carried by the wastewater stream to the Zanjón Grande water stream. The tailing dams along the main units used in San Juan MPU is illustrated in Figure 9.

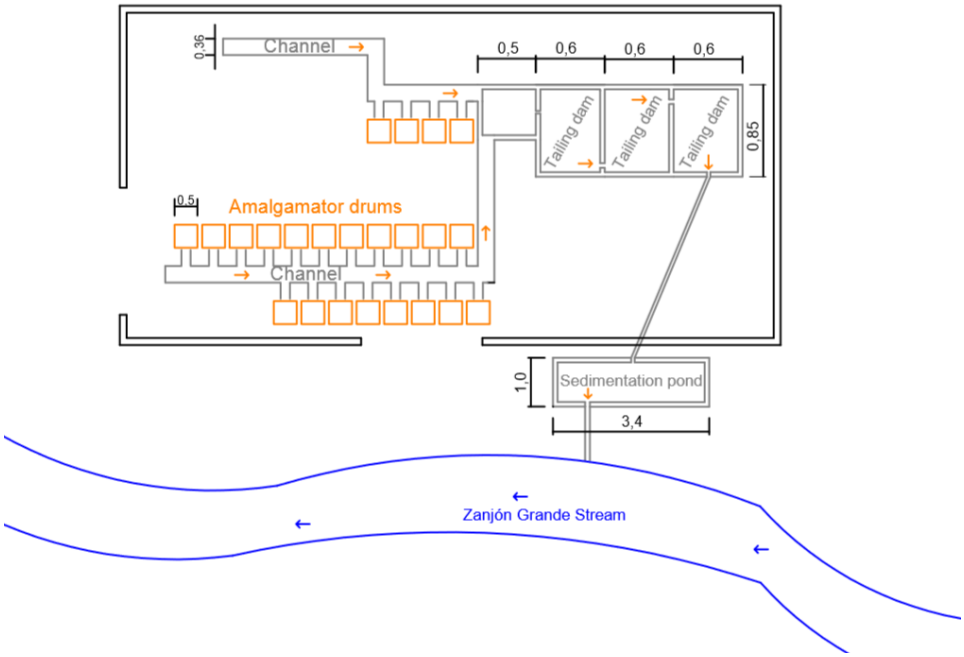

Figure 9. Layout of San Juan mining production unit

4.4 Metal adsorption onto agricultural residues

Activated carbon has been studied as a heavy metal removal alternative for more than three decades. In addition to its adsorption capacity, Smith and Wiechers (1981) stated that this material provides an effective barrier against the passage of toxic metals, particularly cadmium, silver, lead, mercury and arsenic. This technology has several mechanisms by which active carbon treatment may effect trace metal removal, including chemisorption and precipitation.

The importance of adsorption in the removal of heavy metals has directed the attention to study other adsorbent sources that may offer better results with less economic limitations. Waste slurry (Srivastava et al., 1989), oxides (Rauf et al., 1989), live biomass (Veglio & Beolchini, 1997) and agricultural waste (Gupta & Ali, 2004) are some of the materials that have been studied for heavy metal removal (Wan Ngah & Hanafiah, 2008). To generate adsorbent materials out of waste, the carbonaceous residues present in agriculture is a topic of growing interest for small-scale companies that need to comply with strict effluent standards and keep the treatment costs under reasonable prices. Selecting the waste residues implies advantages because of their low cost and the abundance of these materials in nature (Vargas et al., 2008).

According to Paraskeva et al. (2008), traditionally, typical precursors for activated carbon production were coal, peat and lignite. However, in recent years, there has been a growing interest in the production of activated carbons from agricultural by-products and residual wastes. Agricultural by-products, such as shells, kernels, fruit stones, fruit seeds, hulls and husks are produced during the harvesting and processing of commercial crops. Depending on the crop, some of these by-products have found uses as feedstock for animals, fillers in plasterboard, additives in paper making, as a material resource for combustion and co-generation processes, etc.
Despite these applications, there is a large quantity of such by-products produced annually that requires disposal and thus poses an environmental problem. Agricultural by-products are rich

sources of cellulosic material with an average composition of 40-50 % cellulose, 20-30 % hemi-cellulose, 20-25 % lignin and 1-5 % ash, which makes them an attractive source for activated carbon production (Paraskeva et al., 2008).Using agricultural residues for the adsorption of heavy metals has been studied thoroughly. Acheampong (2013) summarized studies on biosorption using different agricultural and plant bio sorbents to remove Cu^{+2}, Cr^{+4}, Pb^{+2}, Zn^{+2}, Cd^{+2}, As^{+3}, As^{+5}, Co^{+2}, Ni^{+2}, and Fe^{+3}. Jain et al. (2016) evidenced a classification of plant based bio sorbents for heavy metals removal (Table 2) Table 2.

Despite the diverse waste agriculture materials studied by the different authors, mercury is only present a few times in relation with the rest of studies in this literature data. This may suggest that few attention has been paid to agricultural and plant bio sorbents for mercury removal (Acheampong, 2013; Jain et al., 2016). On the other hand, Yu et al. (2016), established a systematic review of the literature from 2011 to 2014 on mercury removal by adsorption with modified activated carbon, nanotubes, iron oxides, bacterial species, biomass and others. *Phoenix dactylifera* biomass, *Phragmites karka* and rice residues have been studied in the last years regarding mercury sorption showing important results (Rajamohan et al., 2014; Raza et al., 2015; Song et al., 2015).

Table 2. Classification of plant based biosorbents for heavy metals removal

Biomass source	Species	Metal	pH	Adsorption capacity (mg/g)	References
Seed	Papaya	Cu(II)	6	212.7	Hadi et al. (2011)
	Polyalthia longifolia	Cd(II)	6	20.7	Rao and Rehman (2012)
Leaf	Pine	As(V)	4	3.3	Shafique et al. (2012)
	Moringa oleifera	Ni(II)	6	163.9	Reddy et al. (2012)
Root	*Eichhornia crassipes*	Cu(II)	5-6	32.5	Li et al. (2013a, 2013b)
	Oil palm	Pb(II)	7	150	Bhaumik et al. (2014)
Bark	*Acacia leucocephala*	Cd(II)	5	167.7	Munagapati et al. (2010)
	Eucalyptus	Cr(VI)	2	45	Sarin and Pant (2006)
Peel	Casava	Pb(II)	8	5.80	Owamah (2014)
	Pomegranate carbon	Fe(II)	6	18.52	Moghadam et al. (2013)
Stalk	Corn (acrylonitrile modified)	Cd(II)	7	12.73	Zheng et al. (2010a, 2010b)
	Sunflower	Pb(II)	5	182	Jalali and Aboulghazi (2013)
Husk	Coffee	Zn(II)	4	5.6	Oliveira et al. (2008)
	Rice	Cr(III)	5-6	30	Sobhanardakani et al. (2013)
Fiber	Coconut fiber (modified with pristine)	Hg(II)	5	8	Velazquez-Jimenez et al. (2013)
	Sugarcane bagasse	Hg(II)	4	35.71	Khoramzadeh et al. (2013)
Shell	Walnut shells (modified with $ZnCl_2$)	Hg(II)	5	151.5	Zabihi et al. (2009)
	Annona squamosa	Pb(II)	5	90.93	Isaac and Sivakumar (2013)

Source. Adapted from Jain et al. (2016)

This review shows that, only few studies have carried out mercury removal studies using agricultural waste materials. Thus, further research is required in this field, especially in developing countries where small scale companies can use low cost technologies for meeting their effluent quality requirements.

4.4.1 Characterization methods of activated carbon for adsorption of mercury

4.4.1.1 Pore size

Different techniques have been used to determine the pore sizes of the adsorbent material. Information about the structure of activated carbons can be obtained by the adsorption characteristics of different adsorbates, such as methylene blue and iodine. Adsorption experiments of these molecules are easy and habitually done to characterize activated carbons with the purpose of obtaining information on the adsorption capacity of the materials (Nunes & Guerreiro, 2011). Blue methylene index is used when carbon have a mesoporous structure. The presence of mesopores on methylene blue adsorption can be understood from information on the adsorption sites occupied by methylene blue molecules (Lei et al., 2006). To determine the methylene blue number for the Langmuir model, a q_{eq} plot is made as a function of C_e. The Langmuir parameters (q_{max} and K_L) are found by a least square regression (Nunes and Guerreiro, 2011).

The iodine number test is a measure of the micropore content of the activated carbon (0-20 Å, or up to 2 nm) by adsorption of iodine from solution. It is equivalent to the surface area of carbon between 900 and 1100 m^2/g (Elliott et al., 1989). This test method covers the determination of the relative activation level of unused or reactivated carbons by adsorption of iodine from aqueous solution. The amount of iodine absorbed (in milligrams) by 1 g of carbon using the studied test conditions is called the iodine number. The iodine number is a relative indicator of the porosity of activated carbon. It does not necessarily provide a measure of the carbon's ability to absorb other species. It varies with changes in carbon raw material, processing conditions, and pore volume distribution. The presence of adsorbed volatiles, sulfur, and water extractables may affect the measured iodine number of an activated carbon (ASTM, 2006). Acorn shell and bagasse have been characterized at different activation temperatures and activating agents through the iodine number in terms of pore size (Saka, 2012; Juang et al., 2002). Studies on mercury adsorption revealed that coconut buttons isotherm indicates the micro-mesoporous structure of the carbon (Anirudhan and Sreekumari, 2011) and coffee waste adsorption on KOH as activating agent was related to the meso or macroporus characteristics (Giraldo and Moreno, 2012).

4.4.1.2 Surface area and porosity

Surface area and pore volume are two very important physical characteristics when studying a precursor material for adsorption. Surface area is measured by the Brunauer-Emmett-Teller (BET) method (Brunauer et al., 1938), using a nitrogen multilayer adsorption measured at different pressures at the temperature of liquid nitrogen (77 K). The surface area according to BET is then determined by the product of the cross-sectional area of the nitrogen molecule, of the Avogadro's number and of the specific monolayer capacity of nitrogen, which is obtained by an equation proposed by BET with further modifications. For the pore volume

determination, the procedure more commonly used also uses nitrogen adsorption isotherm data (Nunes and Guerreiro, 2011). For the calculation of total volume, nitrogen adsorption isotherms are used with the Dubinin-Radushkevich equation (Castro et al., 2000).

Different surface areas and pore volumes can be obtained depending on the activation conditions. The physical properties of the activated carbon prepared at different impregnation ratios is presented in Table 3. As shown in the literature, the surface areas and total pore volumes of the $ZnCl_2$-activated and KOH-activated carbons increases from ACZ2 to ACZ3 at 700˚C and ACK2 to ACK3 at the same temperature (Giraldo & Moreno, 2012).

Nguyen et al. (2013) stated that the particle size of agriculture waste by-products can influence their adsorption capacities due to the change in total surface area which is necessary for metal adsorption. The lower particle size provides more active biosorption sites on the surface of adsorbent for metal ions for powder adsorbents (Jain et al., 2016). Rajamohan et al. (2014) also reported that smaller particle size always provides more sorption sites through increased surface area and hence, higher metal uptake.

Table 3. Characterization of synthetized activated carbons

Sample	S_{BET} (m^2/g)	V_o (cm^3/g)	V_{meso} (cm^3/g)	V_t (cm^3/g)	V_o/V_t
ACZ2	745	0.61	0.17	0.80	0.76
ACZ3	823	0.68	0.22	0.92	0.74
ACK2	934	0.78	0.28	1.02	0.77
ACK3	1058	0.85	0.34	1.23	0.69

S_{BET} = Superficial area; V_o = Micropore volume; V_{meso} = Mesopore volume; V_t = Total pore volume; ACZ2 = Carbon impregnated into $ZnCl_2$ at a 2:1 chemical to sorbent mass ratio; ACZ3 = Carbon impregnated into $ZnCl_2$ at a 3:1 chemical to sorbent mass ratio; ACK2 = Carbon impregnated into KOH at a 2:1 chemical to sorbent mass ratio; ACK3 = Carbon impregnated into KOH at a 3:1 chemical to sorbent mass ratio.
Source. Adapted from Giraldo & Moreno (2012)

4.4.1.3 Sorption capacity

Batch tests can be carried out to determine the adsorption capacity by measuring the weight of the sorbent material and the adsorbate concentration. To maintain high adsorption capacity and low precipitation effects, Rahman & Islam (2009) suggest to adjust the pH of the solutions with 0.1 M NaOH or 0.1 M H_2SO_4. After equilibration, the suspension of the adsorbent is separated from the solution by filtration. The concentration of heavy metal ions remaining in solution can be measured and the results of these studies are used to obtain the optimum conditions for maximum heavy metals removal from aqueous the solution. The percentage of heavy metal removal is calculated using the following equation:

$$Removal\ capacity\ (\%) = \frac{C_o - C_e}{C_o} * 100 \quad (1)$$

Where C_o is the initial concentration (mg l^{-1}) of the test solution and C_e is the equilibrium concentration (mg l^{-1}) of the test solution. The amount of metal sorbed per weight of adsorbent used is calculated using the following equation:

$$q_e(mg/g) = \frac{(C_o - C_e) * V}{m} \quad (2)$$

Where q_e is the equilibrium adsorption capacity (mg/g), C_o is the initial concentration (mg l^{-1}) of the metal ions in solution, C_e is the equilibrium concentration (mg l^{-1}) of metal ions in the solution, V is the volume of aqueous solution (mL) and m is the dry weight of the adsorbent (g/L). Besides, models are used to establish and analyse the relation between a solute adsorbed on a sorbent´s surface. The Freundlich equation is an empirical equation based on the sorption on heterogeneous surface, described by the following equation (Freundlich, 1906):

$$q_e = K_F C_e^{\frac{1}{n}} \quad (3)$$

where K_F and $1/n$ are the Freundlich constants related to the adsorption capacity and the adsorption intensity, respectively.The Freundlich equilibrium constants can be evaluated from the intercept and the slope, respectively, of the linear plot of ln q_e versus ln C_e. The Freundlich equation can be linearized in logarithmic form for the determination of the Freundlich constants as shown below:

$$log q_e = log K_F + \frac{1}{n} log C_e \quad (4)$$

4.4.1.4 Apparent (bulk) density

According to the Standard test method D 2854-96, the apparent (bulk) density can be determined by the ratio of the mass to a given volume. Apparent density (bulk density) is determined on a granular sample by measuring the volume occupied by a free fall from a vibrating feeder into an appropriately sized graduated cylinder and determining the mass of the known volume. Other packing procedures can result in different apparent densities (ASTM, 2004).

4.4.2 Activation and modification of biosorbents

Different methods have been used for enhancing the adsorption potential/capacity of the materials. According to Hadi et al. (2015a) the porous structure of the activated carbons can be manipulated by altering the activation parameters, such as the type of activation (physical and/or chemical), activating agent, pyrolysis/activation temperature, impregnation ratio, among others. Usually, the physical and chemical activation techniques are the most common approaches to achieve a high internal porosity and proper pore size.

4.4.2.1 Physical activation

Physical activation generally requires two processes, carbonization and activation. The first one involves carbonization of the material, at high temperatures under an inert atmosphere (N_2, argon). During this stage, the material decomposes into three fractions: chars, tars and gases. During the production of activated carbon, the heating is usually done at medium temperatures and slow heating rates, in order to maximize the fraction of char (Paraskeva et al., 2008). In the second process, the char is subsequently activated at elevated temperatures, usually above 700 °C, under a partial oxidizing atmosphere.

The aim of the activation stage is to produce a highly porous structure from the weakly-developed porous char. The activation process entails the reaction of the oxidizing agent with

tar decomposition products blocking the pores to volatilize carbon oxide, which in turn opens the closed pores, widens the existing small pores and forms new pores (Hadi et al., 2015b).

Hadi et al. (2015a) established a summary of a few studies on the production of chars or activated carbons via pyrolysis or physical activation methods. Table 4 shows the comparison of the textural properties of the activated carbons/chars produced by physical treatment techniques. The surface area, pore size and micropore fractions are inseparable properties that must be concurrently optimized for better adsorption capacities. As seen from Table 4, a lot of literatures are confined to reporting only the surface area, while few researchers have comprehensively investigated the porous structure of the produced activated carbons.

4.4.2.2 Chemical activation

In chemical activation, a chemical agent is used prior to activation. The commonly used chemicals include H_2SO_4, H_3PO_4, KOH, NaOH and $ZnCl_2$. The processes involve impregnation of the material with the chosen chemical in solid or liquid form. Such impregnation can take up to 24 h depending on the chemical used, the precursor and the subsequent processes. Apart from temperature and retention time, the ratio of chemical to precursor is of great importance. A washing step of the material is also involved, either with distilled water or a mild acid, to remove the residual chemicals from the material (Paraskeva et al., 2008). It has been found that chemical activation using various activating agents yields more superior adsorbents with high specific surface area than physical activation methods (Hadi, et al., 2015a). However, while proposing a solution for a small, medium or large industry, the economic and ecological perspective must be considered during the activation process because physical and chemical activation have a high - energy demand and a considerable amount of chemical agents involved.

Table 4. Textural properties of the chars/activated carbons produced by physical treatment or carbonization

Carbonization conditions			**Activation conditions**			**S_{BET}**	**v_t**	**V_{micro}**	**D_p**	**pH**
T (°C)	**Time (h)**	**A. atm**	**T (°C)**	**Time (h)**	**A. atm**	**(m^2/g)**	**(cm^3/g)**	**(cm^3/g)**	**(nm)**	
750	0.5	N_2				34.3				
750	0.5	CO_2				60.7				
300	1	N_2	850	0.67	Steam	130				
300	1	N_2	850	0.67	Steam	280	0.286	0.038	1.178	
600	6	Air				22			50-60	
600	6	Steam				70			50-60	
800	4	CO_2				97		0.9		
400	4					91		0.7		
200	2	N_2	700	5						
500	3	N_2							45.4	
650	0.5	N_2				60	0.09	0.04		
300	1	N_2				51	0.058			
500	0.5	N_2				18				6.0
300						4				
450	1.5	N_2				60	0.1			
400	2	N_2				23.7				
450	1	N_2	275	4	Air	105		0.04		7.7
450	1	Inert								6.3

T = Temperature; A. atm = Activating atmosphere; S_{BET} = Superficial area according to the Brunauer-Emmett-Teller (BET) theory; V_{micro} = Micropore volume; D_p = Particle diameter; V_t = Total pore volume
Source. Adapted from Hadi et al. (2015b)

4.4.3 Physical and chemical adsorption

Adsorption is not only achieved by physical mechanism. Rahman and Islam (2009) stated that the metal uptake depends on the active sites of the adsorbent as well as on the nature of the metal ions in solution. Biosorption could be performed by ion exchange mechanism or by hydrogen bonding due to the -COOH groups and -OH groups present in most of adsorbents. Jain et al. (2016) stated that the mechanisms involved in biosorption: physiosorption, chemisorption, micro-precipitation, ion exchange and chelation. The adsorption mechanism for Hg species removal is still not well explained. Computer simulation of the interactions between the adsorbents and the Hg species still needs to be investigated deeply (Yu et al., 2016). It is important to understand the physical adsorption and focus on the chemical adsorption performed by the functional groups present on the adsorbents.

4.4.3.1 Physical adsorption

The physical adsorption or physisorption occurs because of the attraction forces that exist between the sorbent and the adsorbate. These forces are called the van der Waal's forces. This mechanism can be reversed when pressure is decreased or temperature is increased. In this case, there is no formation of compounds and no activation energy is required.

4.4.3.2 Chemical adsorption

Chemisorption explains the affinity of mercury and surface functional groups on the activated carbon. Weak van der Waal's interaction has been proven inefficient in promoting mercury adsorption; however, surface functional groups revealed that, especially the oxygen functional groups on the carbon surface were observed to be the active sites for elemental mercury adsorption. Mercury is adsorbed onto the charged functional group. In the presence of water, certain functional groups tend to lose its proton at aqueous condition and become ionized. The unbalanced charge is expected to have a strong interaction/affinity for mercury, where significant electron transfer might occur (Sun et al., 2011).

The surface functional groups and the textural properties of the adsorbents can be controlled by the activating agent type and the pyrolysis and activation conditions, whereas the surface charge of the activated carbons can be well-manipulated by altering the pH of the adsorption system. Most of the studies consider only one of these properties (textural or surface properties), while it is necessary to take both of these crucial factors into consideration concurrently (Hadi et al., 2015a). Although the functional groups of the activated carbons have been considered to be crucial in chemisorption, the effect of oxygen-containing functional groups on mercury adsorption capacity and rate has not been comprehensively examined. Despite an inverse relationship between the percentage of oxygen functional groups and the total surface area of the adsorbent material, both of which are regarded positive factors for mercury adsorption capacity, no trade-off graph between these two crucial parameters has been provided to optimize the efficiency of adsorption (Hadi et al., 2015b).

4.4.4 Isothermal studies and kinetics

The biosorption equilibrium models are used to determine the maximum sequestration of metals at variable optimum parameters. An isotherm model describes the relationship between the

amount of metal adsorbed by the adsorbent and the metal concentration remaining in the solution (Jain et al., 2016). To analyze the adsorption data, four adsorption isotherms models can be used: Langmuir, Freundlich, Temkin and Dubinin-Radushkevich (D-R). Important information such as adsorption mechanism, favorability of the adsorption process and adsorbate-adsorbent affinity may be obtained (Inyinbor et al., 2016). It is very important to analyze the rate of metal sorption onto an agricultural residue, which is usually calculated from kinetic studies and it is a key factor when designing a column biosorption process. Kinetics models are used to investigate the biosorption mechanism and parameters involved in the experimental setup (Jain et al., 2016). Song et al. (2015) showed the different pseudo-first order, pseudo-second order and Elovich models along with the isotherm models (Table 5).

Table 5. Isotherm and kinetics equations for biosorption studies

Models		Equation	Parameters
Isotherm	Langmuir	$\frac{C_e}{q_e} = \frac{1}{q_{max}K_L} + \frac{C_e}{q_{max}}$ $R_L = 1/(1 + K_L C_o)$	C_e (mg l^{-1}): equilibrium adsorbate concentration In solution q_e (mg l^{-1}): equilibrium adsorption capacity q_{max} (mg l^{-1}): maximum adsorption capacity K_L (L/mg): Langmuir constant C_o (mg l^{-1}): Initial adsorbate concentration in solution R_L: Favorability of isotherm Unfavorable (R_L>1), Favorable (0<R_L), Irreversible (R_L=0)
	Freundlich	$logq_e = logK_F + \left(\frac{1}{n}\right) logC_e$	K_F (mg/g) $(L/g)^{1/n}$: Freundlich constant n: Heterogeneity factor 1/n<1: Favorable adsorption 1/n>1: Cooperative adsorption
	Temkin	$q_e = B_T lnK_T + B_T lnC_e$	K_T (L/g): Temkin adsorption potential B_T: Temkin constant
	Dubnin-Radushkevich (D-R)	$lnq_e = lnq_{max} - \beta_{\epsilon^2}$ $E_{DR} = \frac{1}{\sqrt{(2\beta)}}$	β ($mmol^2/J^2$): D-R constant ϵ (J/mol): Polanyi potential E_{DR} (Kj/mol): Magnitude of adsorption mechanism E_{DR} < 8: Physic nature 8<E_{DR}<16: Chemisorption E_{DR} > 16: Chemical ion-exchange
Kinetics	Pseudo-first model	$\log(q_e - q_t) = logq_e - \frac{k_1 t}{2.303}$	Q_t (mg/g): Amount of adsorbate concentration at time (t) k_1 (min^{-1}): Pseudo-first-order rate
	Pseudo-second order	$\frac{t}{q_t} = \frac{1}{k_2 q^2{}_e} + \frac{t}{q_e}$	k_2 (g/mg min): Pseudo-second-order rate
	Elovich	$q_t = (b)lnab + (b)lnt$	a (mg/g min): Initial sorption rate constant b (g/mg): Desorption constant

Source. Adapted from Song et al. (2015)

4.4.5 Desorption

To reuse and recover the sorbents is an important aspect for small scale companies. It is one of the critical aspect which determines the economic viability of the process. Thus, it is necessary to regenerate the biosorbents through as many cycles as possible without sacrificing their adsorption performance (Song et al., 2015). According to Asasian and Keghazchi (2015), mercury desorption has been studied and compared using HCl, HNO_3, KCl, KBr, and KI (2 M) as the regenerant. For the desorption experiments the sorbents after sorption are evaluated by considering the initial concentration, adsorbent dosage, initial pH, agitation speed and contact time. Usually, several steps of loading and regeneration cycles should be studied in order to understand the adsorption and desorption process.

4.4.6 Adsorption breakthrough curve

After performing batch tests, it is important to validate the biosorption data obtained under batch conditions. An evaluation of the sorption performance in a continuously operated column is necessary because the sorbent uptake capacity is more efficiently utilized than in a completely mixed system and also the contact time required to attain equilibrium is different under continuous column operating mode (Acheampong, 2013, Sekhar et al., 2003; Vilar et al., 2008). Breakthrough data obtained at a particular operating condition and fitted to adsorption models may enable appropriate design and scale up of the sorption column (Acheampong, 2013).

Different models have been developed to predict and understand the breakthrough curve. For column adsorption, determining the breakthrough curve is a very important issue because it provides the basic, but predominant information for the design of a full-scale adsorption system. Without the information of the breakthrough curve, one cannot determine a rational scale of a column adsorption for practical applications (Xu et al., 2013).

CHAPTER 5

Materials and methods

The methodology used in this study involved different activities organized in a logical and strategic order. In order to optimize the time and resources, some activities were carried out in parallel, while others were performed sequentially. Figure 10 shows the flow chart of adopted methodology and the sequence followed in the present research.

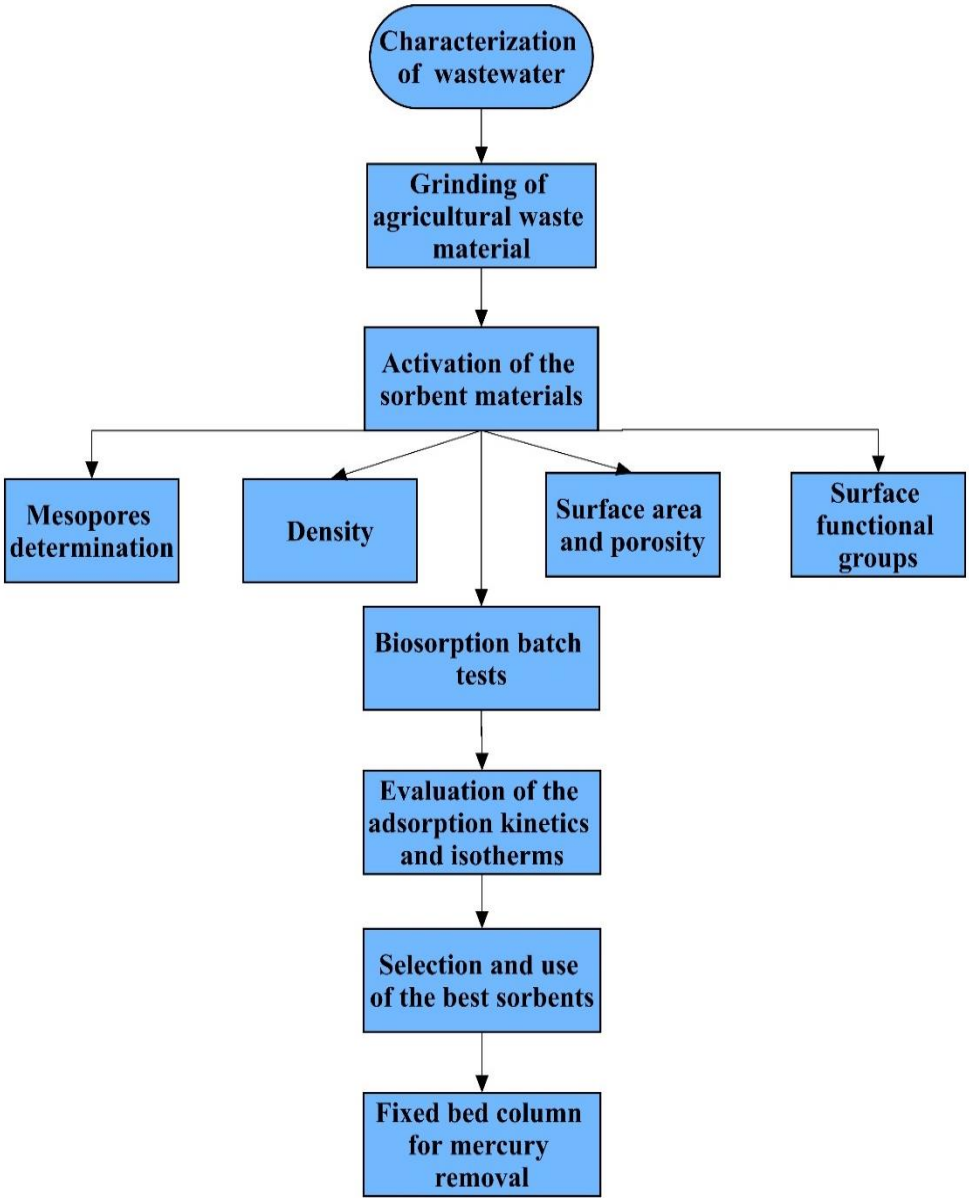

Figure 10. Flow chart of applied methodology

5.1 Comparatively analysis of Hg adsorption capacity on coconut (*Cocos nucifera*) shell and coffee (*Coffea sp.*) husk in batch tests

5.1.1 Physical-chemical characterization of the wastewater from San Juan mining production unit

For the characterization of the MPU, some procedures were defined in order to establish a clear methodology by considering the standard methods and the production process which generates the wastewater. The materials and equipment for the sampling campaign are listed below:

- Portable turbidimeter - Hach 2100®
- Portable Multiparameter - Hach HQ40d®
- Portable pH Meter - Scott 850®
- GPS - eTrex 10 Garmin®
- Graduated cylinder
- Nitric acid 65%

5.1.1.1 Sampling points

After visiting the San Juan MPU, the sampling points were established according to the worst scenarios regarding mercury concentration and their possible contamination not only through the discharge to the river but also through infiltration or overflow of the tailing dams. In this manner, the real wastewater was collected from the worst scenarios to perform the batch tests and the continuous fixed bed reactor in order to evaluate the efficiency of activated carbon. Despite the recirculation of sludge containing mercury and gold in the tailing dams for the recovery of gold and mercury, there is no concrete slab or any impervious material/liner on the bottom of every dam to prevent mercury infiltration through the ground. Hence, the first sampling point was selected as the mixing tank before the tailing dams where no mercury losses of this nature is expected. The effluent discharge to the Zanjón Grande water stream was selected as a second sampling point in order to analyze if the effluent met the wastewater quality standards of Colombia. Figures 12 and 13 show the sampling point location in the tailing dams and effluent discharge, respectively.

Figure 11. Sampling point #1 Tailing dams

Figure 12. Sampling point #2 Effluent discharge

5.1.1.2 Sampling campaign

Composite samples were grabbed by dividing the total volume between the total number of samples collected every hour, from 9:00 am to 1:00 pm. This allowed to cover the period when mercury is released into the wastewater stream and is discharged to the river. Each individual sample was mixed and added into the container destined to have the composite sample. Three sampling events were selected under maximum, average and minimum production time. This production depends on the number of crushing drums used. In this way, the results of every sampling campaign allowed to establish a range on the variation of every parameter. Figure 11 shows the onsite measurement of several easily monitorable parameters. Table 6 shows the parameters analyzed and the used methods.

Table 6. Water quality parameters and methods analysed

Simple sample			Composite sample		
Parameter	**Units**	**Instrument**	**Parameter**	**Units**	**Method**
Temperature	°C	Multiparameter meter Hach HQ40d (Onsite)	Total Suspended Solids	mg l^{-1}	SM: 2540 - D Total suspended solids 1049 - 105°C
			Total Dissolved Solids	mg l^{-1}	SM: 2540 - C Total dissolved solids 180°C
			Biochemical Oxygen Demand	mgO_2 l^{-1}	SM: 5210 Test BOD_5
			Chemical Oxygen Demand	mgO_2 l^{-1}	SM: 5220 C Closed reflux, titrimetric
			Turbidity	NTU	SM: 2130 B. Nefelometric / Portable turbidimeter - Hach® (Onsite)
pH	pH units		Sulphates	mg l^{-1}	SM: 4500-SO_4^{-2} E Turbidimetric
			Total Hg	mg l^{-1}	SM: 3112 B Cold-Vapor atomic absorption spectrometry
Dissolved Oxygen	mgO_2 l^{-1}		Total Fe	mg l^{-1}	SM: 3111 B Direct air-acetylene flame
Electrical Conductivity	µS cm^{-1}		Total Pb	mg l^{-1}	SM: 3113 B Atomic absorption spectrometry oven-electrothermal
			Total Cu	mg l^{-1}	SM: 3111 B direct air-acetylene flame

Mercury and regular physical and chemical parameters like temperature, pH, dissolved oxygen, electrical conductivity, suspended solids, COD, and BOD were the target parameters that were analyzed in order to evaluate the reactor performance and meet the Colombian effluent quality standards. However, other parameters such as sulphates, Fe, Pb and Cu were analyzed during a sampling campaign to evidence possible mercury removal dynamics inside the tailing dams and also determine presumed metals in the water that may interfere with the mercury adsorption technology.

Temperature, pH, dissolved oxygen, electrical conductivity and turbidity were measured in-situ as shown in Figure 11. These parameters were measured four to five times at the same intervals

than that of the collection of composite samples which were analyzed in the laboratory. Dilutions were needed to measure turbidity because the concentration exceeded the maximum value of the equipment.

Figure 13. Measurement of in situ parameters

5.1.1.3 Conservation procedure

Two containers were used for every sampling point, one for BOD, COD, TSS, TDS and cyanide in 3 L, the other one used for sampling heavy metals was of 1 L capacity. Nitric acid (65%) was added to the container for heavy metals in order to keep a pH value under 2 units and avoid metals to react with any compound in the wastewater sample or be adsorbed by the container material. After collecting the composite samples, every container was hermetically sealed, labeled and refrigerated at 4 °C until delivery to the lab for further analysis.

5.1.1.4 Flow rate measurement

The method used to measure the flow in every sampling campaign was volumetric measurement. A known volume of water was collected from the effluent, every hour, during the time of the sampling campaign of wastewater. The flow rate was monitored and measurements were repeated for 3 times and the average values were reported.

5.1.1.5 Settled sludge and river sediments sampling

Settled sludge and sediments from the water body were also sampled according to the national standards for sediment sampling for metals determination (IDEAM, 2009). This procedure was carried out in the tailing dams by collecting sludge from the dams, at a height of 10 cm, from the bottom of the tank. In the case of the river, the sample was collected from the bottom of the water stream. A total of 300 g was collected for every sample in a polyethylene bag that was previously washed with nitric acid (10 %) and rinsed with deionized water.

5.1.2 Primary treatment assessment and re-design

Considering the high solids concentration of the wastewater discharged to the river, a proper primary treatment was required before using efficiently the activated carbon at the real scale. Firstly, an evaluation of the mercury losses throughout the tailing dams was done to analyze this treatment train of the industry in order to advice the owner with solutions regarding the appropriate design of the tailing dams. If a tailing dam is properly designed, solids and mercury will be removed in some proportion from the system before the use of activated carbon.

5.1.2.1 Mercury balance to estimate mercury losses

As a first step, a methodology was designed to measure the ideal conditions of gold processing for future design of the wastewater treatment in terms of mercury, water and mineral amounts. At the same time, it was used to evidence the losses and distribution of mercury in the current tailing dams. The tailing dams were not working properly as solids settlers and might be releasing wastewater by infiltration to the ground due to inappropriate construction materials and no impervious conditions or liners at the bottom of the dams and walls. Therefore, possible losses of mercury from the wastewater and settled sludge through the tailing dams were occurring; hence, a mercury mass balance was carried out in this study.

The mercury load and concentration in all the stages of the gold unit production was calculated by reducing the production to a minimum load and limiting the wastewater to pass only through the first tailing dam before being discharged. This led to establish how much mercury enters the system, how much is recovered manually after amalgamation and how much is discharged to the environment not only through the effluent discharge but also through the losses in between the process described in Section 4.3.11. The following equation defines the mercury mass balance:

$$Hg_{added} = Hg_{Recovered} + Hg_{Sludge} + Hg_{Discharged} + Hg_{Lost} \quad (5)$$

Where,

Hg_{added} (g) = Quantity of mercury that enters the production system.

$Hg_{Recovered}$ (g) = Quantity of mercury recovered in the production process.

Hg_{Sludge} (g) = Quantity of mercury that settles in the tailing dams.

$Hg_{Discharged}$ (g) = Quantity of mercury discharged into the rivers after passing through the dams.

Hg_{Lost} (g) = Quantity of mercury lost through different processes.

The first and second tailing dams that receive all the wastewater before discharge were cleaned and emptied. A nipple-joint to enlarge the pipe between the two dams was provided to simulate a free discharge to the river and allow flow rate measurement. This balance was carried out under ideal water consumption patterns and conditions of the two crushing drums, each one with a capacity of 40-50 kg. The first tailing dam was filled with water before it reached the orifice height that links to the second dam. This simulated/provided normal operational condition in the dams. Afterwards, all water supplies were stopped. The schematic of the tailing

dams are shown in Figure 14Figure 14. The amount of mineral and mercury added to the drums by the workers were registered.

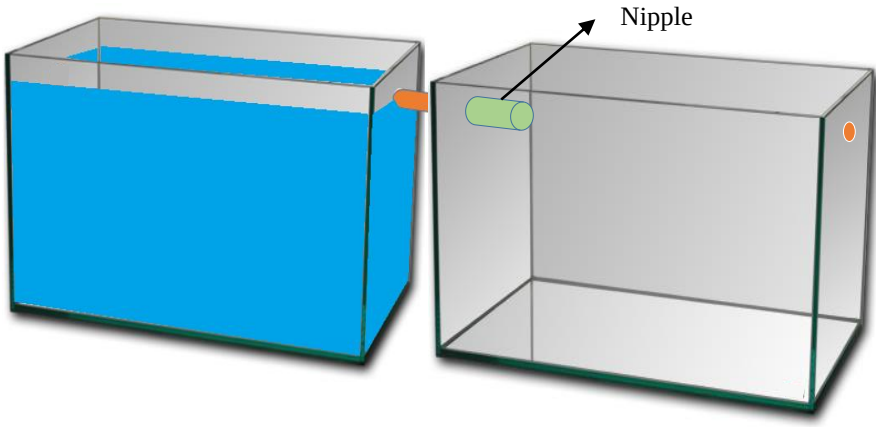

Figure 14. First and second tailing dams before starting the mass balance procedure

Once the first washing step after amalgamation began, the amount of mercury (g) recovered were registered. A composite sample of wastewater was collected once every 20 minutes from the discharge to the second tailing dam as soon as mercury was in contact with the wastewater produced in the drums. The flow rate was measured once every 20 minutes as soon as the wastewater was discharged through the nipple-joints. Once the washing steps were completed, all water supplies were stopped. After eight hours, a sludge sample from the first tailing dam was collected.

The mercury load was calculated using the flow rate, grams of mercury weighed and concentration of mercury in sludge and water. Figure 15 shows the schematic of the crushing drums and the first tailing dam.

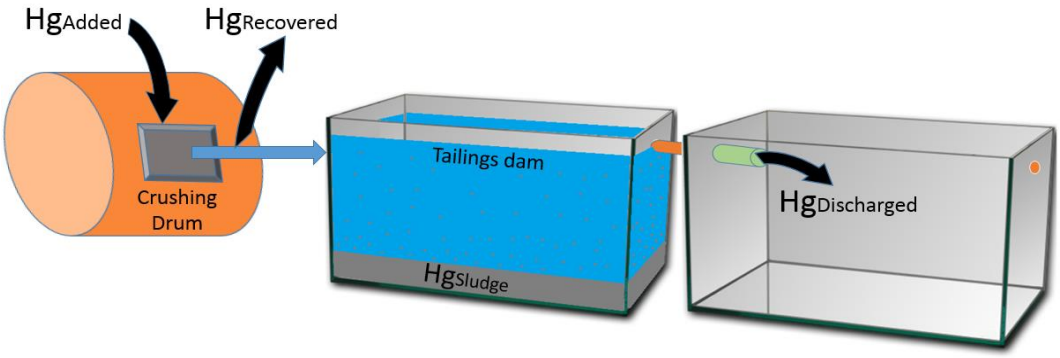

Figure 15. Mass balance of mercury

5.1.2.2 Tailing dams optimization and design

An optimization of the tailing dams design as a fundamental and primary unit of this industry was carried out according to the wastewater characteristics, the mercury balance and the structure evaluation of the MPU and its process. Based on the Stoke´s law, the variable and constant information was established for the design of conventional settling tanks as tailing dams:

$$V_S = \frac{981}{18} \times \frac{\rho s - 1}{\mu} \times d^2 \quad (6)$$

Where:

V_S = Settling velocity (cm s^{-1})
g = Gravity acceleration (m s^{-2})
ρs = Relative density of the particle
d = Particle diameter (cm)
μ = Water kinematic viscosity (cm^2 s^{-1})

The kinematic viscosity was assumed from Table 7, while the size of the particles were obtained from Table 8, respectively.

Table 7. Water kinematic viscosity as a function of temperature

Temperature (°C)	Kinematic viscosity (cm^2 s^{-1})	Temperature (°C)	Kinematic viscosity (cm^2 s^{-1})
0	0.01792	18	0.01059
2	0.01763	20	0.01007
4	0.01567	22	0.00960
6	0.01473	24	0.00917
8	0.01386	26	0.00876
10	0.01308	28	0.00839
12	0.01237	30	0.00804
14	0.01172	32	0.00772
15	0.01146	34	0.00741
16	0.01112	36	0.00713

Source: Adapted from Lopez (1999)

Table 8. Soil classification according to particle diameter variations

Type of soil	Particle diameter (mm)
Very coarse sand	2 – 1
Coarse sand	1 - 0.5
Medium sand	0.5 - 0.25
Fine sand	0.25 - 0.125
Very fine sand	0.125 - 0.0625
Silt	0.0625 - 0.0039
Clay	Less than 0.0039

Source: Adapted from Osorio (2010)

Considering Reynolds formula:

$$\mathrm{Re} = \frac{V_s \times d}{\mu} \quad (7)$$

When Reynolds number isn't appropriate for Stokes´ law application, the settling velocity can be adjusted by considering the particle settling in a transition regime using the diameter and the setting velocity data. The superficial area was determined as a function of the flow and the settling velocity:

$$A_s = \frac{Q}{V_s} \quad (8)$$

Where:

Vs = Settling velocity (m s^{-1})
Q = Flow (m^3 s^{-1})

5.1.3 Grinding of agricultural waste material

Coconut shell and coffee husk were obtained from nearby locations, these materials were washed with distilled water and dried at 100 °C degrees for 24 h. These materials were ground into sizes smaller than 0.5 mm with a Retsch Blade Mill SK100 as shown in Figure 16.

Figure 16. Retsch Blade Mill used for grinding coconut shell and coffee husk

5.1.4 Sorbent material activation

The physical activation was carried out in a Terrigeno muffle furnace model D8 (Figure 17) with a capacity of 8.8 L which works at temperatures of up to 1200 °C. This muffle is

appropriate for carbon transformation and allows to create a reducing atmosphere inside with the addition of nitrogen gas.

Although this process is successful, it is not a sustainable process when it is carried out in laboratory conditions because it is not a closed system and produces high losses of energy and nitrogen. On the contrary, when applied in industrial conditions with specialized machines, it becomes a good cost-benefit process. Considering the amount of activated carbon required for this research, the laboratory scale furnace was the best choice. Steam was used as the activating agent during carbonization and activation. It was produced in a flask with water. The steam flow rate was controlled at 2.5 mL min^{-1}. The carbonization and activation temperatures and times for every step of the process and the gas injection to the muffle furnace are shown in Table 9 and Figure 17, respectively.

Table 9. Carbonization and activation temperatures and time for the precursor materials

Test	Precursor material	Carbonization temperature (°C)	Carbonization time (min)	Activation temperature (°C)	Activation time (min)
1	Coffee husk	400	60	700	60
2	Coffee husk	300		600	
3	Coconut shell	400		700	
4	Coconut shell	300		600	

Figure 17. Set up for nitrogen gas injection to the muffle furnace for activation

Before the carbonization temperature was reached, nitrogen injection to the furnace was programmed for 30 minutes as the temperature increased. Nitrogen was also injected for 30 minutes after the carbonization step and at the end of the activation step during the cooling period, this maintained a reducing atmosphere when no activating agent was added. Figure 18 shows the temperature changes at a carbonization temperature of 400 °C and an activation temperature of 700 °C.

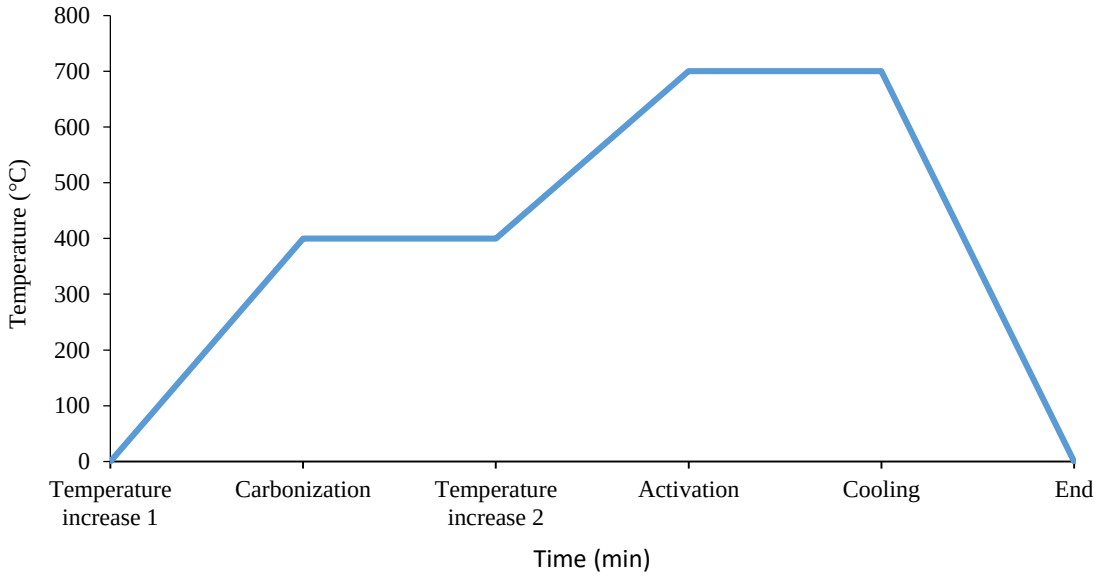

Figure 18. Temperature changes during carbonization at 400 °C and activation at 700 °C

5.1.5 Sorbent material characterization

In this research, all materials used in the laboratory were washed under strict national protocol applied for the determination of heavy metals (IDEAM, 2009). Initially, the materials were washed with neutral phosphate free soap, thereafter, the materials were submerged in HNO_3 and finally rinsed with distilled water.

5.1.5.1 Surface area

To characterize the surface area of every sorbent, an analysis was performed by a Micromeritics Accelerated Surface Area and Porosimetry System ASAP 2020 V4.01. The ASAP 2020 has two independent vacuum systems that allowed the simultaneous preparation of two samples and the analysis of a third one. It also has specific software that allows the automatic and manual control of the equipment, pre-treatment conditions, sample analysis and data treatment from the resulting isotherm. Some of the models that the equipment uses for the determination of superficial area are the BET theory, Langmuir and T-Plot, respectively. In this manner, the surface area, according to the BET theory, and the micropore volume, according to the t-Plot method, were obtained in this study.

5.1.5.2 Mesopore determination

The pore size distribution was characterized by the capacity of the adsorbents to uptake methylene blue. The blue methylene index test was applied in order to analyze which of the activated materials has a higher proportion of mesopores. Since water vapor was used as an activating agent, it was expected that the enhancement of the removal of volatiles in the steam pyrolysis result in significant increase of pore volume, surface area and increase of the adsorption capacity. However, Budinova et al. (2006) suggested that steam activation promotes the formation of narrower micropores in the carbons. The author also states that the smaller width of these narrow pores make them accessible for nitrogen, but not for iodine. Therefore, the iodine number test was omitted to analyze micropores because elemental mercury is slightly

larger than iodine and hence, mercury, in its different species are not target substances for micropores. Nevertheless, the micropore volume according to the T-Plot method result is provided as an extra data from the surface area determination. In this way, a methylene blue stock solution of 1000 mg l^{-1} was used to prepare all the solutions with distilled water. A linear least squares regression was applied with concentrations varying from 0.1 to 4.5 mg l^{-1}, prepared in the stock solution. This allowed to calculate the real concentrations used for the adsorption experiments.

Four solutions of 10, 25, 50 and 100 mg l^{-1} were prepared for the adsorption study under the conditions shown in Table 10. The batch tests (48 h) for the adsorption of methylene blue were developed for each sorbent material, and the final concentrations was determined using an UV spectrophotometer Hach DR2700. The amount of methylene blue adsorbed for every 0.01 g of activated carbon was calculated according to Equation 2. The stock solutions and the rest of the solutions prepared in this study are shown in Figure 19Figure 19.

Table 10. Adsorption conditions for the methylene blue index test

Volume (mL)	Initial concentration (mg l^{-1})	Mass of activated carbon (g)	pH	Agitation speed (rpm)	Temperature (°C)	Time (h)
10	10 - 100	0.01	7	200	30	48

5.1.5.3 Density

Density was measured according to the Standard test method for apparent density of activated carbon D2854-96. The samples were preheated at 105 °C for an hour in order to remove the moisture and residual volatile compounds. A 25 mL graduated cylinder was used to measure the volume occupied by a mass of activated carbon. The activated carbon was added carefully to the cylinder, while the mass and volume were noted down to calculate the apparent density (Equation 9). Figure 20 shows the determination of the mass for one of the activated carbons.

$$Aparent\ density = \frac{mass\ of\ activated\ carbon\ in\ grams}{volume\ of\ activated\ carbon\ in\ mililiters} \qquad (9)$$

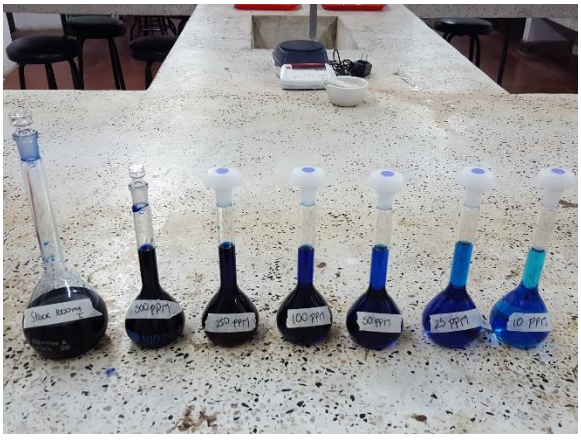

Figure 19. Blue methylene solutions for the determination of mesopores.

Figure 20. Mass determination for aparent density calculation.

5.1.6 Biosorption batch experiments

Batch experiments were carried out in duplicate for every sorbent material under the same conditions. Wastewater from San Juan MPU was used for these tests, the initial and final concentrations were analyzed according to SM: 3112 B Cold-vapor atomic adsorption spectrometry.

Before starting the test, a solid settling process was carried out in Imhoff cones of 1000 mL, for 5 h, in order to simulate the proper function of the tailing dams that were designed. After the removal of solids, adsorption tests were conducted and further, 2 additional tests were performed to evaluate the changes in the sample without activated carbon. Conditions used for a total of 10 tests are shown in Table 11.

Table 11. Adsorption conditions for the batch tests for all the biosorbents

Type of wastewater	Volume (mL)	Mass of activated carbon (g)	pH	Agitation speed (rpm)	Temperature (°C)	Time (h)
Collected from industry	200	2	7	200	25	48

After the samples were agitated for 48 hours, they were filtered using a 0.45 µm filter paper and acidified to pH < 2.0 units before analyzing their concentrations by atomic absorption spectrometry (AAS). The mercury uptake of the activated carbon q_e and the removal capacity were calculated according to Equations 1 and 2, respectively. Figures 21 and 22 show the batch test flasks, before and after 48 h of experiments using coconut shell activated at 400-700°C, respectively.

Figure 21. Coconut shell 400°C - 700°C and wastewater before starting the batch test.

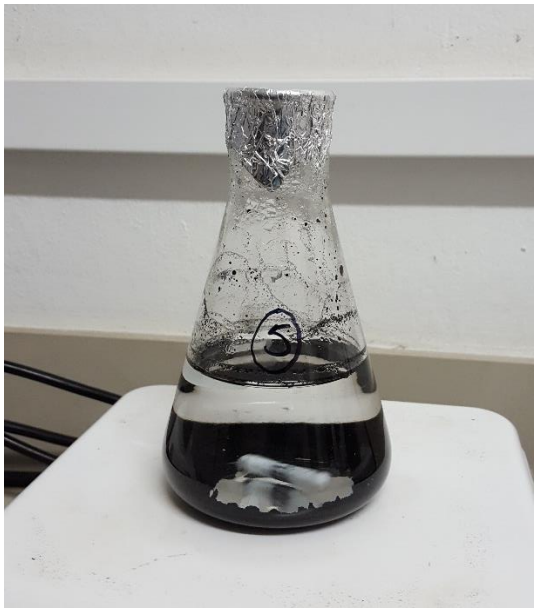

Figure 22. Coconut shell 400°C - 700°C after 48 hours.

5.1.7 Batch desorption test

The biosorbent that showed the best performance in terms of high adsorption capacity was evaluated under two cycles of sorption and desorption. The adsorption conditions for these cycles are shown in Table 12. These tests were carried out in duplicate. After the first adsorption step, the metal-loaded sorbent was washed according to a strict protocol. First, any residual solution from the sorption step was carefully drained ensuring no sorbent was lost in this process. The flask was then filled with demineralized water (400 mL) and filtered, again ensuring no loss of sorbent. The flasks were filled and filtered a total of 3 times to ensure that only bound metal remained on the sorbents. The filtered activated carbon was collected and desorption was carried out (Acheampong, 2013).

Table 12. Mercury batch tests conditions for sorption - desorption cycles

Step	Solution	Volume (mL)	Mass of activated carbon (g)	pH	Agitation speed (rpm)	Temperature (°C)	Time (h)
Sorption	Wastewater collected from MPU	200	1	7	200	25	24
Desorption	0.1M HCl	200	1	1	200	25	24

The desorption step was carried out using 200 mL of 0.1 M HCl in a 250 mL volumetric flask, at 25 °C, for 24 h. After this time, the samples were filtered and then the HCl solution was analyzed for total mercury concentration using AAS as well as the ones from the adsorption step. After the desorption step, the sorbent was carefully washed to remove the desorption solution, the new mass was registered and then the next sorption/desorption cycle was performed (Acheampong, 2013). The desorption efficiency η_d was calculated with the following equation:

$$Desorption\ Efficiency\ (\eta_d) = \frac{C_{fd}}{C_o C_{fs}} \times 100 \qquad (10)$$

Where C_o (mg l^{-1}) is the initial concentration of Hg in the solution, C_{fs} (mg l^{-1}) is the final Hg concentration in solution after sorption, and C_{fd} (mg l^{-1}) is the final Hg concentration in solution after desorption.

5.2 Evaluation of the adsorption constant parameters and correlation coefficients for various adsorption models

Although researchers have developed various isotherm models in the past decades, it is clear that none of them fit well with all cases, and thus, one has to determine the best suitable isotherm experimentally (Xu et al., 2013). On the other hand, a kinetics study of adsorption can be used to describe the adsorption rate and investigate the adsorption mechanism. In this study, therefore, several kinetic and isotherm models available in the literature were tested in order to describe the adsorption mechanism of activated carbon generated with coconut and coffee residues. The review was conducted using the following criteria:

- Adsorption of mercury in liquid solutions.
- Coconut *(Cocos nucifera)* and Coffee (*Coffea sp.*) as the biosorbents.
- Studies published in indexed scientific journals.

Based on the review, graphs evidencing the Lagergren first order, pseudo- first, pseudo-second and Elovich kinetics analysis, as well as the Langmuir, Freundlich and Dubinin Radushkevich isotherm curves were shown to be promising for this study.

5.3 Performance of a fixed bed column for mercury removal using the most suitable adsorbent

5.3.1 Fixed-bed column design and set up

The sorbent material with the best performance during batch test was used to evaluate the adsorption capacity in a down flow semi-continuous reactor. According to the reactor design presented in the literature (Acheampong, 2013), a 1:2 inner diameter/depth ratio column was constructed with 2.54 cm inner diameter and 5 cm of effective bed depth. The column was constructed using PVC pipes; a fitting was assembled in the middle to set two layers of high density polyethylene which were used as support material for the activated carbon. A PVC cap was assembled at the outlet of the reactor with an orifice of 0.5 cm.

The reactor was fed with wastewater collected from San Juan MPU using an IV infusion set for flow control connected to the bottom of a plastic container of 35 cm by 25 cm area. The container was placed at a height of 60 cm from the reactor on a stirring plate at 200 rpm to obtain completely mixed water before it entered the reactor. The water column inside the container did not exceed a height of 1 cm to avoid pressure changes in the incoming flow of the reactor. Figure 23 shows the fixed bed reactor configuration that was constructed and used in this research.

5.3.2 Start up and monitoring of fixed bed

An 8 hours daily average working period of the San Juan MPU was considered to estimate the amount of wastewater generated from that unit. This information was used to establish the working period of the laboratory scale reactor. An additional five more hours were assumed because of hydraulic retention time considerations, i.e. based on a conventional settler that is a part of the primary treatment in wastewater treatment. In this manner, the fixed bed reactor was evaluated for an average of 12 h operation. Wastewater was collected from the initial tank that passes wastewater to the tailing dams. This was done to avoid mercury losses along the tailing dams and this information was considered in the mercury balance. The collected wastewater was transported to the laboratory by following standard laboratory guidelines (low temperatures and pH < 2.0).

At the laboratory, the collected wastewater (11 L) were settled in Imhoff cones (Figure 24) for 5 hours in order to simulate a proper primary treatment and avoid saturation of the activated carbon due to suspended solids. Then, the clarified wastewater was mixed in a tank and split into 0.8 L samples where its initial concentration was measured. The pH was raised to 7.0 units

only when the wastewater was settled or used in the column to meet the real conditions. The column was monitored for 10 days, 1 sample per day and at a flow rate of 1.1 $cm^3 min^{-1}$. Initial and daily Hg concentrations were analyzed using AAS.

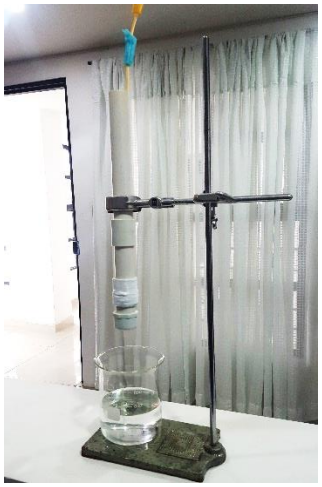

Figure 23. Fixed bed reactor configuration

Figure 24. Wastewater settling for fixed bed reactor evaluation

5.3.3 Performance analysis of the fixed bed adsorption column

During the reactor tests, the outlet mercury concentrations were measured as a function of the operation time of the column. According to Johari et al. (2016), the mercury adsorption data were plotted as a dimensionless adsorption breakthrough curve, wherein the normalized concentration term was defined as the ratio of C/C_o.

Based on the study of Ahmad & Hameed (2010), the maximum column capacity, q_{total} (mg) for a given set of conditions was calculated from the area under the curve of the adsorbed Hg concentration, C_{ad} (mgL^{-1}), versus time:

$$q_{total} = \frac{QA}{1000} = \frac{Q}{1000}\int_{t=0}^{t=t_{total}} C_{ad}dt \qquad (11)$$

Where $C_{ad} = C_i - C_e$ ($mg\ l^{-1}$), t_{total} is the total flow time (min), Q is the flow rate ($mL\ min^{-1}$) and A is the area under the breakthrough curve (cm^2). The equilibrium uptake $(q_{e\ (exp)})$, the amount of Hg adsorbed (mg) per unit dry weight of adsorbent ($mg\ g^{-1}$) in the column, was calculated as follows:

$$q_{eq(\text{exp.})} = \frac{q_{total}}{W} \qquad (12)$$

Where W is the total dry weight of adsorbent in the column (g).

CHAPTER 6

Results and discussion

6.1 Analysis of Hg adsorption capacity on coconut (*Cocos nucifera*) shell and coffee (*Coffea sp.*) husk in batch tests

6.1.1 Physical-chemical and heavy metal characterization of the wastewater from San Juan mining production unit

As mentioned in Section 5.1.1, three sampling campaigns were chosen in terms of the number of amalgamator drums used. Table 13 shows the characteristic of wastewater. Maximum production refers to a day when the ore extracted from the different mines of the region are transferred to the UPM and the total number of barrels or crushing amalgamator drums come into operation.

Table 13. Characteristic of wastewater from the San Juan mining production unit

Parameter	Unit	Tailing dams			Effluent discharge		
		Max p	Med p	Min p	Max p	Med p	Min p
Flow	$L\ s^{-1}$	N-A	N-A	N-A	1.67	1.50	1.35
pH	pH unit	7.4	8.79	6.39	6.77	8.96	6.70
Temperature	°C	26.6	24.5	24.6	25.8	24.7	24.3
Dissolved oxygen	$mgO_2\ l^{-1}$	2.89	5.67	3.81	4.50	5.77	5.58
Electrical conductivity	$\mu S\ cm^{-1}$	105.85	145.16	138.23	106.38	131.58	120.58
Turbidity	NTU	15328	3858	5838	7472	4990	3372
Total suspended solids	$mg\ l^{-1}$	18496	3318	12085	14015	3334	10625
Total dissolved solids	$mg\ l^{-1}$	185	172	135	188	177	121
COD	$mgO_2\ l^{-1}$	303	181	145	232	201	133
BOD_5	$mgO_2\ l^{-1}$	46	37	29	39	57	26
Sulfates	$mg\ l^{-1}$	22	37	105	23	36	91
Free and dissociable cyanide	$mg\ l^{-1}$	<0.002	0.008	0.004	<0.002	0.005	0.005
Total Hg	$mg\ l^{-1}$	2.00	7.71	2.56	2.19	0.97	2.38
Hg in sludge/sediment	$mg\ 100g^{-1}$ sludge	N-A	62.58	2.46	N-A	9.19	1.36
Total Pb	$mg\ l^{-1}$	N-A	0.0088	N-A	N-A	0.068	N-A
Total Fe	$mg\ l^{-1}$	N-A	397.6	N-A	N-A	249.1	N-A
Total Cu	$mg\ l^{-1}$	N-A	4.21	N-A	N-A	1.98	N-A

Max p = Maximum production; Med p = Medium production; Min p= Minimum production; N-A = Not available

The most representative days for this production are Saturdays and Sundays. During these days, the miners extract the gold from the process and sell it in order to shop all the groceries for their families. In the case of average production, the MPU does not have the total number of barrels in operation; nevertheless, at this production stage, the resulting sludge from the tailing dams and the one that is settled in the channels is re-processed in 7 or 8 drums.

The minimum production refers to the days of the week when the facilities of the MPU has the least production and works with not more than four amalgamators drums. It is important to mention that during these days there is no re-processing of sludge, but there is stacking of the sludge contained in the tailing dams near the drums.

According to the data shown in Table 13, it can be seen that the majority of parameters sampled in the wastewater of the San Juan MPU exceeded the permissible discharge limits prescribed by the Colombian Resolution 0631 of 2015, on the discharge of effluent to surface water bodies (MADS, 2015). It evidences high levels of mercury in the water produced by the UPM, an analysis of the most significant parameters is the sections below.

6.1.1.1 Temperature

The temperature is a very important parameter due to its effect on aquatic life. The average temperature in the residual water is ~25ºC produced in the effluent of the San Juan mining unit. The temperature limit for industrial wastewater according to resolution 631 of 2015 (article 5) sets a maximum permissible limit value of 40°C for all industrial activities that discharge water to surface water bodies. It is important to emphasize that, every day in the MPU, none of the work started at the same time; however, the wastewater was measured for the same period of time as soon as wastewater was produced. According to the results of the analyzes carried out in-situ (Figure 25), the temperature variations for the tailing dams (a) fluctuates between 24 and 28 ºC, while for the discharge (b), its values ranges from 24 to 26 ºC.

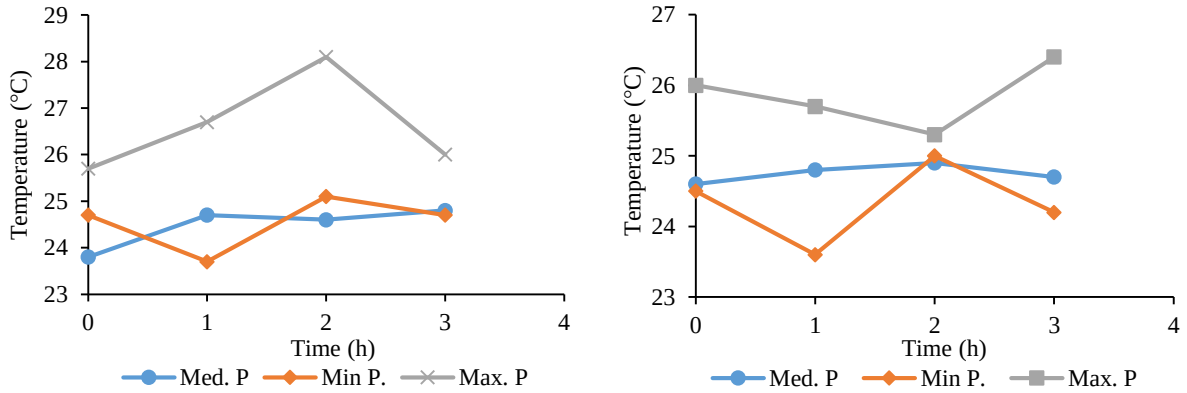

Figure 25. Temperature variation in the tailing dams (a), and discharge (b) of San Juan MPU

It is important to mention that the variations of temperature in wastewater from the mining industry are directly related to the production schedule of the MPU. Therefore, a significant increase in the maximum production days occurs due to the prompt generation of wastewater during the milling of each drum under elevated temperature. Temperature changes generate alterations or effects on the oxygen concentrations and as a consequence, a decrease in the dissolved oxygen can be noticed in these waters. On the other hand, Hadi (2015) stated that

higher temperatures result in higher mercury uptake due to the endothermic nature of this process. It is also estimated that higher temperatures increase the mobility of the mercuric ion leading to enhanced intra-particle diffusion rate.

6.1.1.2 Dissolved oxygen

Concentrations of dissolved oxygen in natural water depend on the physicochemical characteristics and biochemical activity of microorganisms in water bodies. Dissolved Oxygen analysis is fundamental for the control of pollution in natural water and industrial or domestic wastewater treatment processes (Gaitán, 2004). Figure 26 shows the changes in oxygen concentrations in both the tailing dams (a) and the discharge (b), respectively. It is worth mentioning that the increase of organic matter in water is a factor that contributes to the changes in dissolved oxygen levels due to the consumption of oxygen during the decomposition process. According to Table 14, waters with oxygen levels below 5 mg l^{-1} can be dangerous to aquatic life, causing organism to disappear.

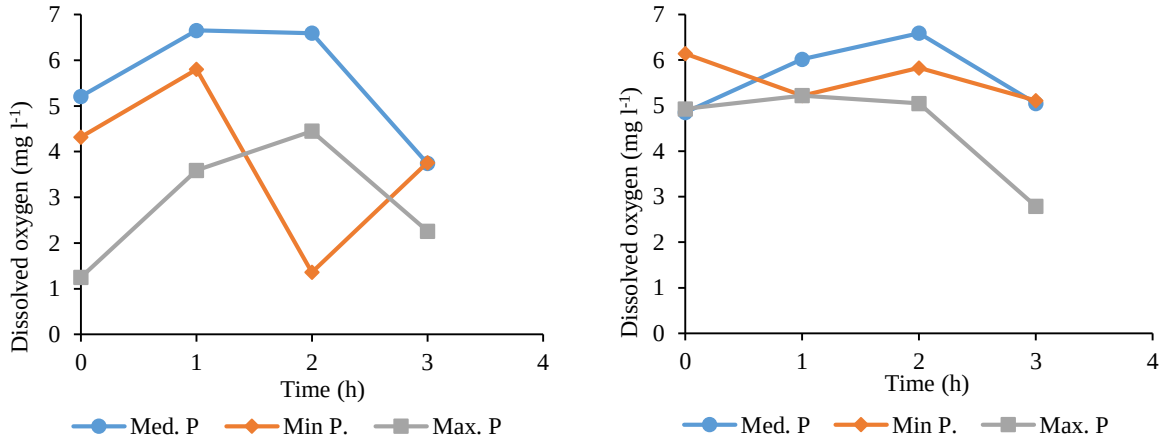

Figure 26. Dissolved oxygen characterization in the tailing dams (a), and discharge (b) of San Juan MPU

The concentrations of dissolved oxygen shown in Figure 26, in the tailing dams (a) vary from 1 to 6 mg l^{-1}, while the discharge (b) are registered between 3 and 6 mg l^{-1}. This indicates that after the settling of solids in the tailing dams, the wastewater only reaches an acceptable level of oxygen saturation in the water. This may be occurring because of the surface aeration and turbulence of the last units prior to discharge. There is a slight improvement in the oxygen content of the water in the discharge, this is related to the solids concentrations, in this way the higher solids and turbidity found in maximum and medium production decrease the dissolved oxygen in the wastewater stream. The lowest solids concentration was found under medium production so there is a tendency of higher DO concentrations in both tailing dams and discharge for medium production conditions.

6.1.1.3 pH

Figure 27 shows the pH variation during the sampling campaigns. With respect to pH, the results and their variations for the tailing dams (a) and the discharge (b) range from 6.0 to 8.0.

This indicates that the effluents discharged from the mining production unit generate a slight acidity in the receiving source.

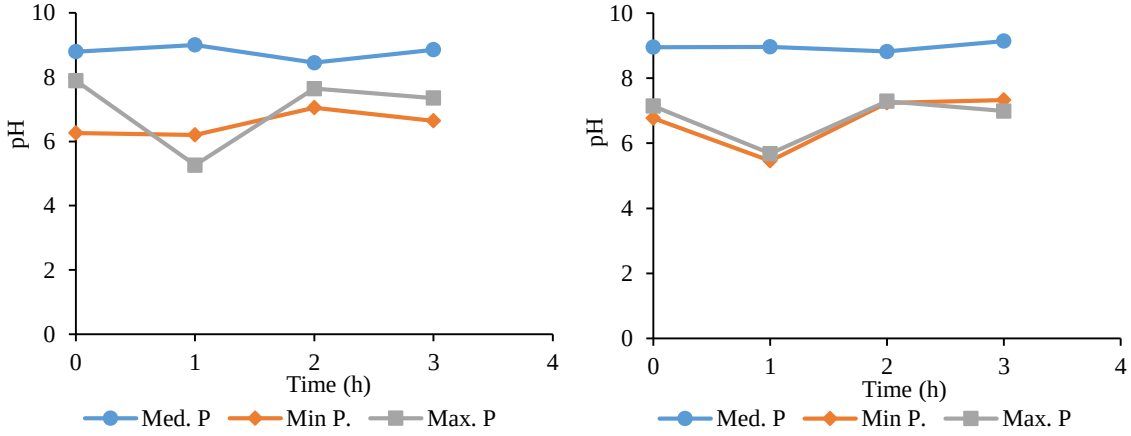

Figure 27. pH characterization in the tailing dams (a), and discharge (b) of San Juan MPU

These results evidence that the values are within the minimum and maximum permissible limits according to Resolution No. 0631 of 2015. This law establishes maximum values permissible in terms of pH for industrial waters, i.e. between 6.0 and 9.0 during mining activities. Adsorption of mercury is a highly pH dependent process. As the pH value of the solution increases, more mercury uptake occurs. The increased adsorption of mercury ion has been shown to be related to the species of mercury present in a solution. Higher pH values result in the presence of more soluble mercuric species which, in turn, promotes the effective contact between the adsorbate molecules and the adsorbent materials thus enhancing the possibility of the mercury uptake by the porous adsorbent particles (Hadi et al., 2015).

6.1.1.4 Electrical conductivity

Figure 28 shows the variations of the electrical conductivity of the two sampling points. The high concentration of electrical conductivity in San Juan MPU is mainly due to the presence of the dissolved matter of the mineral salts and the metal ions remaining in the water after the grinding and milling of a pyrite and chalcopyrite rich mineral, which have metal ions like Fe and Cu.

According to the chemical composition of the pyrite (FeS_2), it contains 46.4% Fe and 53.6% sulfur, respectively. The pyrite acts as a cathode and is protected, while the chalcopyrite acts as an anode and its oxidation increases. This pair is of great interest since they are usually minerals that are found together and is usually in contact with each other. In addition, when the ferric ion concentration increases in the solution, the acidity also increases (Velasco, 2009).

It was expected to find higher levels of electrical conductivity in the day of maximum production due to the amount of material crushed, however, the values of the conductivity during medium production days in the dam (a) and discharge (b) were higher than the maximum and minimum production days. This phenomenon can be associated to the alternative activities to the grinding and crushing of materials that can be performed on any day of the week; for example, the accumulation of sludge during the week.

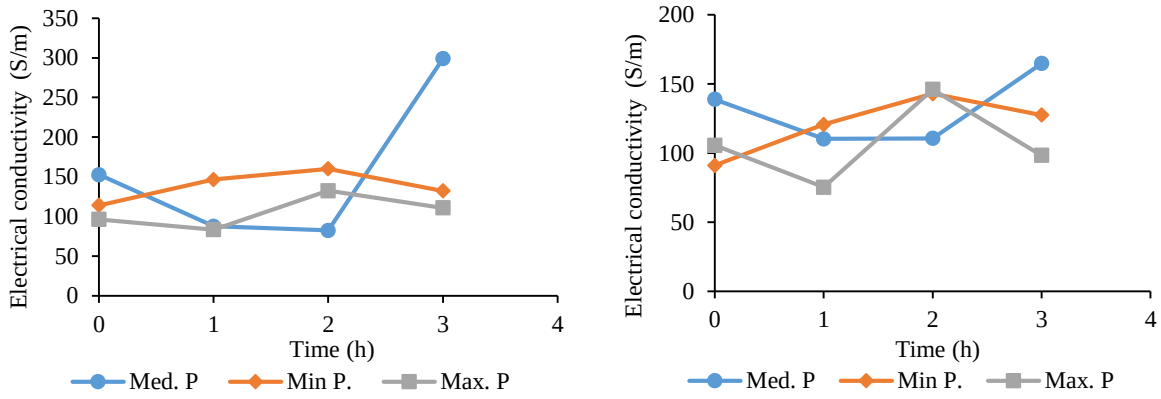

Figure 28. Electrical conductivity characterization in the tailing dams (a), and discharge (b) of San Juan MPU

6.1.1.5 Total suspended solids and turbidity

As seen in Figure 29 and Figure 30, the high values obtained during the analysis of the total suspended solids and the turbidity shows relationship between these parameters. From Figure 29, it is clearly observed that the values of the total suspended solids from the tailing dams (a), have significantly higher values with respect to the concentrations obtained in the discharge (b) point. According to resolution 0631 of 2015, a maximum permissible value of total suspended solids in point-source wastewater discharges can be only 50 mg l^{-1} (red line).

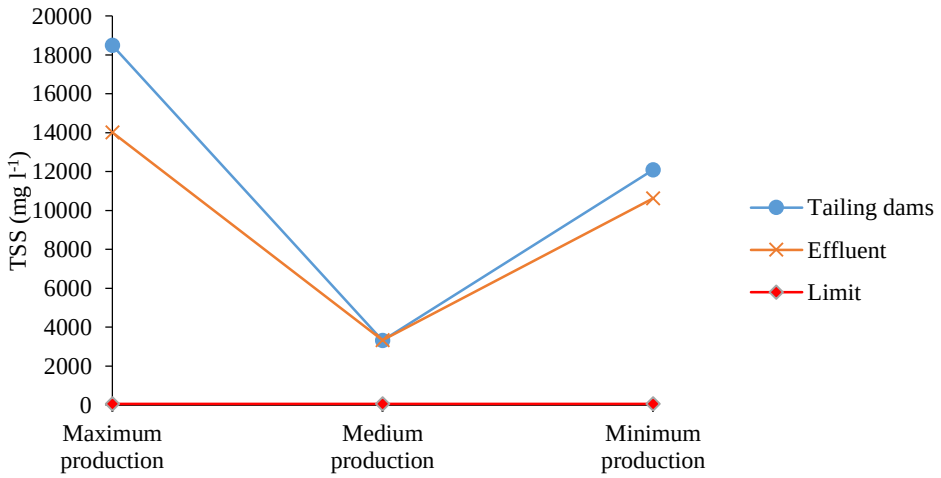

Figure 29. Total suspended solids characterization in the tailing dams and discharge of San Juan MPU

Wastewater from the mining industry generates a large amount of total suspended solids. During its productive stages, especially the gold benefit process, the crushing activities results in a liquid medium providing suspended matter to the waste stream. These solids that are suspended are colloidal material that does not dissolve in water, and they consist of fine silts that are transported to the sedimentation tanks.

As shown in the effluent discharge of Figure 29 and Figure 30, it can be observed that there is a decrease of the total suspended solids and turbidity, respectively, from the beginning of the tailing dams until the discharge to the water body during maximum production. Since the tailing

dams have a solids settling function, they reduce a portion of the TSS load from the water. This phenomenon is performed in San Juan MPU under optimum condition on maximum production day because it's the time when the tailing dams have been previously dislodged and maintenance activity was carried out.

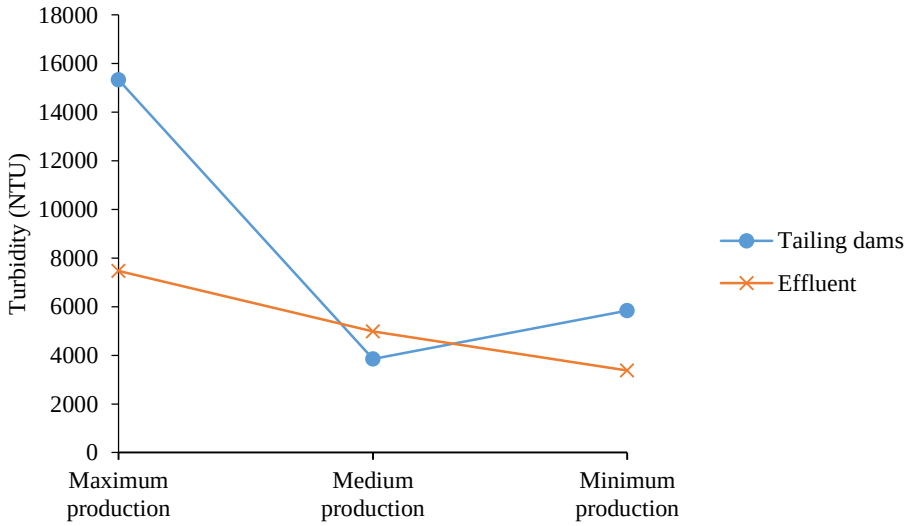

Figure 30. Turbidity characterization in the tailing dams and discharge of San Juan MPU

It is important to emphasize that, during maximum production there is a representative difference in the generation of suspended matter causing negative contributions to the water quality of the receiving body, thus affecting its visual appearance and water transparency as an impediment to the passage of light. The mercury adsorption process requires low TSS concentrations so the mercury will not compete with solids and other compounds to be adsorbed.

6.1.1.6 Chemical oxygen demand

The Resolution 0631 of 2015 states that the values obtained for the chemical oxygen demand shall not exceed the maximum allowed limits, i.e. 150 mg l^{-1} of COD. The majority of the values shown in Figure 31 are above the allowed value. However, it is possible to establish that the three results for each sampling point are within a narrow range, which indicates that there are no significant differences in the distributions of the samples.

Chemical oxygen demand is established as the amount of oxygen that is consumed by the pollutants that are in that water for a certain time, whether organic or inorganic pollutants. There is no significant difference between the results obtained in the tailing dams and effluent, it can be estimated that there are not many reactions involving an oxygen demanD happening inside the tailing dams prior to the effluent discharge. This statement can be supported with the BOD results shown in 6.1.1.7.

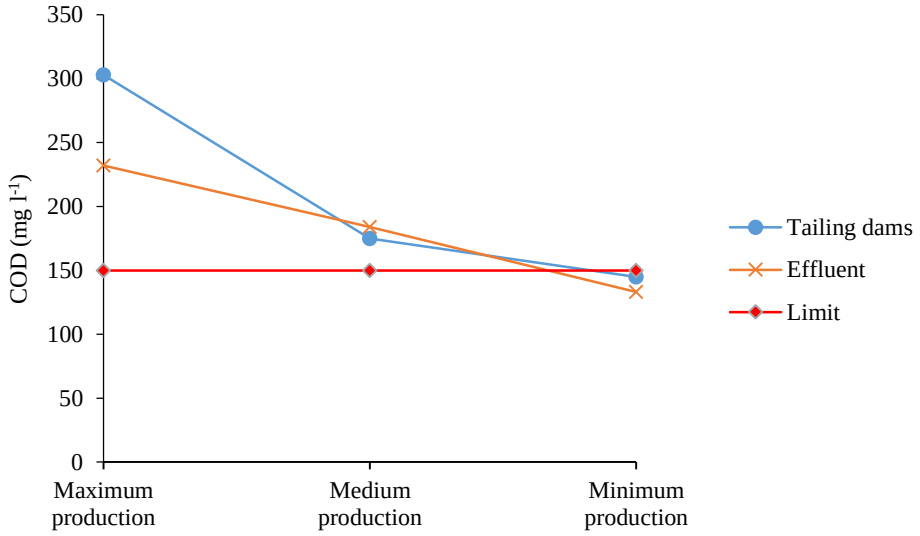

Figure 31. Chemical oxygen demand characterization in the tailing dams and discharge of San Juan MPU

6.1.1.7 Biochemical oxygen demand

One of the most important tests to establish the relationship of the sample with organic matter is the five-day BOD test. The concentrations of BOD_5 can be generated in this case by the organic material dissolved in the water that was used as influent for the benefit of gold or the organic matter that is present in the mineral that was processed. From Figure 32, it can be observed that at the point of discharge for the medium production, the permissible limit has been exceeded. However, in these cases there is no need to think of a biological treatment to reduce these concentrations in the effluent. According to the Colombian legislation related to a certain mining activity, a limit value of BOD_5 has been recommended as 50 mg O_2 l^{-1}. Further analyzes should be carried out in order to measure the influent BOD concentration and this has to be subtracted from the effluent BOD concentration.

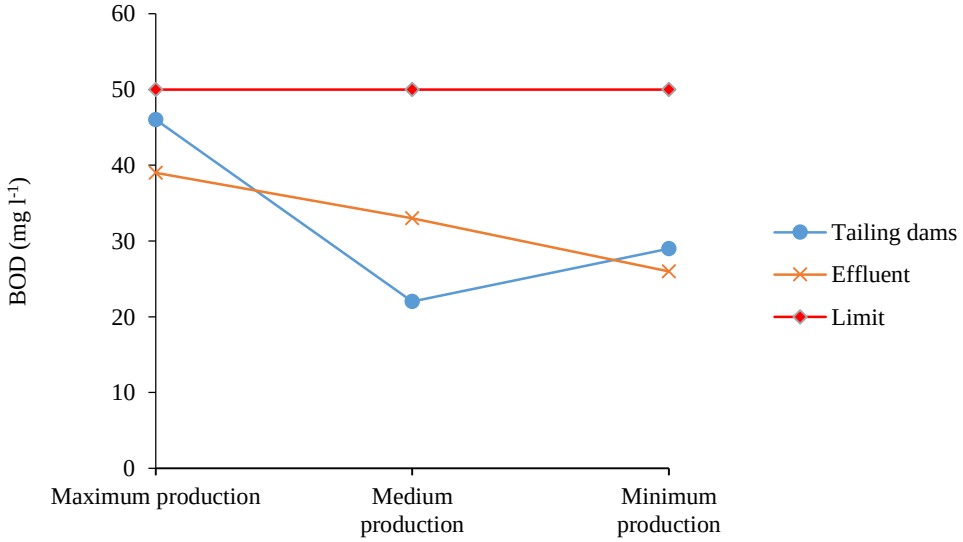

Figure 32. Biochemical oxygen demand characterization in the tailing dams and discharge of San Juan MPU

The average BOD/COD ratio was calculated as the average of BOD concentrations in tailing dams and effluent over the average of COD concentrations in tailing dams and effluent. The

resulting ratio was 1,17 which indicates that the wastewater is mainly characterized by inorganic compounds such as minerals and metals and is not likely to be treated with a biological treatment.

6.1.1.8 Sulphates

Sulphate (SO_4^{2-}) is widely distributed in nature and can be present in natural water in concentrations ranging from a few milligrams per liter to a few grams per liter. Some mining drains can contribute to large amounts of sulphates through the oxidation of pyrite. Particularly, the presence of sulphates in the wastewater of the mining industry are due to the high mineralization of rocks. Besides, there is also the presence of free sulphur which yields high sulphate levels because the minerals of the municipality of Suárez are rich in pyrite and chalcopyrite contents. From Figure 33, it is evident that the sulphate concentrations in the tailing dams (a) and discharge (b) do not exceed the maximum permissible limit established in resolution 0631 of 2015 (1,200 mg l-1). However, it is important to measure this parameter periodically to estimate the pathways of mercury removal or immobilization from the aqueous medium, since sulphides can react with the mercury.

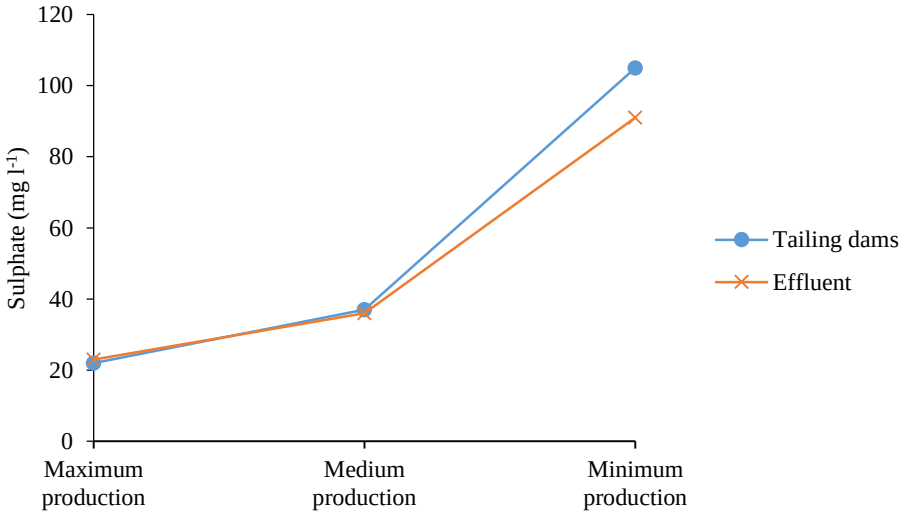

Figure 33. Sulphate concentration in the tailing dams and discharge of San Juan MPU

Sulphide is produced by the reduction of sulphate. The reduction of sulphates via bacterial route is the main mechanism that produces sulphides, under sedimentary conditions. There is also the possibility that at high temperatures, sulphate can be chemically reduced to H_2S, and this phenomenon may occur inside the amalgamator drums.

This sulphide and sulphate interaction with mercury may lead to precipitation of mercuric sulphide compounds under circumstances of high temperatures inside the drums where the amalgamation takes place. Its formation in the water is subject to high concentrations of sulphides and the absence of oxygen. HgS have low solubility in water and are difficult to methylate. It is formed as soon as the divalent mercury and sulphide ions are present simultaneously. The sulphide ion on which the HgS is formed may be sulphides such as FeS and CaS, and if an excess of free sulphide ions is present, the ionized HgS^{2-} complex will be formed. In this case mercury present in the settled sludge of the tailing dams may be inmobilized

by the presence of sulphides that are formed under anoxic conditions due to the long sludge retention time and nule aeration. Further studies must be conducted in order to understand the dynamics of mercury in the sludge since no treatment or proper disposal is applied in the region.

HgS can also be formed from monomethylmercury, in the presence of sulphide ions, where the equilibrium is:

$$2CH_3Hg^+ \leftrightarrow Hg^{2+} + (CH_3)_2H \quad (11)$$

$$Hg^{2+} + S^{2-} \rightarrow HgS \quad (12)$$

The equilibrium reactions shown in Equation 11 and Equation 12 can move to the right if Hg^{2+} is removed by the formation of HgS in the reaction of Equation 12. As dimethyl mercury is volatile and very sparingly soluble in water, it will also be removed from the aqueous phase after it is formed (Jimenez, 2005). Once the mercury sulphides are formed they are precipitated in the form of gas.

6.1.1.9 Mercury

Mercury concentration in wastewater under maximum, medium and minimum production are shown in Figure 34. The orange line shows the maximum permissible limit of the Colombian legislation.

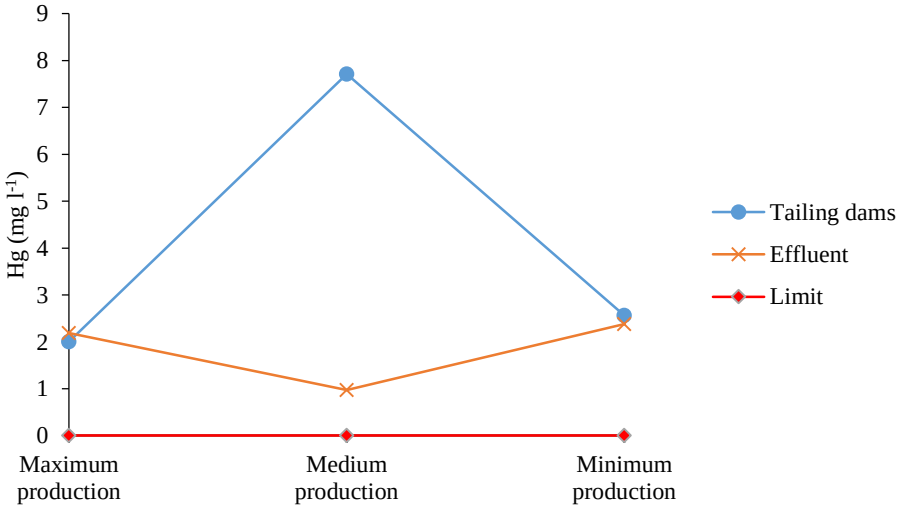

Figure 34. Mercury characterization in the tailing dams and discharge of San Juan MPU

As it was stated in Section 4.3, mercury is present in nature in different oxidation states and as organic and inorganic compounds. They may appear in the gaseous phase in elemental Hg form (dimethylmercury), as liquid (elemental Hg) in mineralized soils and in anaerobic sediments mercury appears as cinnabar. In the wastewater from the San Juan MPU, mercury levels range from 0.97 to 7.71 mg l^{-1}. Based on resolution 0631 of 2015, the reported mercury concentrations exceed the maximum allowable limits (0.02 mg l^{-1}).

The previous information indicates that the environmental and health risk of miners and the general population is extremely high. The routes of exposure may be through food which is the main source of mercury transport to the community. For this reason, it is important to conduct further studies that are directed at the contamination of mercury generated in the UPM, its losses

in the process and its possible routes of contamination by means of performing a mass balance of mercury that is presented in later sections of this thesis.

There are a great variety of heavy metals in the wastewater of the mining industries such as lead, copper and iron, but the most well-known and abundant is Fe. Once present in water, Fe forms a wide variety of complexes of metals ions and organic matter.

The presence of these metals and their concentrations in the water of the MPU is vital to consider any type of treatment for the removal of mercury and other metals present. It is highly important to evidence the presence of other metals that may compete with mercury in the adsorption process using activated carbons. Table 15 shows the Cu, Pb and Fe concentrations measures in the tailing dams and the discharge and the maximum limit that is permissible according to the legislation.

Table 14. Heavy metals concentrations and the maximum limit allowed

Parameter	Unit	Máximum limit allowed	Tailing dams	Discharge
Cu	mg l^{-1}	1.00	4.21	1.98
Pb	mg l^{-1}	0.20	0.0088	0.068
Fe	mg l^{-1}	2.00	397.6	249.1

6.1.1.10 Cyanide

Table 13 shows the reported concentrations of free and dissociable cyanide in wastewater from the San Juan UPM. Although there is no use of this substance, these concentrations may occur due to poor handling of reagents, use of contaminated tools and through infiltration of the residual water with cyanide contents, which can be contacted by tailings afterwards. It is important to mention that the mining industry uses large amounts of cyanide in order to recover all the gold particles that are not usually recovered by the amalgamation process.

Resolution 0631 of 2015 establishes the maximum permissible limit of cyanide in wastewater in the mining industry as 1. mg l^{-1}. However, in this study, concentration levels do not exceed the permissible limits. From an environmental and health point of view, it is important to monitor them because it is an element that in very low concentrations can have negative effects on aquatic life and be fatal to human health. A new, its toxicity depends directly on its concentration, and other factors such as temperature, pH, and volatility at neutral or alkaline pH.

6.1.1.11 Mercury in sediments and settled sludge

It is important to consider how much mercury is settled in the sludge from the tailing dams and the sediments of the water body. As it was expected, mercury concentrations in both the locations are significantly high. Taking into account the fact that, at present, in Colombia there is no regulation that recommends the maximum values permissible for mercury levels in sediments generated during the mining process. Therefore, it becomes necessary to analyze the

mercury data with the Peruvian Supreme Decree No. 002 of the 2013-MINAM. In that Supreme Decree, the threshold permissible mercury values have been stated, and for sediments from industrial activities, a maximum value of 24 mg kg^{-1} has been recommended. Figure 35 shows the results of mercury in the sludge and sediment samples, while the maximum permissible value from Peru is shown by means of an orange line.

As shown in Figure 35, the mercury levels found in sediments evidence the variation of the concentration in the tailing dams and the discharge points. During medium production, the value ranges from 91 to 650 mg kg^{-1} of sludge. The Hg content in the sludge is higher and exceed the limit values recommend by the Supreme Decree of 2013 of Perú. It is important to mention that these concentrations can also vary depending on the stage of production of the MPU and the type of unit operation in a specific mining site.

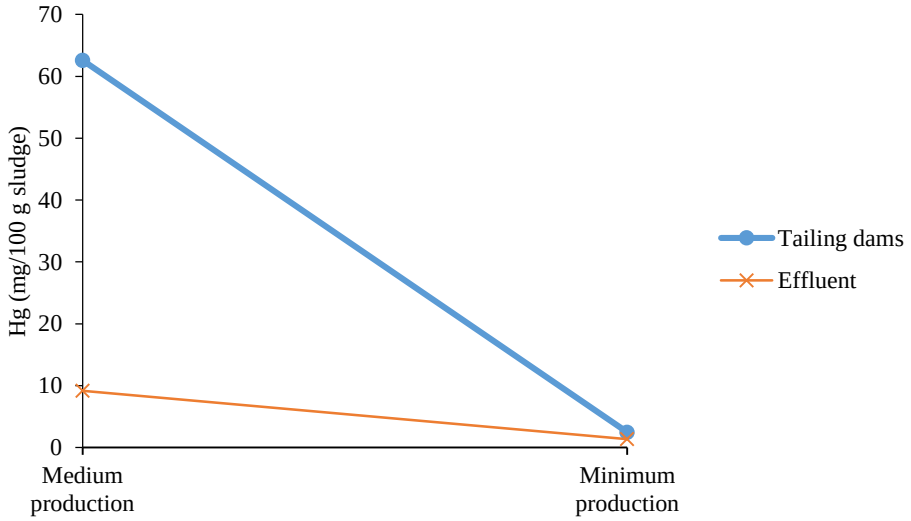

Figure 35. Mercury concentration in the settled sludge from tailing dams and sediment concentration in the discharge of San Juan MPU

6.1.2 Primary treatment assessment and re-design

6.1.2.1 Mercury balance and losses determination

The mass balance was performed in order to estimate the amount of mercury present in water and sludge after the amalgamation and mercury recovery process due to the productivity stage, under controlled conditions of ore, mercury and water. For the mass balance determination, a washing step of the units and structures was carried out in order to determine the levels of mercury that was lost during these unit operations. Water and sediment samples were taken under minimum flow conditions, i.e. during the production of wastewater, to determine the possible losses. Besides, during the amalgamation process, the amount of mercury is very small or negligible.

The mercury concentrations present in water and sediment samples are shown in Table 16. As it can be seen, the mercury concentration in the water effluent was 5.85 mg Hg l^{-1} which is significantly higher than the permissible limit of 0,002 mg l^{-1}, while in the sediments, a value

of 2.01 g kg^{-1} Hg of sludge was observed. Besides, it was possible to establish the mercury losses in the process of gold processing at the MPU of San Juan and also justify the original hypothesis that the tailing dams were not efficiently designed and they pose a significant risk/danger in causing severe mercury pollution to the environment and potential human health damage.

Table 15. Mass balance for mercury in the amalgamation and wastewater production process

Measurement	Value
Mercury added	311.845 g
Mercury recovered	226.796 g
Mercury settled in sludge	2.01 g Hg kg^{-1}
Mercury discharged to water body	5.85 mg Hg l^{-1}
Mass of ore processed	80 kg
Water flow	0.67 L s^{-1}

To estimate the amount of mercury present in the sludge, the volume of the sludge and its density were taken into account according to the following calculations:

$$Sludge\ Volume = Width \times Length \times Height \quad (13)$$

$$Sludge\ Volume = 0.6m \times 0.85m \times 0.04m = 0.0204m^3 \frac{1000L}{1m^3} = 20L$$

Considering the fact that the volume of solids present in the aqueous medium is diluted in the total mixture, the density of sludge was assumed as 1.15 kg l^{-1} and the mass of sludge as well as the mass of mercury were calculated.

$$\text{Mass}_{\text{Sludge}} = \text{Density of sludge} * \text{Sludge volume} \quad (14)$$

$$\text{mass}_{\text{Sludge}} = 1.15 \frac{\text{kg}}{\text{L}} \times 20\text{L} = 23\text{kg}$$

$$\text{mass}_{\text{Hg}} = \text{Mercury concentration in sludge} * \text{mass}_{\text{Sludge}} \quad (15)$$

$$\text{m}_{\text{assHg}} = 2.01 \frac{\text{g Hg}}{\text{Kg sludge}} \times 23\ \text{Kg} = 46.23\ \text{g Hg}$$

To estimate the amount of mercury that reaches the receiving body through the wastewater, the volume of wastewater generated was also considered as shown below.

$$\text{Volume}_{Water} = 1608\ \text{L}$$

$$\text{mass}_{\text{Hg in wastewater}} = \text{Mercury concentration in water} * \text{Volume}_{Water}$$

$$\text{mass}_{\text{Hg in wastewater}} = 5.85 \frac{\text{mg}}{\text{L}} \times \frac{1\ \text{g}}{1000\ \text{mg}} \times 1608\ \text{L} = 9.4\ \text{g Hg}$$

From Equation 5, the mercury losses in the San Juan mining production unit were quantitatively determined with the purpose of knowing the exact values and the performance of the sludge retention unit after material washing.

Therefore,

$$Hg_{added} = Hg_{Recovered} + Hg_{Sludge} + Hg_{Discharged} + Hg_{Lost} \quad (16)$$

$$Hg_{Lost} = Hg_{added} - Hg_{Recovered} - Hg_{Sludge} - Hg_{Discharged}$$

$$Hg_{Lost} = 311.845 \text{ g Hg} - 226.796 \text{ g Hg} - 46.23 \text{ g Hg} - 9.4 \text{ g Hg}$$

$$g_{Lost} = 29.42 \text{ g Hg}$$

After the calculation of the losses, it was estimated that the processes which are carried out in the MPU generate significant amount of mercury to the environment, i.e. through unknown pathways or due to a wrong technique and poor recovery of the metal during the washing step and through the tailing dams. The operation of the tailing dam is not optimal for retention and removal of suspended matter.

It was presumed that, during the retention of suspended solids in the wastewater of the MPU, mercury losses occurred through the bottom of the retention units, and they mobilized to deeper soil layers. The mobility of mercury in the MPU of the Municipality of Suárez should be investigated further.

Mercury losses in the system were 29.42 g and that these losses were related to the deficient design of the tailing dams. This result suggests that during a day of average production more than 300 g of mercury are lost, this amount of mercury may contaminate water and soil drastically. Therefore, the next step was to re-design a proper primary treatment system that is able to settle the suspended solids and contain the mercury present in sludge in impervious units.

6.1.2.2 Conventional settlers design

Design principles

According to the Colombian Technical Regulation of the Drinking Water and Basic Sanitation Sector RAS - 2000, title E, basic criteria should be taken into account and minimum requirements should be met for the different processes involved in the conceptualization and treatment of wastewater.

- The design period, taking into account economic and technical criteria is 8 to 16 years.
- The number of parallel minimum units is four (4) for maintenance purposes.
- The operating period is 24 hours per day.
- The retention time will be between 2 and 6 hours.
- The surface load will be between 2 and 10 $m^3/m^2/day$.
- The depth of the settler is between 1.5 and 2.5 m.
- The ratio of the length and width dimensions (L/B) is between 3 and 6.
- The bottom of the unit should have a slope between 5 and 10% to facilitate sliding of the sediment.
- The speed in the holes should not be greater than 0.15 m s^{-1} to avoid creating disturbances within the sedimentation zone.
- The sludge discharge must be located in the first third of the unit, since 80% of the volume of the sludge is deposited in that area.

For the sedimentation design, the flow rate established from the mass balance calculation was taken into account, which corresponds to the ideal conditions of water consumption. This is contrary to those found during the three days in the MPU. By selecting a kinematic viscosity from Table 7 and a particle diameter form Table 8, the required data is shown in the table below.

Table 16. Data for the conventional settlers

Data	Value
Maximum flow	0.67 L s^{-1}
Relative density silt	1.8
Particle diameter	0.001 cm
Water temperature	25 °C
Kinematic viscosity (μ)	0.00896 cm^2 s^{-1}

Based on Stoke's law (6), the settling velocity (Vs) can be determined as follows:

$$V_S = \frac{981}{18} \times \frac{\rho s - 1}{\mu} \times d^2 \quad (17)$$

$$V_s = \frac{1}{18} \times \frac{981 cm}{s^2} \times \frac{1.8 - 1}{0.00896 \frac{cm^2}{s}} \times (0.001\ cm)^2 = 0.0049\ cm/s$$

$$Vs = 0.0049 \frac{Cm}{s} \times \frac{1\ m}{100\ m} = 0.000049\ m/s$$

Flow for design:

$$Q = 670 \frac{ml}{S} \times \frac{1\ m^3}{1000000\ ml} = 0.000670\ m^3/s$$

The superficial area is determined (AS) accordingly:

$$A_s = \frac{Q}{V_s} = \frac{0.000670\ m^3/Sg}{0.000049\ m/Sg} = 13.77\ m^2$$

The width of the settler is assumed and the length can be calculated as follows:

$$B = 2.3m \ \text{Asumed}$$

$$L_2 = \frac{A_s}{B} = \frac{13.77}{2.3} = 5.98\ m$$

The separation distance between the inlet and the diffusor screen was assumed, as follows:

$$L_1 = 1.0\ m \ \text{Assumed}$$

Therefore, the total length is:

$$L = L_1 + L_2 = 1.0\ m + 5.98\ m = 6.98\ m$$

This corresponds to a certain L/B ratio:

$$\frac{L}{B} = \frac{6.98\ m}{2.3\ m} = 3.03\ m$$

A depth of 2.0 was assumed and the L/H ratio was calculated as follows:

$$\frac{L}{H} = \frac{6.98\ m}{2.0\ m} = 3.49\ m$$

Horizontal velocity was calculated (V_H) using Equation 18, as follows:

$$V_H = \frac{100 \times Q}{B \times H} \quad (18)$$

$$V_H = \frac{100 \times 0.000670\ m^3/s}{2.3\ m\ \times\ 2.0\ m} = 0.014\ m/s$$

With an outlet weir having a crest length equal to the width of the unit, the water height over the weir can be calculated as follows:

$$H_2 = \left[\frac{Q}{1.84\ \times\ B}\right]^{\frac{2}{3}} \quad (19)$$

$$H_2 = \left[\frac{0.000670\ m^3/s}{1.84\ \times\ 2.3\ m}\right]^{\frac{2}{3}} = 0.0029\ m^2$$

For the diffuser screen a velocity through the orifices was assumed as:

$$V_O\ = 0.1\ \frac{m}{s}$$

The total area of orifices was estimated as follows:

$$A_O = \frac{Q}{V_0} = \frac{0.000670\ m^3/s}{0.1\ m/s} = 0.2\ m^2$$

$$\text{Diameter of each orifice } (d_o) = 0.075\ m$$

$$\text{Area of each orifice } (a_o\ ) = 0.0044\ m^2$$

$$\text{Number of orifices} = \frac{A_0}{a_0} = \frac{0.2\ m^2}{0.0044\ m^2} = 45$$

Thereafter, the portion of height for the diffusor screen was calculated as follows:

$$h = H\ -\ \frac{2}{5} \times H = 2.0\ m - \frac{2}{5} \times 2.0\ m = 1.2\ m$$

The number of rows of orifices was assumed as:

$$n_f = 5$$

Hence, the number of column is:

$$n_c = 9$$

$$\text{Space between rows } (a_l) = \frac{h}{n_f} = \frac{1.2\ m}{5} = 0.24\ m$$

$$\textit{Space between columns } (a_2) = \frac{B - a_l(n_c - 1)}{2} = \frac{2.3\ m - 0.24\ m\ (9 - 1)}{2} = 0.19m$$

After calculating all the dimensions, every unit can be divided into 4 parts or zones, each one of these zones has a specific function. Figure 36 and Figure 37 show the dimensions and the zones of one of the conventional settler and a description of the zones are provided below.

- Inlet zone: Transitional hydraulic structure, which allows a uniform flow distribution within the settler.
- Settling zone: It consists of a rectangular channel with volume, length and flow conditions suitable for sedimentation of the particles. The flow direction is horizontal and the velocity is the same at all the points (piston flow).
- Outlet zone: It consists of a weir, several gutters or pipes with perforations that have the purpose of collecting the effluent without disturbing the sedimentation of the deposited particles.
- Sludge collection zone: It consists of a hopper with adequate capacity to deposit the sedimented sludge, and a pipe and valve for periodic evacuation (Ruiz, 1999).

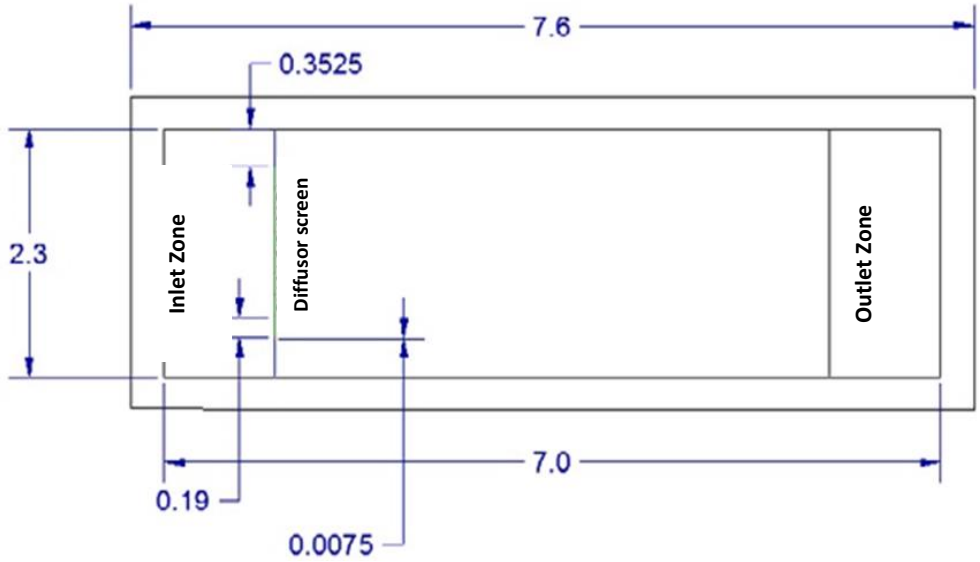

Figure 36. Plan view of the conventional settler design (unit = m)

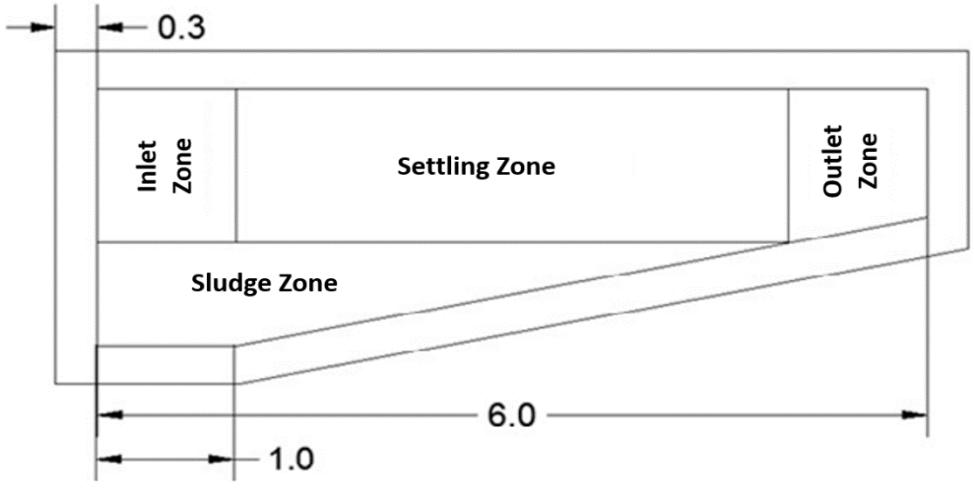

Figure 37. Profile view of the conventional settler design (unit = m)

6.1.3 Grinding of agricultural waste material

Figure 38 and Figure 39 show the washing process of the materials, which were rinsed 3 times with distilled water and later filtered. After drying for 1 day at 80 °C in a furnace, they were immediately ground. The grinding of coconut shell and coffee husk was carried out to particles smaller than 0.5 mm. One kg of ground coconut shell and 1 kg of ground coffee husk were obtained. Figure 40 shows the drying step of coffee husk.

Figure 38. Washing of the precursor materials

Figure 39. Washed coffee husk

Coconut shell needed to be smashed with a hammer before grinding in order to decrease the size of the material in order to be milled and also to soften this material which has a higher hardness than the coffee and could get stuck to the blades of the mill. Figure 40 shows the dried and smashed coconut shell, while Figure 42 shows the coconut shell after the grinding step. Figure 43 shows the coffee husk after the three stages, namely, washing, drying and grinding.

Figure 40. Drying step for coffee husk

Figure 41. Dried and smashed coconut shell

Figure 42. Ground coconut shell

Figure 43. Coffee husk after washing (on the left), drying (in the middle) and grinding step (on the right)

6.1.4 Coconut shell and coffee husk activation

Coconut shell and coffee husk were activated with steam as the activating agent and nitrogen gas was used to create a reducing atmosphere. The consumption of nitrogen gas and steam flow rate were measured for every test in order to ascertain how much materials and resources were required to generate the activated carbon under these laboratory conditions. Steam flow rate was calibrated by measuring the water volume consumed in an Erlenmeyer flask when heating with a specific level of heat. The flow rate was 2.5 mL min^{-1} and it was repeated 3 times before the start of any test. Both precursor materials were placed in the muffle furnace, in shallow layers, because the injection of substances is generated in the middle of the muffle furnace door and contact of the substance with the coconut shell and coffee husk only takes place in the top layer. A high amount of nitrogen was consumed during carbon activation. Table 18 shows the conditions that were measured and controlled for every experiment.

Table 17. Parameters and results of the carbonization - activation process

Precursor material	**Coffee husk**		**Coffee husk**		**Coconut shell**		**Coconut shell**	
	Carb 400 (°C)	**Activ 700 (°C)**	**Carb 300 (°C)**	**Activ 600 (°C)**	**Carb 400 (°C)**	**Activ 700 (°C)**	**Carb 300 (°C)**	**Activ 600 (°C)**
Time (min)	60	60	60	60	60	60	60	60
Temperature rise time (min)	30	30	30	30	30	30	30	30
N_2 consumed in rise time (psi)	100	100	100	100	100	150	120	100
Steam volume consumed (mL)	150	140	140	160	170	150	160	160
Steam flow rate (mL min^{-1})	2.50	2.33	2.33	2.67	2.83	2.50	2.67	2.67
N_2 Pressure rate (psi)	5	5	5	5	5	5	5	5
Cooling step								
Time elapsed (min)	210		196		160		97	
N_2 Pressure rate (psi)	10		10		10		10	
N_2 consumed (psi)	650		700		750		900	

Carb = Carbonization step; Activ = Activation step

The cooling step is inefficient in terms of nitrogen consumption, i.e. the time required to cool down the activated carbon is certainly values that is higher than the time required to raise the temperature for carbonization and activation. It is a very important step and it should be carried out carefully until the muffle temperature reaches 150°C and there is no chance of carbon combustion. For the carbonization step, activation and cooling period, a total of 3870 psi was consumed, which equals to 2 industrial nitrogen cylinders of 6.5 m^3 each.

A more efficient way of injecting nitrogen and steam and also enhance the contact with the precursor material would be to use a plate that injects the substances from the bottom of the plate and since the gas flows upwards, the substance is going to move upwards and make

contact with all the precursor material over the plate efficiently. This approach would increase the yield of activated carbon production in a single experiment without having problems of activation only in the top layer of the material inside the muffle furnace. Nevertheless, if one would like to consider in scaling this process/treatment a real scale for San Juan MPU, the carbon needs to be activated with an industrial oven that can optimize the use of chemical substances. The yield of every experiment was calculated by measuring the mass of every precursor material that entered the muffle furnace and the final mass of the activated carbon. Table 19 shows the yield of every experiment.

Table 18. Biosorbent mass yield of every activation experiment according to the mass obtained

Activation experiment	**Coffee husk 400 - 700 (°C)**	**Coffee husk 300 - 600 (°C)**	**Coconut shell 400 - 700 (°C)**	**Coconut shell 300 - 600 (°C)**
Mass of precursor material (g)	142	279	240	240
Mass of activated carbon (g)	22.3	66	60	72
Yield	15.7%	23.7%	25.0%	30.0%

Figures 44 to 46 show the experimental set up for the activation of carbon, the precursor material before starting the tests and the resulting activated carbon made from coffee husk and coconut shell, respectively.

Figure 44. Coffee husk before starting the activation process

Figure 45. Coffee husk activated carbon

Figure 46. Coconut shell activated carbon

6.1.5 Sorbent material characterization

6.1.5.1 Surface area and micropore volume

The characterization of surface area and micropore volume was obtained with a Micrometrics ASAP 2020 V4.01, through N_2 adsorption at -196°C. BET model was used to measure the surface area, while the micropore volume was obtained with the T-Plot model. Thus, the four biosorbents were analyzed. Figure 47 shows the results obtained from this study.

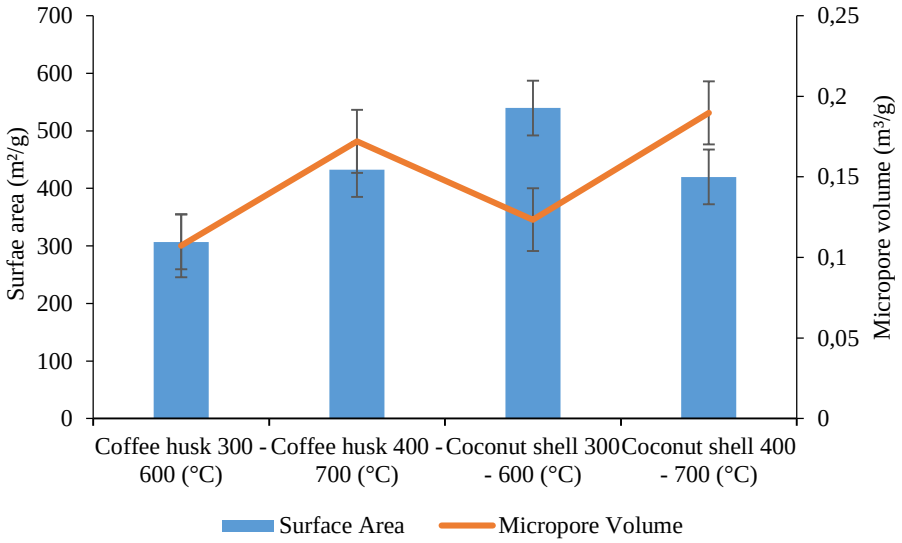

Figure 47. Surface area and micropore volume for coffee husk and coconut shell as the biosorbents

As seen in Figure 47, the BET surface area of the coconut shell, at a carbonization temperature of 300 °C and an activation temperature of 600 °C, was found to reach a maximum value of 539.6 m^2 g^{-1} which suggests that lower temperatures for carbonization/activation generate a higher surface area. Contrary to coconut shell, the coffee husk activated carbon showed a higher surface area of 432.7 m^2 g^{-1} when activated under higher temperature. From Figure 47, it was estimated that the carbonization/activation temperature has a different effect on the precursor materials. Moreover, the micropore volume data show an increase in the micropore volume as the carbonization/activation temperature increases. In this way, the micropore volume of coffee husk and coconut shell at a carbonization temperature of 400 °C and an activation temperature of 700 °C were found to reach a maximum of 0.17 cm^3 g^{-1} and 0.19 cm^3 g^{-1}, respectively.

6.1.5.2 Mesopore determination

Based on the stock solution containing 1000 mg l^{-1} of blue methylene, the solutions of 10, 25, 50 and 100 mg l^{-1} were prepared and were tested with 10 mg each of the respective activated carbon. In addition to these solutions, less concentrated solutions from 0.1 to 4.5 mg l^{-1} were also prepared to plot the graph in order to obtain the linear least squares regression. Figure 48 shows the result for the absorbance of blue methylene.

Considering Figure 48, the Equation 20 was established to calculate the methylene blue concentrations for the adsorption tests. Figure 49 and Figure 50 show the color change noticed

during this adsorption process. Absorbance was measured for all the initial concentrations and the required dilutions were made in order to read the absorbance value within the detection limits of the spectrophotometer. After completing 48 hours, the samples were measured for its final absorbance.

$$BMconcentration = \frac{Absorbance + 0.0135}{0.2216} \quad (20)$$

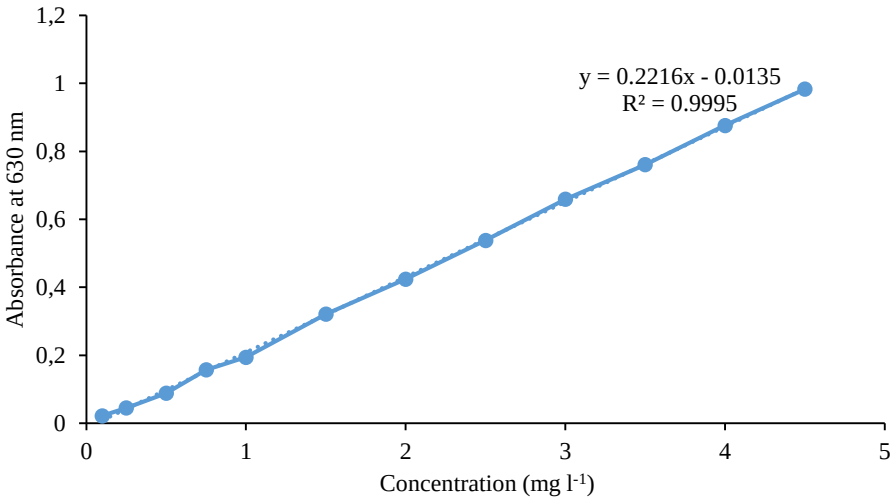

Figure 48. Linear least squares regression for determining the blue methylene concentrations determination

Figure 49. Methylene blue adsorption test under different adsorbate concentrations

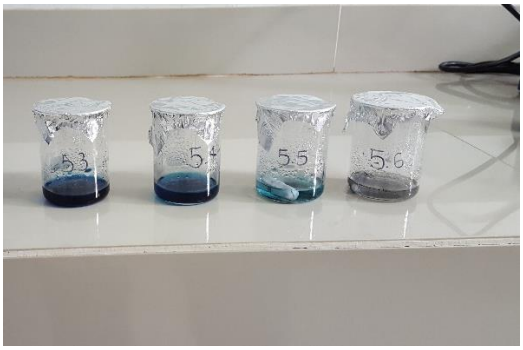

Figure 50. Methylene blue adsorption test after 48 hours under different adsorbate concentrations

Equation 2 was used to calculate the adsorption capacity of each biosorbent under different initial concentrations. For this calculation, the mass of activated carbon used and the volume of solution were registered in Table 20. Methylene blue adsorption results clearly shows the proportion of mesopores in a particular activated carbon. From Table 19 and Table 20, it can be estimated that coffee husk, at carbonization temperature of 400 °C and activation temperature of 700 °C, developed a higher amount of mesopores than the rest of the activated carbons. It showed a methylene blue removal of 74.3 %, while the tests at an initial concentration of 111.2 mg l^{-1} showed a maximum adsorption capacity of 28.6 mg g^{-1} for this biosorbent.

Table 19. Methylene blue adsorption results

Biosorbent	Theory initial concentration (mg l^{-1})	Real initial concentration (mg l^{-1})	Mass of biosorbent (g)	Methylene blue final concentration C_e (mg l^{-1})	q_{eq} (mg g^{-1})
Coffee husk 400 - 700 (°C)	10	8.51	0.01	1.15	7.4
	25	23.52	0.01	8.52	14.3
	50	53.14	0.01	38.24	14.7
	100	111.24	0.01	83.26	28.6
Coffee husk 300 - 600 (°C)	10	8.51	0.01	4.58	3.9
	25	23.52	0.01	15.85	7.4
	50	53.14	0.01	44.34	8.7
	100	111.24	0.01	97.7	13.5
Coconut shell 400 - 700 (°C)	10	8.51	0.01	1.11	7.4
	25	23.52	0.01	4.46	18.2
	50	53.14	0.01	30.35	22.6
	100	111.24	0.01	97.25	13.6
Coconut shell 300 - 600 (°C)	10	8.51	0.01	4.44	4.1
	25	23.52	0.01	19.91	3.2
	50	53.14	0.01	45.92	7.2
	100	111.24	0.01	94.54	15.9

On the other hand, coconut shell, at a carbonization temperature of 400 °C and an activation temperature of 700 °C, showed the highest adsorption capacity among the two coconut shell activated carbons in the test with an initial methylene blue concentration of 50 mg l^{-1}. As it was expected, when steam was used as an activating agent, it favors the presence of mesopores and there was a clear correlation of the higher proportions of mesopores to the high carbonization/activation temperatures in coconut shell and coffee husk activated carbons, respectively. Figure 51 shows the methylene blue adsorption behavior under different initial concentration, for both coconut shell and coffee husk, activated at a carbonization temperature of 300 °C and an activation temperature of 600 °C. They present a similar behavior on the adsorption of different concentrations and the adsorption capacity results were closer to the results of coconut shell and coffee husk activated at 400° to 700 °C, respectively.

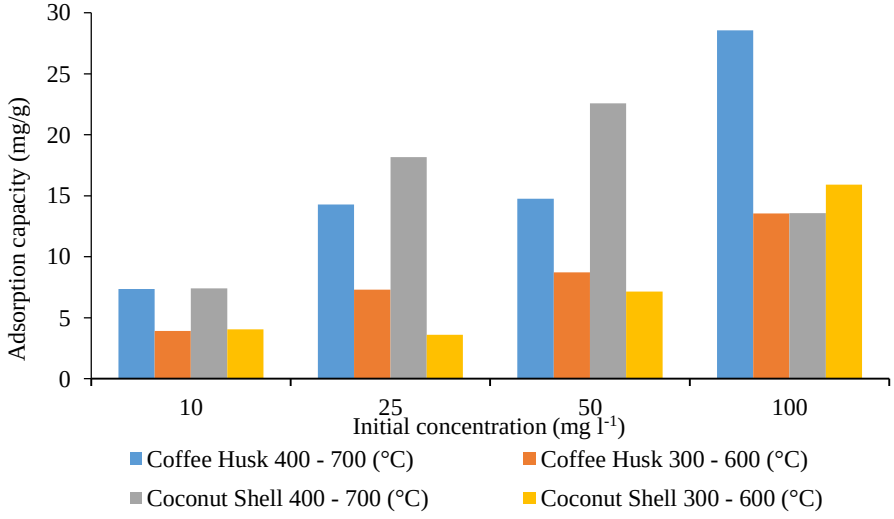

Figure 51. Methylene blue adsorption onto coconut shell and coffee husk

6.1.5.3 Density

Bulk or apparent density was determined on an analytical balance, and the results are shown in Table 21. The density was used in order to calculate the mass of activated carbon used in the fixed bed reactor. As seen in Table 21, the minimum density was found in the coffee husk biosorbent at a carbonization temperature of 300 °C and an activation temperature of 600 °C. This table also shows the surface area, micropore volume and the average mesopore adsorption capacity found in the previous tests.

Table 20. Effect of carbonization and activation temperature on the physical properties of the biosorbents

Biosorbent at carbonization - activation temperature	**Density (g ml^{-1})**	**BET surface area (m^2 g^{-1})**	**Micropore volume (cm^3 g^{-1})**	**Mesopore adsorption (mg g^{-1})**
Coffee Husk 300°C - 600°C	0.44	306.85	0.11	8.37
Coffee Husk 400°C - 700°C	0.47	432.68	0.17	16.23
Coconut Shell 300°C - 600°C	0.60	539.59	0.12	7.68
Coconut Shell 400°C - 700°C	0.59	419.76	0.19	15.43

BET surface area = Superficial area according to the Brunauer-Emmett-Teller (BET) theory

6.1.6 Biosorption batch test results

The mercury adsorption in batch tests were performed for 48 hours with an initial concentration of 0.144 mg l^{-1} of mercury present in the wastewater collected for the whole experiment. For the mercury concentrations obtained for the batch experiments, the control test carried out without the biosorbent showed a lower concentration than the one measured as initial concentration. For the test #1, the control test showed a mercury concentration of 0.033 mg l^{-1}, while, for the test #2, the mercury concentration in the control was 0.044 mg l^{-1}. This may occur due to the adherence of mercury to the glass material of the flasks used for the test or the plastic material used to transport the wastewater to the laboratory in charge of analyzing the mercury concentrations. In order to calculate the adsorption capacity and the percentage of mercury removal with Equation 2 and Equation 1, the results obtained as control tests were assumed as the new initial concentrations. Table 22 shows the equilibrium concentrations, C_e, after the batch tests, the adsorption capacity q_e and removal capacity for coconut shell and coffee husk with the new initial concentrations C_o.

Table 21. Adsorption and removal capacity of biosorbents under different carbonization/activation temperatures

Biosorbent	**C_o = 0.033 (mg l^{-1})**			**C_o = 0.044 (mg l^{-1})**		
	C_{e1} (mg l^{-1})	**q_{e1} (mg g^{-1})**	**Removal Capacity (%)**	**C_{e2} (mg l^{-1})**	**q_{e2} (mg g^{-1})**	**Removal Capacity (%)**
Coffee Husk 300°C - 600°C	0.025	0.0008	24.2%	0.024	0.002	45.5%
Coffee Husk 400°C - 700°C	0.03	0.0003	9.1%	0.013	0.0031	70.5%
Coconut Shell 300°C - 600°C	0.0098	0.0023	70.3%	0.0078	0.0036	82.3%
Coconut Shell 400°C - 700°C	0.02	0.0013	39.4%	0.0097	0.0034	78.0%

As seen in Table 22 the maximum removal capacity was achieved using coconut shell as the sorbent at a carbonization temperature of 300 °C and an activation temperature of 600 °C with a removal capacity of 82.3%. According to this result, it was estimated that coconut shell material has a higher removal capacity when it was activated at lower temperatures. Despite the high removals of over 80%, the mercury concentration remaining in the wastewater doesn´t meet the national standards for wastewater discharge for the mining sector of gold extraction and precious metals. The permissible limit is 0.002 mg l^{-1}, which in this case, would need a biosorbent with a removal capacity of 95.5 %. This result suggests that a pre-treatment step is required for mercury removal. Figure 52 shows the adsorption capacity of the four sorbents.

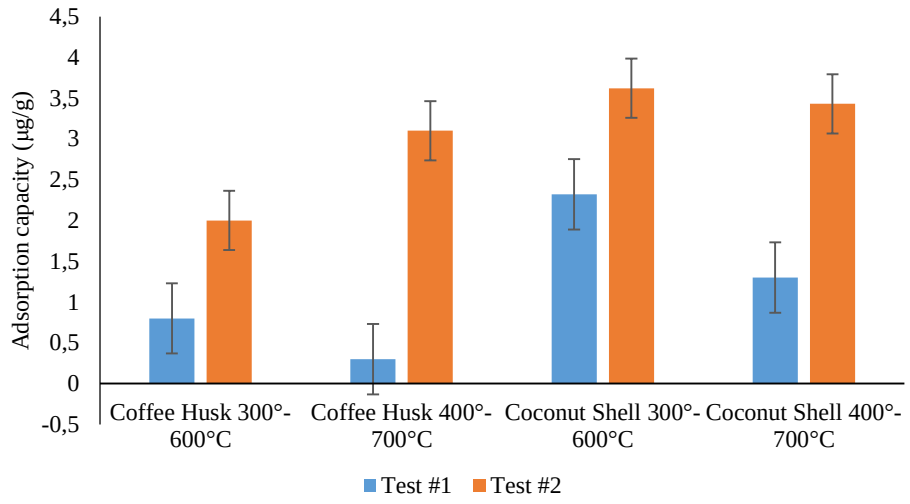

Figure 52. Adsorption capacity of coffee husk and coconut shell at different cabonization - activation temperatures in batch tests #1 and #2

The results suggest that for test #1 and test #2, the coconut shell biosorbent at a carbonization temperature of 300 °C and an activation temperature of 600 °C evidenced the higher adsorption and removal capacity. From the results observed for coffee husk, it cannot be established whether the highest adsorption or removal capacity corresponds to test #1 and test #2. Further studies should be performed to establish whether coffee husk has a higher adsorption capacity when is activated under lower temperatures or has a higher performance when it is activated under higher temperatures

6.1.7 Desorption test results

Coconut shell with a carbonization temperature of 300°C and an activation temperature of 600°C was selected as the best sorbent according to the performance in the batch test. This sorbent was evaluated under two cycles of sorption and desorption. In order to consider possible adherence of mercury to the glass or plastic materials, similar to batch test results, the adsorption cycle results were multiplied by the percentage of the proportion that had to be assumed as the new initial concentration during batch test. Figure 53 shows the results of mercury concentrations in wastewater when treated with 0.1 M HCl after each adsorption and desorption step.

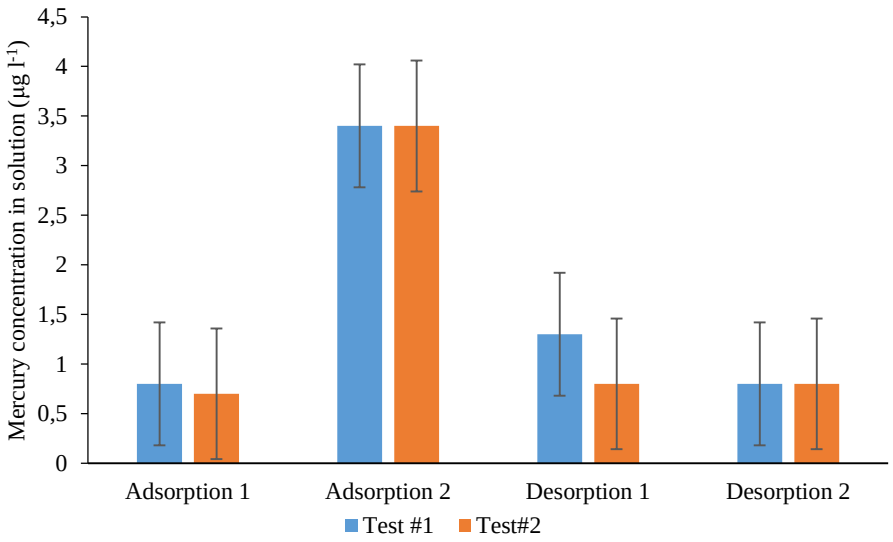

Figure 53. Mercury concentrations in solutions after the adsorption and sorption cycles

As seen from Figure 53, the mercury concentration remaining in the wastewater after the second adsorption step raises drastically. These evidences a weak desorption capacity of HCl on coconut shell and therefore a weak recovery of mercury. The maximum desorption concentration was found in the first desorption step with 1.3 µg l^{-1}, which is significantly low compared to the initial concentration of mercury in the water (27.15 µg l^{-1}). To assess these results, the removal capacity, adsorption capacity q_e and the desorption efficiency η_d were calculated according to Equation 1(1, Equation 2 and Equation 10, respectively.

Table 22. Adsorption, removal capacity and desorption efficiency for the sorption-desorption cycles

Test	C_o (mg l^{-1})	Cycle 1			Cycle 2		
		q_{e1} (mg g^{-1})	Removal capacity (%)	n_{d1} (%)	q_{e2} (mg g^{-1})	Removal capacity (%)	n_{d2} (%)
#1	0.0271	0.0053	97.1%	4.9%	0.0052	96.2%	3.1%
#2	0.0311	0.0061	97.7%	2.6%	0.0060	96.7%	2.7%

Despite the high removal capacities observed during the sorption step, the results shown in Table 23 clearly reveals that the desorption efficiency was not favorable. After the second desorption cycle, the desorption efficiency for test #1 and test #2 were only 3.1 % and 2.7 %, respectively. This clearly shows that, from the amount of mercury adsorbed by the coconut shell activated carbon during test # 1 and #2, only 3.1 % and 2.7 % were recovered in the HCl solution. Further studies are therefore required to determine which chemical solution may offer a better desorption efficiency under these conditions and for these materials.

6.2 Evaluation of the adsorption constant parameters and correlation coefficients for various adsorption models

6.2.1 Review of kinetics and isotherm studies on mercury adsorption with coconut and coffee residues

Few or no studies have been proposed to evaluate the adsorption capacity of coconut shell and coffee husk to remove mercury from the liquid phase. Nevertheless, some studies have evaluated another type of biomass residue obtained from coconut and coffee. The possible mercury adsorption mechanism as well as adsorption rates may be envisaged through kinetics analyses. Different authors have studied the kinetic of the adsorption of mercury in solution using the pseudo-first order, pseudo-second order, Elovich models as is presented in Table 5.

Anirudhan and Sreekumari (2011) developed a biosorbent with coconut buttons. This material was treated with a H_2SO_4 solution and heated to 400 °C inside a muffle furnace with a steam flow rate of 3 mL min^{-1} for 1 h. Considering the initial concentrations of 25, 50, 75 and 100 mg l^{-1}, a temperature of 30 °C, an adsorbent dose of 2 g l^{-1} and pH of 7.0 units, the fittings of pseudo first (PFO) and second-order (PSO) were evaluated as shown in Figure 54 to test the experimental kinetic data and determine the rate controlling step of the adsorption process.

The values found for R^2 for the PSO kinetic model were found to be higher than 0.990. Moreover, the half-life time was found to vary with the initial concentration, indicating the assumption of a PSO adsorption mechanism rather than first order one. In this way, the half-life time increased from 5 to 15 min for mercury when the initial metal concentration was increased from 25 to 100 mg l^{-1}. The calculated q_e values from PSO equation were in good agreement with the experimental values. Therefore, it could be established that the sorption reaction belongs to the PSO kinetic model and that the overall rate of the metal adsorption process appears to be controlled by the chemical process *via* ion exchange and/or the complexation process.

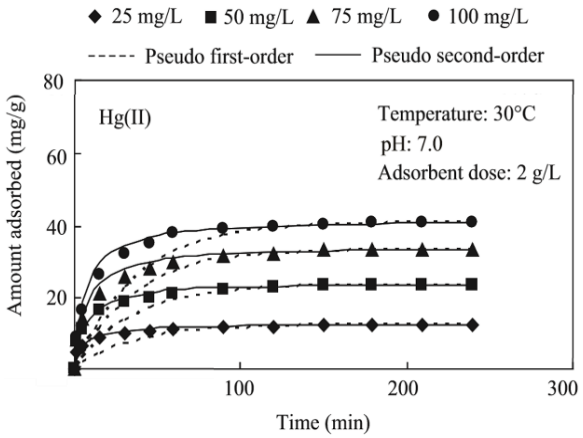

Figure 54. Comparison of experimental contact time data and the fittings to PFO and PSO kinetic models for adsorption of Hg(II) onto activated carbon Source: Adapted from Anirudhan & Sreekumari (2011)

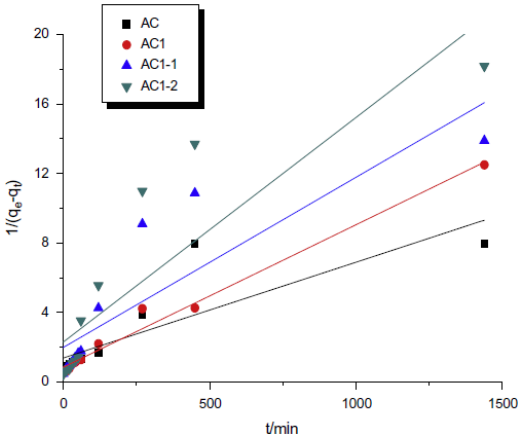

Figure 55. The Lagergren second order model for Hg^{2+} adsorption on samples
Source: Adapted from Lu et al. (2014)

Lu et al. (2014) used commercial coconut activated carbon as a precursor material to achieve surface modification by heating to 850 °C with steam flow and subsequently oxidation at 25 °C using H_2O_2 (30%) at a ratio of 1:2 and 2:5 (*m*:*v*). The kinetics were evaluated at 283 K with a mercury (Hg^{2+}) concentration of 7.2 mg g^{-1} for 4 different activated carbons depending on the modification process applied as shown in Figure 55. In the first 120 min, the adsorption rate increased rapidly with increasing time, after which, the rate increased only slowly and reached adsorption equilibrium at 500 min.

The data for the adsorption of mercury on activated carbon were fitted to the Lagergren first-order model, the Lagergren second-order model and the Lagergren pseudo-second-order model. Lagergren pseudo second order model fitted the results slightly better. The results of kinetic study suggested that the process of mercury (Hg^{2+}) adsorption onto activated carbon was a two-step process involving both rapid adsorption and slow adsorption.

Coconut pith was used by Saman et al. (2015), wherein, a char generated in a closed vessel at 700 °C, at a heating rate of 10 °C min^{-1} and an activated carbon prepared by adding a KOH solution at a mass ratio of 1:4 (CP to KOH) were compared. The amount of mercury adsorbed increased rapidly at the early stage of adsorption and became slow with an increase in the contact time. The minimum time taken to reach equilibrium for mercury ($MeHg^{+}$) adsorption onto char and activated carbon was 60 min and 30 min, respectively, which is faster than mercury (Hg^{2+}), which was 360 min for both char and activated carbon.

In this study, four kinetic models, namely, (i) intra-particle diffusion, (ii) PFO, (iii) PSO, and (iv) Elovich were applied. Based on the R^2 of the linear plot, the PSO kinetic model resulted in the highest values. Therefore, the PSO kinetic model was chosen as the kinetic model described the kinetics of mercury adsorption. This model suggested chemisorption mechanism as a rate-limiting step, which is related to the adsorption at the active site on the surface of the adsorbent. Figure 56 and Figure 57 show the results of this model.

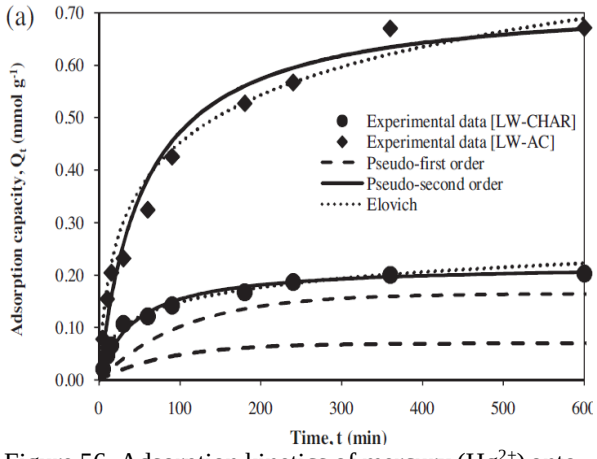

Figure 56. Adsorption kinetics of mercury (Hg^{2+}) onto char and activated carbon adsorbent
Source: Adapted from Saman et al. (2015)

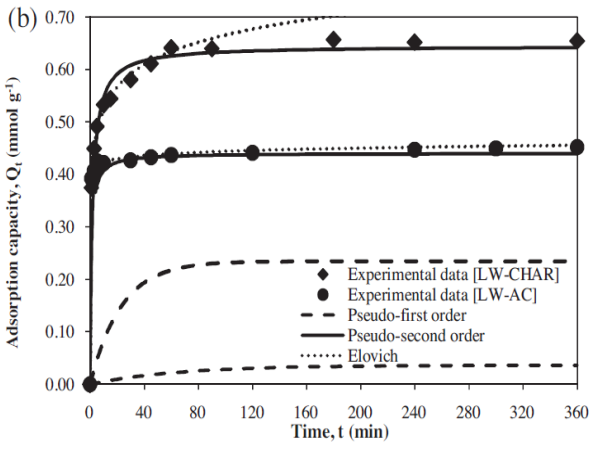

Figure 57. Adsorption kinetics of Mercury ($MeHg^{+}$) onto char and activated carbon adsorbent
Source: Adapted from Saman et al. (2015)

Carro et al. (2009) used exhausted coffee ground as biosorbent without any type of activation. In this case, 0.25 g of dry biomass was added to 100 mL of mercury (Hg^{+2}) solution (100 mgL^{-1}). The mixture was placed in a thermostated cell at 25.0 °C, and the pH was continuously

monitored and adjusted to 5.0 units. The results from that study showed that the exhausted coffee ground attained ~80% of maximum mercury uptake within 4 h. Experiments carried out using exhausted coffee grounds provided 50% of total mercury uptake in less than 1 h. Figure 58 shows the plot of kinetics for the mercury adsorption on exhausted coffee grounds.

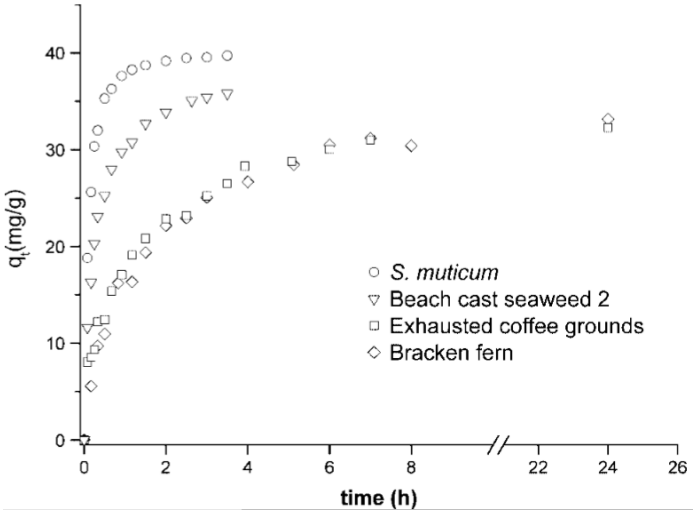

Figure 58. Mercury uptake values as a function of time by exhausted coffee grounds and other biosorbents
Source: Carro et al. (2009)

The biosorption equilibrium models are normally used to determine the maximum sequestration of metals at variable optimum parameters. An isotherm model describes the relationship between the amount of metal adsorbed by adsorbent and metal concentration remaining in the solution (Jain et al., 2016). Besides, important information such as the adsorption mechanism, the favorability of the adsorption process and the adsorbate-adsorbent affinity may be obtained from these models (Inyinbor et al., 2016).

Anirudhan & Sreekumari (2011) calculated the adsorption constants for concentration ranging between 10 and 300 mg l^{-1} according to the least squares fitting method. The validity of the isotherm models was tested by comparing the experimental and calculated data, at 30°C, with the coconut buttons activated carbon. Based on the correlation coefficients, R^2, it was clear that the adsorption of mercury onto activated carbon best fitted to the Freundlich adsorption isotherm model for the entire range of concentrations.

The fact that the Freundlich isotherm fitted the experimental data very well may be due to the heterogeneous distribution of active sites on the carbon surface, since the Freundlich equation assumes a heterogeneous surface. The values of *n* for the Freundlich isotherm were found to be greater than 1, indicating that the metal ions were favorably adsorbed by the activated carbon. Figure 59 shows the results obtained by these authors. In a study carried out by Lu et al. (2014) with commercial coconut activated carbon, the classical Langmuir isotherm and Freundlich isotherm were used to fit the data of adsorption of mercury (Hg^{2+}). It was found out that the correlation coefficients, R^2, were greater than 0.95, and the Langmuir model fit the results slightly better than the Freundlich model. The Langmuir model suggests that the surface of the adsorbent is uniform. Figure 60 shows the Langmuir plots for every carbon used in their tests.

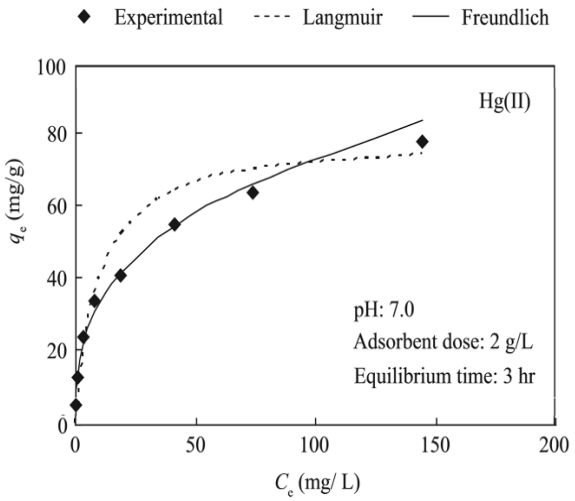

Figure 59. Comparison of model fits to the experimental data for the adsorption of mercury onto activated carbon
Source: Adapted from Anirudhan & Sreekumari (2011)

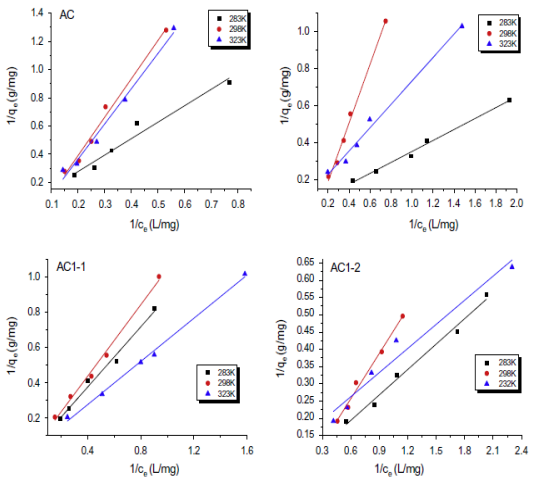

Figure 60. Langmuir plots of mercury (Hg^{2+}) at different temperatures
Source: Adapted from Lu et al. (2014)

Their result match the results obtained by Saman et al. (2015), where the adsorption isotherm data were analyzed by using the Langmuir, Freundlich, and Dubinin-Radushkevich isotherm models. In the latter, the Langmuir prediction curve showed better fit to the experimental data as compared to other models (Figure 61 and Figure 62).

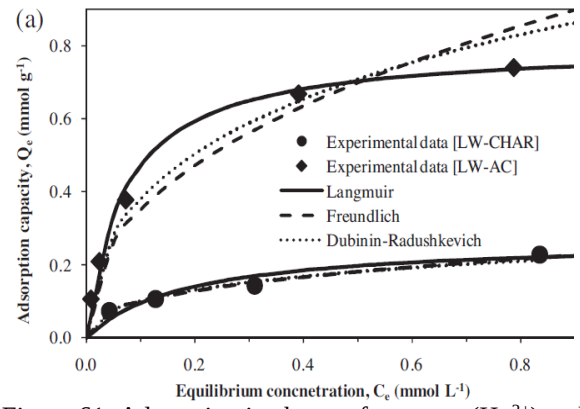

Figure 61. Adsorption isotherm of mercury (Hg^{2+}) and onto char and activated carbon adsorbents
Source: Adapted from Saman et al. (2015)

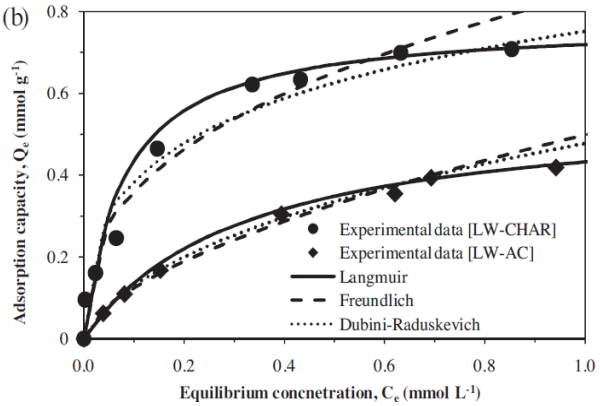

Figure 62. Adsorption isotherm of mercury ($MeHg^{+}$) onto char and activated carbon adsorbent
Source: Adapted from Saman et al. (2015)

Coffee pulping has been used as a biosorbent to evaluate mercury removal from water by Giraldo and Moreno (2012). This material was activated by physical activation of 700 °C with CO_2 flow, followed by a chemical activation with KOH and $ZnCl_2$. Adsorption isotherms were modelled using the Freundlich's equation (Figure 63). The values of Freundlich's isotherm parameter, *1/n* lower than 1 show a favorable adsorption of mercury onto the activated carbon from coffee pulping. Besides, in their results, the equilibrium adsorption capacity value was also high, ranging from 0.002 to 0.380 $mmol \cdot g^{-1}$ for mercury on the activated carbon impregnated with KOH, at a chemical to coffee pulping ratio of 3:1.

Carro et al. (2009) studied the adsorption isotherms for exhausted coffee husks at 25° C. The data was fitted to the Langmuir isotherm model as shown in Figure 64. Based on the Langmuir constant values, a great affinity between the biomass and the metal ion was observed at low metal concentrations. Table 24 shows a summary of the literature results on mercury adsorption/removal from liquid phase onto coconut and coffee residues.

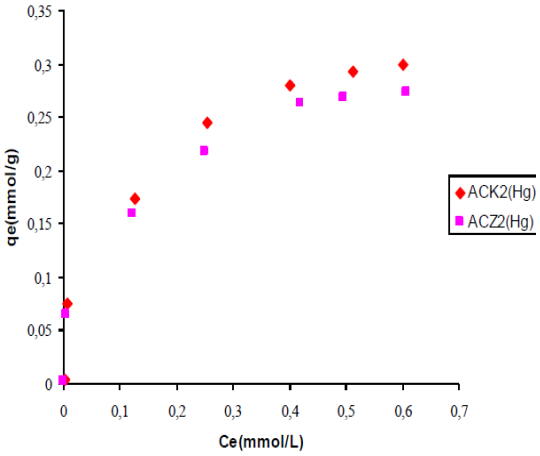

Figure 63. Isotherm of mercury adsorption onto the activated carbons
Source: Giraldo & Moreno (2012)

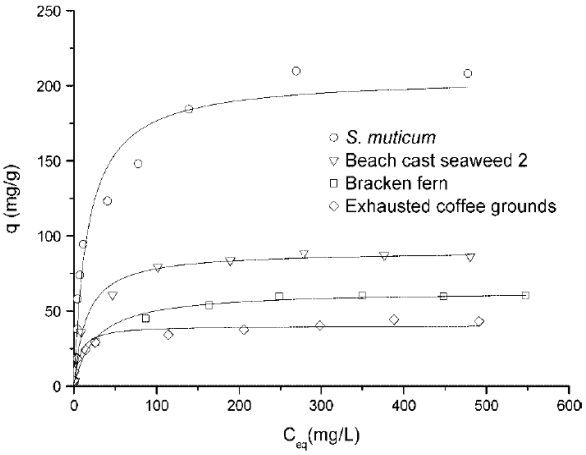

Figure 64. Isotherm of mercury using exhausted coffee grounds and other sorbent materials
Source: Carro et al. (2009)

Table 23. Mercury adsorption in liquid phase onto coconut and coffee residues

Precursor material	Activation - modification	Tests initial conditions	Best fitted kinetics	Adsorption mechanism or main remark	Best fitted isotherm model	Reference
Coconut Buttons	H_2SO_4, 400° - Steam	Initial concentrations 25, 50, 75 and 100 mg l^{-1}, temperature 30°C, adsorbent dose 2 g l^{-1} and pH 7.0 units	Pseudo second-order	Ion exchange and/or complexation process	Freundlich	Anirudhan & Sreekumari (2011)
Coconut Activated Carbon	850°C - Steam, H_2O_2 (30%)	Hg^{2+} initial concentration 7.2 mg g^{-1}, temperature 283 K	Lagergren second-order model	Two-speed process, both rapid adsorption and slow adsorption	Langmuir	Lu et al. (2014)
Coconut Pith	700°C, KOH solution at 1:4 (CP to KOH)	Hg^{2+} initial concentration 1 mM, pH 4.5, temperature 30°C. $MeHg^{+}$ initial concentration 1 mM, pH 4.0, 3.0, Temperature 30 °C	Pseudo second-order	Chemisorption	Langmuir	Saman et al. (2015)

Precursor material	Activation - modification	Tests initial conditions	Best fitted kinetics	Adsorption mechanism or main remark	Best fitted isotherm model	Reference
Coffee Pulping	700˚C - CO_2, KOH, $ZnCl_2$	Initial concentrations 20 to 100 mg l^{-1}, Adsorbent dose 0.5 g l^{-1} and pH 5.1 units	N-A	N-A	Freundlich	Giraldo & Moreno (2012)
Exhausted Coffee ground	N-A	Initial concentration 100 mg l^{-1}, temperature 25 °C, adsorbent dose 0.25 g and pH 5.0 units	N-A	50% of total mercury uptake in less than 1 h	Langmuir	Carro et al. (2009)

Hg^{+2} = Mercury as mercuric ion; $MeHg^{+}$ = Mercury as Methyl mercury

Based on table 24, the kinetics and isotherm models it can be stated that the adsorption of mercury with biosorbents generated with coconut shell and coffee husk has a good performance and there is a good relationship between the adsorbate and the adsorbent. The kinetics prove that the material removes a great concentration of mercury during the first hours and the isotherms show favorable conditions for adsorption under different concentrations and physico - chemical conditions.

6.3 Performance of a fixed bed column for mercury removal using the most suitable adsorbent

6.3.1 Fixed bed start up and monitoring

Coconut shell, at a carbonization temperature of 300 °C and an activation temperature of 600 °C, showed good performance and was therefore selected as the best sorbent from batch tests. The density of coconut shell activated carbon, calculated as shown in section 6.1.5.3, was used to calculate the mass of activated carbon required to pack the column at the desired effective bed depth (Equation 21 and Equation 22).

$$Volume_{biosorbent} = Area_{Column} \times Effective\ bed\ depth \tag{21}$$

$$Volume_{biosorbent} = \left(\frac{1.27cm^2 \times \pi}{2}\right) \times 5cm = 12.67cm^3$$

$$Mass_{biosorbent} = Density_{biosorbent} \times Volume_{biosorbent} \tag{22}$$

$$Mass_{biosorbent} = \frac{0.6g}{cm^3} \times 12.67cm^3 = 7.6g\ of\ biosorbent$$

To obtain an average flow of 1.1 cm^3 min^{-1}, a conversion of 20 drops of wastewater per 1 cm^3 was assumed. Calculations were applied to obtain the desired flow through the infusion that was previously set at four drops for every 11 seconds. An initial test with deionized water was applied to the system to check the correct flow. This was monitored for 2 times per minute during the first 20 minutes and 2 times every hour during a total of 5 hours. In this manner, an

average volume of 0.8 L was fed to the reactor every day, for 12 hours, at the rate of 1.1 cm^3 min^{-1}. Samples were collected at the end of every day and their pH was adjusted to 2.0 units and refrigerated to be analyzed at the end of the test.

6.3.2 Performance analysis of the fixed bed adsorption column

The results obtained during the 10 days of experimentation confirmed mercury removals > 75% (Figure 65). The results also indicate that that sorbent bed did not clog during continuous operation and was able to maintain its performance.

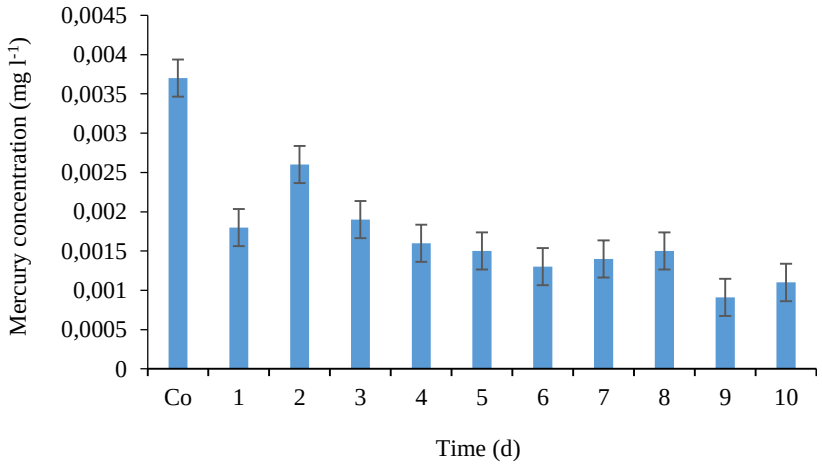

Figure 65. Daily mercury concentration obtained during the monitoring of the fix bed reactor.
C_o = Initial conditions of mercury concentration obtained for the test

Since the reactor was not saturated even after 10 days of operation, the breakthrough curve shown in Figure 66 does not show the trend of a typical adsorption breakthrough profile. This phenomenon could occur due to insufficient time to perform a proper breakthrough analysis, and therefore, the behavior of the column could not be ascertained properly. However, further studies are required to understand the behavior of the reactor in terms of the saturation of the active sites and changes in surface properties of the sorbent due to mercury adsorption.

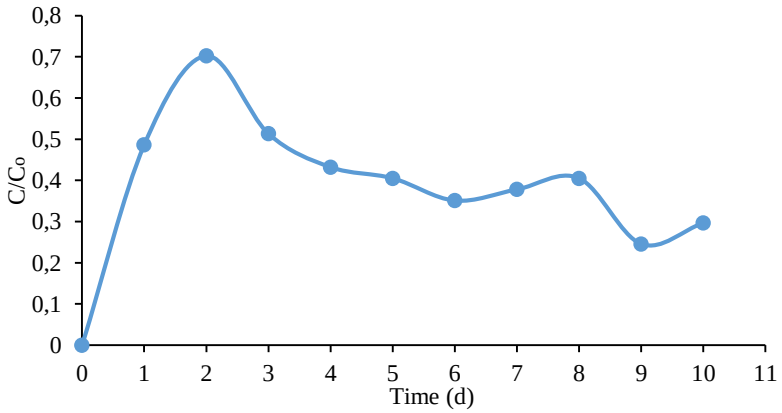

Figure 66. Breakthrough curve for mercury adsorption onto coconut shell activated at a carbonization temperature of 300 °C and an activation temperature 600 °C
C = Mercury concentration over the monitoring; C_o = Initial mercury concentration

As shown in Equation 23, the maximum column capacity, q_{total}, was calculated from the area under the curve of the adsorbed mercury concentration:

$$q_{total} = \frac{QA}{1000} = \frac{Q}{1000}\int_{t=0}^{t=t_{total}} C_{ad}\,dt \quad (23)$$

$$q_{total} = \frac{Q}{1000mL} \times \frac{0.02139mg * d}{L}$$

$$q_{total} = \frac{1.1mL/min}{1000mL} \times \frac{0.02139mg * d}{L} \times \frac{86400min}{d} = 1.680\ mgHg$$

Considering the total dry weight or mass of the sorbent in the column, the equilibrium uptake capacity, i.e. $q_{eq\ (exp.)}$, was calculated as the amount of mercury adsorbed per unit of dry weight of adsorbent (mg g^{-1}):

$$q_{eq(\text{exp.})} = \frac{q_{total}}{W} \quad (24)$$

$$q_{eq(\text{exp.})} = \frac{1.680\ mgHg}{7.6g} = \frac{0.221\ mgHg}{g\ of\ sorbent}$$

Figure 66. Breakthrough curve for mercury adsorption onto coconut shell activated at a carbonization temperature of 300 °C and an activation temperature 600 °C
C = Mercury concentration over the monitoring; Co = Initial mercury concentration

Based on the results obtained from this column study, there was a decrease in the mercury concentrations in the outlet. This allows to meet the Colombian standard for the discharge of wastewater produced in the mining industry of precious metals. Nevertheless, only day 2 does not meet this standard. However, considering the initial characterization results, a higher level of mercury was expected to be found at the inlet as minimum and maximum concentrations were 0.97 and 7.71 mg l-1, respectively. This situation was also noticed during the batch tests. This can be attributed to the previous treatment step when the settleable and the suspended solids were removed as a simulation of an existing primary treatment process. When solids are removed in the primary treatment step, mercury can also be attached to the solids particles that get settled. This tendency of mercury adsorption indicates that mercury removal using a fixed bed reactor packed with coconut shell sorbent can be used as a polishing step for wastewater treatment in MPU with excellent Hg removal capacity.

Once the activated carbon is generated from these two agricultural residue, the process of applying this technology is easy and can be performed by the miners in this region and extended to all the mining departments in Colombia. There are great amount of coconut shell and coffee husk in Colombia that have no proper disposal. This evidences a good opportunity to connect the interests of two industries that need to improve their environmental management of their activities and processes. Further studies are to be done in the removal of other metals as well as other activation methods that require less energy and resources

Conclusions and recommendations

- The wastewater effluent quality from San Juan MPU discharges a water stream containing high mercury, turbidity, solids and other heavy metals concentrations that have direct negative impacts on the environment and population. These contaminants concentrations are above the permissible limits in Colombia. These concentrations are not regulated or controlled by the authorities yet since it is part of an informal mining process.
- There are strong evidences to state that, mercury is not only present in the effluents, but it also percolates from the tailing dams and the sludge accumulated for dehydration on a side of the units. This contaminates the soil and nearby areas. Therefore, retro-fitting the existing units with suitable liners or concrete based wall is urgently required as a preventative approach.
- The existing tailing dams need to be re-designed in order to achieve a higher sludge retention rate and avoid extremely high concentrations of solids in the effluent discharge.
- Mercury concentrations are exceedingly high in the sludge. Sludge stabilization or decontamination of sludge is urgently required. Even if the existing law orders to eliminate mercury from these industry, the sludge is still a problem to address for the next years.
- The adsorption capacity performed by coconut shell and coffee husk is satisfactory and can be applied on a real scale in down flow filters with high efficiency. They prove to have good affinity with specific contaminants such as mercury. Coconut shell biosorbent at a carbonization temperature of 300 °C and an activation temperature of 600 °C evidenced the higher adsorption and removal capacity of 0.0036 mg g^{-1} and 82.3% respectively.
- Coconut shell activated carbon can be used as a polishing treatment step as long as a primary and secondary treatment is developed. Otherwise, clogging of the reactor may occur and solids and other compounds may compete with mercury during the adsorption process.
- Conventional sedimentation, coagulation - flocculation processes may be combined in addition to the adsorption step using coconut shell activated carbon for the removal of solids and mercury from the mining industry.
- The higher desorption efficiency obtained was 4.6 % after the first desorption cycle indicating low desorption capacity of HCl applied to the coconut shell.
- The physical activation becomes expensive when applied on a laboratory scale; hence, further cost-benefit analysis studies should be carried out using alternative activation methods at the industrial scale.
- The obtained surface area, density and mesoporous of the coconut shell activated carbon are lower that the values of commercial activated carbons, however, the biosorbent proved to show a good affinity with mercury at low concentrations.

- At the regional level, environmental education and proper awareness must be promoted for the community and the miners. The possible occupational and environmental risks of using mercury in the amalgamation process should be explained to the workers as a part of the knowledge dissemination process.
- Investigation on low cost treatment alternatives should be continued in order to offer this vulnerable sector a solution to comply with the national quality standards.

CHAPTER 7

References

Acheampong, M., A., Meulepas, R., J., W., Lens., P., N., L., 2010. Removal of heavy metals and cyanide from gold mine wastewater. Journal of Chemical Technology and Biotechnology, 85, 590-613.

Acheampong, M., A., 2013. Sustainable gold mining wastewater treatment by sorption using low - cost materials. CRC Press/Balkema, Wageningen.

Ahmad, A., A., Hameed, B., H., 2010. Fixed bed adsorption of reactive azo dye onto granular activated carbon prepared from waste. Journal of Hazardous Materials, 175, 298-303.

Alcaldía municipal Suárez, 2017. Nuestro municipio, información general 2015, Suárez, Colombia.

Anastopoulos, I., Kyzas, G., Z., 2015. Composts as biosorbents for decontamination of various pollutants: a review. Water, Air, & Soil Pollution, 226, 61.

Anirudhan, T., S., Sreekumari, S., S., 2011. Adsorptive removal of heavy metal ions from industrial effluents using activated carbon derived from waste coconut buttons. Journal of Environmental Sciences, 23, 1989-1998.

Asasian, N., Kaghazchi, T., 2015. Sulfurized activated carbons and their mercury adsorption/desorption behavior in aqueous phase. International Journal of Environmental Science and Technology, 12, 2511-2522.

ASTM, 2006. Standard test method for determination of iodine number of activated carbon. ASTM D 4607-94 ASTM Committee on Standards, Philadelphia, USA.

Aznar, A., 2000. Determinación de los parámetros físico-químicos de calidad de las aguas. Gestión Ambiental, 2, 12-19.

Barakat, M., A., 2011. New trends in removing heavy metals from industrial wastewater. Arabian Journal of Chemistry, 4, 361-377.

Brunauer, S., Emmett, P., H., Teller, E., 1938. Adsorption of gases in multimolecular layers. Journal of the American Chemical Society, 60, 309-319.

Caicedo, L., 2014. Tecnología más limpia en el beneficio de oro sin mercurio. ingeniera de producción biotecnológica, Bogotá, Colombia.

Castro, J., Bonelli, P., B., Cerrella, E., G., Cukierman, A., L., 2000. Phosphoric acid activation of agricultural residues and bagasse from sugar cane: Influence of the experimental conditions on adsorption characteristics of activated carbons. Industrial & Engineering Chemistry, 39, 4166-4172.

Centro panamericano de ingeniería sanitaria y ciencias del ambiente, 2004. Tratamiento de agua para consumo humano: Plantas de filtración rápida. Manual I: Teoría tomo II., Lima, Perú.

Comisión nacional del medio ambiente, 2008. Plan nacional de gestión de riesgos del mercurio, Chile.

Dash, R., Balomajumder, C., Kumar, A., 2009. Removal of cyanide from water and wastewater using granular activated carbon. Chemical Engineering Journal, 146, 408-413.

Díaz, P., Pilar, L., 2011. Minería de oro artesanal y a pequeña escala en Timbiquí - Cauca una aproximación histórica a sus efectos socio ambientales desde la perspectiva de los actores locales, Bogotá, Colombia.

Elliott, C., Colby, T., Iticks, H., 1989. Activated carbon obliterans alter aspiration of activated charcoal. Chest, 672-674.

Español, S., 2001. Toxicología del mercurio. Actuaciones preventivas en sanidad laboral y ambiental, Almadén, España.

Freundlich, H., M., 1906. Over the adsorption in solution. Journal of Physical Chemistry, 57, 385-470.

Gaviria, A., C., Meza, L., A., 2006. Análisis de alternativas para la degradación del cianuro en efluentes líquidos y sólidos del municipio de Segovia, Antioquia y en la planta de beneficio de la empresa mineros nacionales, Municipio de Marmato, Caldas. Dyna, 73, 149, 31-44.

Giraldo, L., Moreno, J., C., 2012. Synthesis of activated carbon mesoporous from coffee waste and its application in adsorption zinc and mercury ions from aqueous solution. Journal of Chemistry, 9, 938-948.

Guiza, L., 2013. La pequeña minería en Colombia: una actividad no tan pequeña. DYNA, 181, 109-117.

Gupta, V., K., Ali, I., 2004. Removal of lead and chromium from wastewater using bagasse fly ash - a sugar industry waste. Journal of Colloid and Interface Science, 271, 321-328.

Hadi, P., Xu, M., Ning, C., Sze, Ki Lin, C., McKay, G., 2015a. A critical review on preparation, characterization and utilization of sludge derived activated carbons for wastewater treatment. Chemical Engineering Journal, 260, 895-906.

Hadi, P., To, M., H., Hui, C., W., Lin, C., S., McKay, G., 2015b. Aqueous mercury adsorption by activated carbons. Water Research, 73, 37-55.

IDEAM, 2004. Determinación de oxígeno disuelto por el método yodo métrico modificación de azida, Bogotá, Colombia.

IDEAM, 2006. Conductividad eléctrica por el método electrométrico en aguas, Bogotá, Colombia.

IDEAM, 2007. Demanda bioquímica de oxígeno 5 días, incubación y electrometría, Bogotá, Colombia.

IDEAM, 2009. Procedimiento para el muestreo de aguas y sedimentos para determinación de metales, Bogotá, Colombia.

IDEAM, 2015. Estudio Nacional del Agua 2014. Bogotá, Colombia.

Itodo, A., U., Abdulrahman, F., W., Hassan, L., G., Maigandi, S., A., Itodo, H., U., 2010. Application of methylene blue and iodine adsorption in the measurement of specific surface area by four acid and salt treated activated carbons. New York Science Journal, 3, 25-33.

Inyinbor, A., A., Adekola, F., A., Olatunji, G., A., 2016. Kinetics, isotherms and thermodynamic modeling of liquid phase adsorption of Rhodamine B dye onto *Raphia hookerie* fruit epicarp. Water Resources and Industry, 15, 14-27.

Jain, C., K., Malik, D., S., Yadav, A., K., 2016. Applicability of plant based biosorbents in the removal of heavy metals: a review. Environmental Processes, 3, 495-523.

Jaramillo, M., C., Zapata, L., F., Marulanda, T., 2015. Fitorremediación de mercurio a partir de *elodea sp*. Ingenierías USBmed, 6, 2, 42-45.

Jiménez, María., 2005. Interacción del mercurio con los componentes del agua residual, Manizales, Colombia.

Johari, K., Saman, N., Song, S., Cheu, S., Kong, H., Mat, H., 2016. Development of coconut pith chars towards high elemental mercury adsorption performance - Effect of pyrolysis temperatures. Chemosphere, 156, 56-68.

Juang R., Wu, F., Tseng, R., 2002. Characterization and use of activated carbons prepared from bagasses for liquid-phase adsorption. Colloids and surfaces A: Physicochemical and Engineering Aspects, 201, 191-199.

Khunphonoi, R., Khamdahsag, P., Chiarakorn, S., Grisdanurak, N., Paerungruang, A., Predapitakkun, S., 2015. Enhancement of elemental mercury adsorption by silver supported material. Journal of Environmental Sciences, 32, 207-216.

Lei, S., Miyamoto, J-I., Kanoh, H., Nakahigashi, Y., Kaneko, K., 2006. Enhancement of the methylene blue adsorption rate for ultramicroporous carbon fiber by addition of mesopores. Carbon, 44, 1884-1890.

López, R., 1999. Elementos de diseño para acueductos y alcantarillados, Bogotá, Colombia.

Lopez, P., E., 2006. Evaluación minero - ambiental del distrito minero de Suárez, Popayán, Colombia.

Lu, X., Jiang, J., Sun, K., Wang, J., Zhang, Y, 2014. Influence of the pore structure and surface chemical properties of activated carbon on the adsorption of mercury from aqueous solutions. Marine Pollution Bulletin, 78, 69-76.

Ministerio de Ambiente y Desarrollo Sostenible, 2015. Resolución 0631 del 17 de marzo de 2015. Bogotá, , Colombia.

Ministerio del medio ambiente, 2002. Diagnóstico y proyecciones de la gestión minero ambiental para las regiones auríferas de Colombia, Bogotá.

Ministerio de Minas y Energía, Unidad de Planeación Minero Energética, Universidad de Córdoba, 2014. Estudio de la cadena del mercurio en Colombia con énfasis en la actividad minera de oro. Bogotá, Colombia.

Mishra, V., K., Upadhyay, A., R., 2008. Phytoremediation of mercury and arsenic from tropical opencast coalmine effluent through naturally occurring aquatic macrophytes. Water, Air, & Soil Pollution, 192, 303-314.

Montenegro, M., Arturo, F., 2002. Evaluación de la contaminación por mercurio en población de mineros artesanales de oro de la comunidad de Santa Filomena - Ayacucho - Perú, Lima, Perú.

Nguyen, T., A., Ngo, H., H., Guo. W., S., Zhang, J., Liang, S., Yue, Q., Y., Li, Q., Nguyen., T., V., 2013. Applicability of agricultural waste and by-products for adsorptive removal of heavy metals from wastewater. Bioresource Technology, 148, 574-585.

Nunes, C., A., Guerreiro, M., C., 2011. Estimation of surface area and pore of activated carbons by methylene blue and iodine numbers. Quimica Nova, 472-476

Oyarzun, R., Higueras, P., Lillo, Javier., 2011. Minería ambiental: una introducción a los impactos y su remediación. Geem, España.

Paraskeva, P., Kalderis, D., Diamadopoulos, E., 2008. Production of activated carbon from agricultural by-products. Journal of Chemical Technology & Biotechnology, 83, 581-592.

Rahman, M., S., Islam, M., R., 2009. Effects of pH on isotherms modeling for Cu(II) ions adsorption using maple wood sawdust. Chemical Engineering Journal, 149, 273-280.

Rai, P., K., Tripathi, B., D., 2009. Comparative assessment of *Azolla pinnata* and *Vallisneria spiralis* in Hg removal from G. B. Pant Sagar of Singrauli Industrial region, India. Environmental Monitoring and Assessment, 17, 75-84.

Rajamohan, N., Rajasimman, M., Dilipkumar, M., 2014. Parametric and kinetic studies on biosorption of mercury using modified *Phoenix dactylifera* biomass. Journal of the Taiwan Institute of Chemical Engineers, 45, 2622-2627.

Rauf, M., A., Hasany, S., M., Hussain, M., T., 1989. Adsorption studies of mercury on zirconium oxide from aqueous solution. Journal of Radioanalytical and Nuclear Chemistry, 132, 397-408.

Raza, M., H., Sadiq, A., Farooq, U., Athar, M., Hussain, T., Mujahid, A., Salman, M., 2015. *Phragmites karkaas* a biosorbent for the removal of mercury metal ions from aqueous solution: effect of modification. Journal of Chemistry, 1-12.

Ruiz, H., 1999. Operación y mantenimiento de plantas de potabilización de agua. Bogotá.

Saavedra, E., E., Sánchez, M., T., 2011. Minería y espacio en el distrito minero Pachuca-Real del Monte en el siglo XIX. Investigaciones Geográficas, 65, 82-101.

Saka, C., 2012. BET, TG-DTG, FT-IR, SEM, iodine number analysis and preparation of activated carbon from acorn shell by chemical activation with $ZnCl_2$. Journal of Analytical and Applied Pyrolysis, 95, 21-24.

Salvatore, G., La Barbera, S., 2005. Control de sedimentos en pequeña minería aurífera en hoja de lata, municipio Sifontes, estado Bolívar, Caracas, Venezuela.

Sekhar, C., Kamala, K., Chary, C., Anjaneyulu., Y, 2003. Removal of heavy metals using a plant biomass with reference to environmental control. International Journal of Mineral Processing, 68, 37-45.

Smith, R., Wiechers, S.G., 1981. Elimination of toxic metals from wastewater by an integrated wastewater treatment/Water reclamation system. Walter S A, 7, 65-70.

Song, S-T., Saman, N., Johari, K., Mat, H., 2015. Biosorption of mercury from aqueous solution and oilfield produced water by pristine and sulfur functionalized rice residues. Environmental Progress & Sustainable Energy, 34, 1298-1310.

Srivastava, S., K., Tyagi, R., Pant, N., 1989. Adsorption of heavy metal ions on carbonaceous material developed from the waste slurry generated in local fertilizer plants. Water Research, 23, 1161-1165.

Sun, X., Hwang, J-Y., Xie, S., 2011. Density functional study of elemental mercury adsorption on surfactants. Fuel, 90, 1061-1068.

Unidad de planeación minero energética, 2007, Producción más limpia en la minería del oro en Colombia. Scripto Impresores S.A, Bogotá, Colombia.

Valderrama, L., Chamorro, J., Olguín, D., Rivera, J., Oyarce, J., 2012. Amalgamación de concentrado de oro obtenido en concentrador knelson. Revista de la Facultad de ingeniería, 27, 33-38.

Vargas, J., E., Giraldo, L., Moreno, J., C., 2008. Obtención y caracterización de carbones activados a partir de semillas de *Mucuna sp*. Revista Colombiana de Química, 37, 67-77.

Veglio, F., Beolchini, F., 1997. Removal of metals by biosorption: a review. Hydrometallurgy, 44, 301 -316.

Velasco, N., 2009. Estudio electroquímico de la lixiviación de pirita, Chile.

Vilar, V., Loureiro, J., Botelho, C., Boaventura, R., 2008. Continuous biosorption of Pb/Cu and Pb/Cd in fixed-bed column using algae Gelidium and granulated agar extraction algal waste. Journal of Hazardous Materials, 154, 1173-1182.

Wan Ngah, W., S., Hanafiah, M., A., 2008. Removal of heavy metal ions from wastewater by chemically modified plant wastes as adsorbents: a review. Bioresource Technology, 99, 3935-3948.

Yu, J., G., Yue, B., Y., Wu, X., W., Liu, Q., Jiao, F., P., Jiang, X., Y., Chen, X., Q., 2016. Removal of mercury by adsorption: a review. Environmental Science and Pollution Research, 23, 5056-5076.

Xu, Z., Cai, J., Pan, B., 2013. Mathematically modeling fixed-bed adsorption in aqueous systems. Journal of Zhejiang University Science A, 14, 3, 155-176.